

DISCRETE CONFORMAL APPROXIMATION OF
COMPLEX EARTHQUAKE MAPS

by

ERIC MICHAEL MURPHY, B.A., M.A.

A DISSERTATION

IN

MATHEMATICS

Submitted to the Graduate Faculty
of Texas Tech University in
Partial Fulfillment of
the Requirements for
the Degree of

DOCTOR OF PHILOSOPHY

Approved

G. Brock Williams
Co-Chairperson of the Committee

Roger W. Barnard
Co-Chairperson of the Committee

Kent Pearce

Edward J. Allen

Accepted

John Borrelli
Dean of the Graduate School

AUGUST, 2005

DISTRIBUTION STATEMENT A
Approved for Public Release
Distribution Unlimited

20050802 092

JUL 27 2005

REPORT DOCUMENTATION PAGE

Form Approved
OMB No. 0704-0188

Public reporting burden for this collection of information is estimated to average 1 hour per response, including the time for reviewing instructions, searching existing data sources, gathering and maintaining the data needed, and completing and reviewing the collection of information. Send comments regarding this burden estimate or any other aspect of this collection of information, including suggestions for reducing this burden, to Washington Headquarters Services, Directorate for Information Operations and Reports, 1215 Jefferson Davis Highway, Suite 1204, Arlington, VA 22202-4302, and to the Office of Management and Budget, Paperwork Reduction Project (0704-0188), Washington, DC 20503.

1. AGENCY USE ONLY (Leave blank)		2. REPORT DATE 26.Jul.05	3. REPORT TYPE AND DATES COVERED DISSERTATION	
4. TITLE AND SUBTITLE DISCRETE CONFORMAL APPROXIMATION OF COMPLEX EARTHQUAKE MAPS.			5. FUNDING NUMBERS	
6. AUTHOR(S) CAPT MURPHY ERIC M				
7. PERFORMING ORGANIZATION NAME(S) AND ADDRESS(ES) TEXAS TECH UNIVERSITY AT LUBBOCK			8. PERFORMING ORGANIZATION REPORT NUMBER CI04-1143	
9. SPONSORING/MONITORING AGENCY NAME(S) AND ADDRESS(ES) THE DEPARTMENT OF THE AIR FORCE AFIT/CIA, BLDG 125 2950 P STREET WPAFB OH 45433			10. SPONSORING/MONITORING AGENCY REPORT NUMBER	
11. SUPPLEMENTARY NOTES				
12a. DISTRIBUTION AVAILABILITY STATEMENT Unlimited distribution In Accordance With AFI 35-205/AFIT Sup 1			12b. DISTRIBUTION CODE	
13. ABSTRACT (Maximum 200 words)				
14. SUBJECT TERMS			15. NUMBER OF PAGES 145	
			16. PRICE CODE	
17. SECURITY CLASSIFICATION OF REPORT	18. SECURITY CLASSIFICATION OF THIS PAGE	19. SECURITY CLASSIFICATION OF ABSTRACT	20. LIMITATION OF ABSTRACT	

Discrete Conformal Approximation of Complex Earthquake Maps

by

ERIC M. MURPHY
Texas Tech University

Using the techniques of circle packing, we construct discrete conformal approximations for complex earthquake maps on the Teichmüller spaces of compact, hyperbolic Riemann surfaces developed by William Thurston and Curtis McMullen, and we show that these approximations are convergent. We then describe earthquake maps on the Teichmüller spaces of compact, Euclidean Riemann surfaces, extending the work of Thurston and McMullen. Using the discrete conformal approximations developed for hyperbolic surfaces, we approximate the action of these new maps with circle packing.

ACKNOWLEDGEMENTS

To the Department of Mathematics and Statistics, Texas Tech University, thank you for taking me in and helping to make these years into years of learning.

To the members of my committee, thank you for your insight, comments, and encouragement. Most particularly, I must thank Dr. Brock Williams for the endless hours of patient help and understanding he has given; I am not at all certain I would be in a position to write these words if it were not for all that you have done for me since you sat in the back corner on the first day of Math 5320 laughing to yourself as we wondered, "Where is the professor?" Thank you, sir.

To the United States Air Force, the United States Air Force Academy, and the Department of Mathematical Sciences, thank you for your faith in me and for allowing me to wear a uniform. Thank you.

To the Department of Mathematics and Statistics at Eastern New Mexico University, thank you for taking a chance on a recovering English major. I would especially like to thank Dr. Kathleen Salter; even now, one of the proudest memories of my mathematical life is that I once earned a perfect score on one your exams. (I still have the exam.) Thank you.

To Mr. (Coach) Frank Dooley, thank you for not for not allowing me quit when I tried to tell myself that calculus was just too hard; it was perhaps a very small thing for you that turned into something not so very small for me. One day, I hope that I make half the impact in the life of a student as you made in mine. Thank you.

It is not possible to thank everyone who has helped to make us who we are, but I want you to know that I remember and cherish all of you who touched and made a difference in my life. Thank you.

Finally, and most important, the greatest thanks go out to my mother and father. Thank you for always telling me to follow my dreams and thank you for understanding when my dreams were not yours. Thank you for teaching me that books are my friends (though I may have taken that a little too much to heart), and thank

you for “suggesting” that, if I insisted on studying English literature, I should study something “useful” at the same time. Thank you for being the little voice in my ear, always telling me to be a better man, and thank you for loving me even when I failed to be. “Thank you” is not enough payment for a debt that can never be repaid, but thank you. I love you both. Thank you for everything.

“Then out spake brave Horatius,
The Captain of the Gate:
‘To every man upon this earth
Death cometh soon or late.
And how can man die better
Than facing fearful odds,
For the ashes of his fathers,
And the temples of his gods,
And for the tender mother
Who dandled him to rest’ ”[34]

(I said I was a *recovering* English major; I did *not* say I was cured.)

CONTENTS

ACKNOWLEDGEMENTS	ii
ABSTRACT	vi
LIST OF TABLES	vii
LIST OF FIGURES	x
CHAPTER	
I. INTRODUCTION	1
II. REAL AND COMPLEX EARTHQUAKES	4
2.1 Preliminaries and Definitions	4
2.2 Shearing Maps and Real Earthquakes	7
2.3 Grafting Maps and Complex Earthquakes	17
2.4 Riemann Surfaces and Teichmüller Theory	21
2.5 Earthquakes on Surfaces	25
2.6 A Conformal Structure on the Images of Hyperbolic Riemann Surfaces under Complex Earthquake Maps	30
III. CIRCLE PACKING	41
3.1 Preliminaries and Definitions	41
3.2 Discrete Function Theory	46
3.3 Hex Refinement	51
3.4 Combinatorial Welding	53
3.5 Density of Packable Surfaces	56
IV. PACKING EARTHQUAKES	61
4.1 Discrete Laminations	61
4.2 Hyperbolic Projections	63
4.3 Discrete Shearing Maps	64
4.4 Discrete Grafting Maps	64
4.5 Convergence of Discrete Earthquake Maps on Hyperbolic Riemann Surfaces	66

V. EARTHQUAKES ON EUCLIDEAN SURFACES	77
5.1 Defining Earthquakes on the Torus	77
5.2 A Conformal Structure on the Images of Tori under Complex Earthquake Maps	80
5.3 Density of Euclidean Earthquakes	94
5.4 Discrete Complex Earthquake Maps on Tori	99
5.5 Earthquakes on Other Surfaces	119
BIBLIOGRAPHY	120
APPENDIX	124
A: DRAWING THE LAMINATION	124
B: ACTION OF A FINITE LEFT EARTHQUAKE	125
C: COMPUTING A MEASURED GEODESIC LAMINATION	126
D: COMPUTING THE PACKING LABEL	128
E: LAYING OUT THE CIRCLE PACKING	133

ABSTRACT

Using the techniques of circle packing, we construct discrete conformal approximations for complex earthquake maps on the Teichmüller spaces of compact, hyperbolic Riemann surfaces developed by William Thurston and Curtis McMullen, and we show that these approximations are convergent. We then describe earthquake maps on the Teichmüller spaces of compact, Euclidean Riemann surfaces, extending the work of Thurston and McMullen. Using the discrete conformal approximations developed for hyperbolic surfaces, we approximate the action of these new maps with circle packing.

LIST OF TABLES

2.1	The Points S and $h(S)$ Used to Compute a Lamination	16
D.1	Computed Packing Labels for \mathcal{K}	130

LIST OF FIGURES

2.1	Examples of Finite Geodesic Laminations	5
2.2	Topological Types of Finite Laminations on $n = 7$ Vertices	6
2.3	Finite Lamination with Dual Graph/Tree of Triangles	6
2.4	Finite Left Earthquake	12
2.5	“Uniqueness” of Finite Left Earthquakes	13
2.6	Measured Geodesic Lamination on S Given $h(s)$	16
2.7	Local Projective Description of a Shearing Map	17
2.8	Hyperbolic Strip in \mathbb{H}	18
2.9	Local Projective Description of a Grafting Map	19
2.10	Local Projective Description of a Complex Earthquake Map	20
2.11	Fundamental Region for a Torus	22
2.12	Moduli Space vs. Teichmüller Space	23
2.13	Action of a Map f with Dilatation $D_f(z_0) > 1$	24
2.14	Geodesics on Surfaces Lift to Geodesics on \mathbb{D}	26
2.15	Shearing Action on a Hyperbolic Surface	27
2.16	Grafting Action on a Hyperbolic Surface	28
2.17	Open Sets to Define a Conformal Structure on \widehat{R}	31
2.18	Construction of Coordinate Charts for Open Sets U_β	32
2.19	Construction of Coordinate Charts for Open Sets U_γ	33
2.20	Construction of Coordinate Charts for Open Sets U_δ	35
2.21	Partition of U into U_α , U_β , and L	39
3.1	An Abstract Triangulation and Pathological Triangulations	42
3.2	An Abstract Triangulation \mathcal{K}	44
3.3	The Carriers of Two Different Circle Packings of \mathcal{K}	45
3.4	Chains of Circles and Flowers	45
3.5	Two Important Types of Circle Packings	46
3.6	Unique Riemann Map $f : \Omega \rightarrow \mathbb{D}$	48

3.7	Approximate Riemann Map with Circle Packing (171 Circles)	49
3.8	Approximate Riemann Map with Circle Packing (342 Circles)	49
3.9	Approximate Riemann Map with Circle Packing (684 Circles)	49
3.10	Hex Refinement	51
3.11	Hex Refinement and Correction on Adjacent Triangle	52
3.12	Welding Action when h Respects the Combinatorics of \mathcal{K}_1 and \mathcal{K}_2 . .	53
3.13	Welding Action with Combinatorial Refinement of \mathcal{K}_1 and \mathcal{K}_2	54
3.14	An Equilateral Surface and the Induced Packable Surface	59
4.1	Approximating a Geodesic L with Combinatorial Geodesics ℓ_k	62
4.2	Action of a Hyperbolic Projection p_k^i	63
4.3	Combinatorial Shearing and Welding	64
4.4	Combinatorial Grafting and Welding	65
4.5	Geodesics, Discrete Geodesics, and Quasicollars	69
4.6	Pullback of Geodesics, Discrete Geodesics, and Quasicollars	71
4.7	Projection of Geodesics, Discrete Geodesics, and Quasicollars	72
4.8	Misalignment under Pullback, Projection, and Shearing	73
5.1	Earthquake Actions on the Fundamental Region of a Torus	79
5.2	Open Sets to Define a Conformal Structure on the Torus \widehat{T}	82
5.3	Construction of Coordinate Charts for Open Sets U_β	82
5.4	Construction of Coordinate Charts for Open Sets U_γ	83
5.5	Construction of Coordinate Charts for Open Sets U_δ	84
5.6	Construction of Coordinate Charts for Open Sets U_ϵ	86
5.7	Partition of U into U_α , U_β , and L	93
5.8	Fundamental Regions in the Normalized Teichmüller Space of Tori . .	95
5.9	Laminations on a Fundamental Region for a Torus	96
5.10	Convergent Euclidean Earthquakes on a Torus T	97
5.11	Secondary Geodesics on T	102
5.12	Geodesics, Discrete Geodesics, and Quasicollars	103
5.13	Pullback of Geodesics, Discrete Geodesics, and Quasicollars	106

5.14	Projection of Geodesics, Discrete Geodesics, and Quasicollars	107
5.15	Misalignment under Pullback, Projection, and Shearing	108
5.16	Explicit Shearing Action on a Torus	114
5.17	Packing, Discrete Lamination, and Earthquake on a Torus	114
5.18	Discrete Shearing Map on a “Coarsely” Packed Torus	115
5.19	Discrete Shearing Map on a “Finely” Packed Torus	116
5.20	Explicit Grafting Action on a Torus	117
5.21	Packing and Discrete Lamination on a Torus and a Packed Cylinder .	118
5.22	Discrete Grafting Maps on a Torus T	118
D.1	A Triangulation \mathcal{K}	129
D.2	Angle Sums	131
D.3	A Triangulation on a Torus	132
E.1	Distinct Circle Packings Induced by Different Boundary Radii	134
E.2	Circle Packing on a Torus	135

CHAPTER I

INTRODUCTION

The concept of shearing maps as generalizations of Dehn twists and transformations on points in Teichmüller space was first developed by Thurston [49, 51], and has been used by Kerckhoff in proving the Nielsen Realization Conjecture [32] and Bonahon in his investigations into Thurston's boundary of Teichmüller space [6]. These earthquakes have been extended by McMullen [35] to include another geologic action, that of grafting, on points in Teichmüller space. Taken together, through composition, we have complex earthquakes.

Essentially, Thurston's shearing earthquake opens a hyperbolic surface (point in Teichmüller space) along a measured geodesic lamination, shears the surface along the seam in a manner determined by the measure, and re-attaches the surface. McMullen's grafting maps, rather than shearing along the lamination, insert or remove a cylinder and re-attach the surface. In Chapter II, we describe these earthquake actions in detail, giving several examples paying particular attention to the geometric nature of the transformations.

A circle packing is a collection of circles with a prescribed pattern of tangencies. Of course, given a collection of circles, there is no guarantee that they can be "fit together" in a particular pattern; in fact, some patterns may not be possible. For example, given that all the circles have the same radius, one circle cannot be tangent to more than six other circles. The "prescribed pattern," is a strictly combinatorial structure with no inherent geometry. As the circles adjust their radii, trying to meet the constraints of the pattern prescribed, a rigid geometry is realized. The interplay between the combinatorial structure and the rigid constraints inherent in the geometry of the circles provides a deep link to geometric function theory and the structure of Riemann surfaces which we will exploit in describing the relationship between earthquakes and circle packing.

Imposing the geometry of a circle implies the existence of a metric; thus we can

speaking about circle packings on any surface with a metric. Consequently, we may discuss circle packing on any Riemann surface. In fact, it is known that given any reasonable pattern of tangencies there exists a unique Riemann surface which supports a circle packing having that pattern of tangencies [4]. Not all surfaces, though, support a circle packing. It has been shown by Brooks [12] and by Bowers and Stephenson [10, 8], however, that these packable Riemann surfaces are dense in Teichmüller space. To go beyond this notion of density and enter into a deterministic discussion of how the pattern of tangencies affects the geometry of the surfaces and their circle packings can be very difficult [4, 8, 10, 42].

In Chapter III, we outline the essential background material in the theory of circle packing. We then prove two results regarding circle packings and surfaces. First, we prove a proposition of independent interest regarding the interaction between the pattern of tangencies and the geometry of a surface and the unique packing on that surface. We then prove a lemma regarding the density of a subclass of packable surfaces; specifically, we show that we can approximate any Riemann surface with a sequence of packable surfaces such that the radii of the circles in the packings admitted on the surfaces tend toward zero.

In Chapter IV, we turn to our main result, using techniques developed by Williams [53, 54] to describe a discrete, conformal (combinatorial or circle packing) version of the earthquakes developed by Thurston and McMullen. This process involves opening a packing along the pattern of tangencies, shearing or grafting within the combinatorics and repacking to obtain a new surface. We then prove that if we have a compact hyperbolic Riemann surface R and a sequence of packable surfaces R_k converging to R with mesh going to zero, then we may approximate the action of a complex earthquake on R through combinatorial earthquakes on the sequence R_k . Further, we show that this sequence of approximations is convergent.

Having constructed approximation methods for earthquakes on hyperbolic Riemann surfaces, we note that the literature contains no reference to earthquake actions on Euclidean surfaces, such as tori. In Chapter V, we extend the work of Thurston

and McMullen by developing a theory of earthquakes on compact tori. Once we have these earthquake actions defined and we demonstrate that the action thus described is a transformation on the Teichmüller space of tori, we develop discrete conformal (combinatorial or circle packing) approximations for these Euclidean earthquakes similar to those described in Chapter IV, and show that these approximations are again convergent. Finally, we discuss earthquakes on the one-point Teichmüller spaces of the remaining compact surfaces, giving a complete characterization of earthquakes on compact Riemann surfaces.

The views expressed in this article are those of the author and do not reflect the official policy or position of the United States Air Force, Department of Defense, or the U.S. Government.

CHAPTER II
REAL AND COMPLEX EARTHQUAKES

2.1 Preliminaries and Definitions

We begin by describing the action of finite left earthquakes on the Poincaré unit disk. We use a definition for finite laminations of the unit disk, $\mathbb{D} = \{z \in \mathbb{C} : |z| < 1\}$, from the excellent exposition of finite left earthquakes by Gardiner and Lakic [23, 24] rather than the original definition for a more general lamination used by Thurston and others [21, 35, 49, 51, 54]. This definition is used here as it is more accessible to geometric and graphical examples, and, as we shall see, this more “accessible” finite definition suffices to demonstrate the results germane to this investigation.

Definition 2.1.1. *Let S be a subset of the unit circle consisting of $n \geq 4$ points. A **finite geodesic lamination** \mathcal{L} of the unit disk \mathbb{D} associated with S is a collection of $n - 3$ disjoint hyperbolic lines (geodesics) joining the points of S so that no line in \mathcal{L} joins adjacent points of S . More generally, a **geodesic lamination** of \mathbb{D} is a, not necessarily finite, collection of pairwise disjoint (in \mathbb{D}) hyperbolic geodesics.*

The collection of disjoint geodesics in a finite geodesic lamination is maximal in the sense that we may place at most $n - 3$ such geodesics. Note that a finite geodesic lamination divides \mathbb{D} into $n - 2$ disjoint hyperbolic triangles. Given such a lamination, we may place a weight (measure) on each geodesic.

Definition 2.1.2. *For a finite set $S \subset \partial\mathbb{D}$ with $n \geq 4$ points and a lamination $\mathcal{L} = \{L_i\}_{i=1}^{n-3}$ associated with S consisting of $n - 3$ disjoint hyperbolic geodesics, L_i , let σ be a non-negative measure on \mathcal{L} . That is, $\sigma : L_i \mapsto \mu_i \in [0, \infty)$, $i = 1, 2, \dots, n - 3$. We call the 2-tuple (\mathcal{L}, σ) a **finite measured geodesic lamination** on \mathbb{D} .*

In Figure 2.1 we see three examples of finite laminations of \mathbb{D} . These are clearly not the only finite geodesic laminations on the given number of points in each case. So, given that we can construct these laminations, we ask the natural question. “How

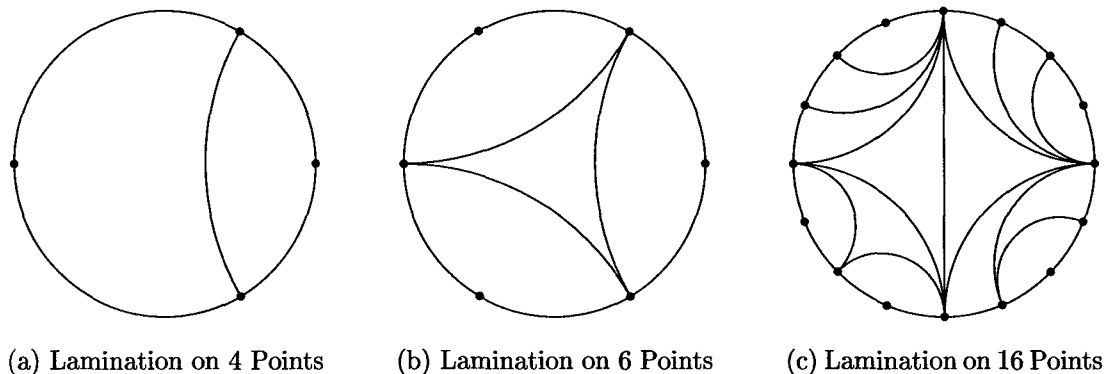


Figure 2.1: Examples of Finite Geodesic Laminations

many distinct laminations are there on a given set of points?” This question is essentially a restatement of Euler’s polygon division problem, Proposition 2.1.1. In placing the n points of S on the unit circle, we divide it into n subarcs; that is, we induce an n -sided polygon. Then, in constructing a lamination through the inclusion of $n - 3$ geodesics connecting points of S , we divide this polygon into three-sided figures or generalized triangles.

Proposition 2.1.1 (Euler’s Polygon Division). *A plane convex polygon of $n \geq 4$ sides can be divided into triangles by diagonals in*

$$C_{n-2} = \frac{1}{n-1} \binom{2n-4}{n-2} \quad (2.1.1)$$

distinct ways, where C_{n-2} is the Catalan number on $n - 2$.

This answer to the question of how many distinct finite laminations are possible on n points has been noted by Gardiner, Hu, and Lakic [23, 24]. See Dörrie [19] for the classic elementary proof of this result. The laminations thus generated will fall into classes of laminations that are unique up to rotations. In Figure 2.2 we see the topological classes of laminations possible on $n = 7$ vertices. Note that there are six distinct classes of lamination and seven laminations possible in each class, obtained by rotations of a representative of the class. Thus, we have $C_5 = 42$ total possible finite laminations on those seven vertices.

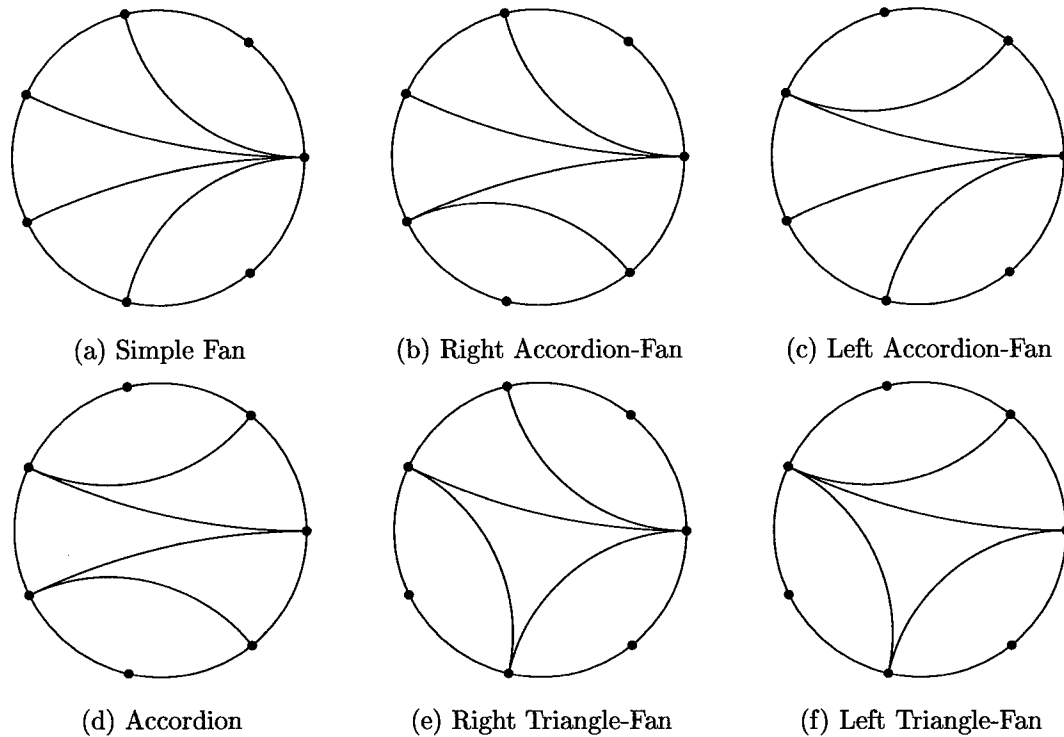


Figure 2.2: Topological Types of Finite Laminations on $n = 7$ Vertices

Definition 2.1.3. *Given a set $S \subset \partial\mathbb{D}$ with $n \geq 4$ points and a lamination \mathcal{L} , the dual graph for the lamination is called the **tree of triangles**.*

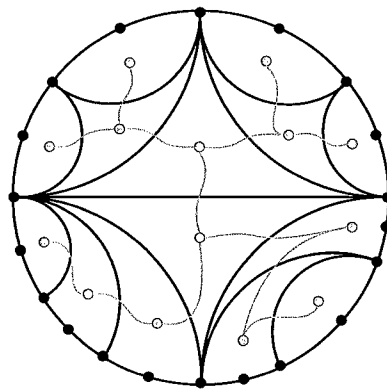


Figure 2.3: Finite Lamination with Dual Graph/Tree of Triangles

In Figure 2.3 we see an example of a finite geodesic lamination and the corresponding dual graph or tree of triangles. To call this dual graph a tree makes combinatorial

sense, since the standard definition of a combinatorial *tree* from graph theory is a connected graph that contains no subgraph isomorphic to a cycle [26]. The constraints placed upon the definition of a finite lamination guarantee that the dual graph will satisfy this definition.

Definition 2.1.4. *Let \mathcal{L} be a finite geodesic lamination of \mathbb{D} on a set S containing $n \geq 4$ points. If a triangle T induced by this lamination has two sides that are arcs of $\partial\mathbb{D}$, then T is called a **border triangle**.*

Again, this definition of a border triangle comes from Gardiner and Lakic [23, 24]. We have a useful, and necessary, result regarding these border triangles.

Proposition 2.1.2. *If \mathcal{L} is a finite geodesic lamination of \mathbb{D} on a set S containing $n \geq 4$ points, then \mathcal{L} contains at least two border triangles.*

2.2 Shearing Maps and Real Earthquakes

The following proposition is frequently used or implied in work on finite earthquakes since it allows an explicit description of a disk automorphism used to construct those earthquakes [23, 24]. Due to the relatively elementary nature of the proposition, however, no proofs appear in the literature. In the interest of a complete exploration of the properties and construction of finite left earthquakes, we prove it here.

Proposition 2.2.1. *Let $L \subset \mathbb{D}$ be a hyperbolic geodesic with endpoints $a, b \in \partial\mathbb{D}$, $a \neq b$; call a and b the left and right endpoints, respectively, of L . Let $\mu \geq 0$. The map*

$$C(z) = \frac{(ae^\mu - b)z + ab(1 - e^\mu)}{(e^\mu - 1)z + (a - be^\mu)} \quad (2.2.1)$$

is a disk automorphism with exactly two fixed points at $a, b \in \partial\mathbb{D}$ such that $C(L) = L$ and points on L are translated a fixed hyperbolic distance μ to the left along the geodesic (away from b and toward a).

Proof. To show that $C(z)$ has exactly two fixed points at $a, b \in \partial\mathbb{D}$ is a simple exercise in algebra; we simply solve the equation $C(z) = z$ for z . This immediately gives that

$C(z)$ has exactly two fixed points at $a, b \in \partial\mathbb{D}$. To prove that the transformation $C(z)$ is a disk automorphism, we recall [38] that a Möbius transformation

$$M(z) = \frac{\omega_1 z + \omega_2}{\omega_3 z + \omega_4}, \quad (2.2.2)$$

where $\omega_1\omega_4 - \omega_2\omega_3 \neq 0$, is a disk automorphism if and only if there exist constants $\alpha \in \mathbb{D}$ and $\theta \in \mathbb{R}$ such that

$$M(z) = e^{i\theta} \frac{z - \alpha}{1 - \bar{\alpha}z}. \quad (2.2.3)$$

Since $(ae^\mu - b)(a - be^\mu) - (e^\mu - 1)(ab(1 - e^\mu)) = e^\mu(a - b)^2 = 0$ if and only if $a = b$, $C(z)$ is indeed a Möbius transformation. We can express $C(z)$ as

$$\frac{(ae^\mu - b)z + ab(1 - e^\mu)}{(e^\mu - 1)z + (a - be^\mu)} = \left(\frac{ae^\mu - b}{a - be^\mu} \right) \left(\frac{z - \frac{ab(e^\mu - 1)}{ae^\mu - b}}{1 - \frac{1 - e^\mu}{a - be^\mu}z} \right). \quad (2.2.4)$$

Therefore, in order to show that $C(z)$ is a disk automorphism we need only verify that the right-hand side of Equation (2.2.4) satisfies the necessary criteria.

$$\left| \frac{ae^\mu - b}{a - be^\mu} \right| = \sqrt{\frac{(ae^\mu - b)(\overline{ae^\mu - b})}{(a - be^\mu)(\overline{a - be^\mu})}} = \sqrt{\frac{e^{2\mu} - 2e^\mu \operatorname{Re}(a\bar{b}) + 1}{e^{2\mu} - 2e^\mu \operatorname{Re}(a\bar{b}) + 1}} = 1 \quad (2.2.5)$$

$$\left| \frac{ab(e^\mu - 1)}{ae^\mu - b} \right| = \frac{e^\mu - 1}{|ae^\mu - b|} = \frac{e^\mu - 1}{\sqrt{e^{2\mu} - 2e^\mu \operatorname{Re}(a\bar{b}) + 1}} < \frac{e^\mu - 1}{\sqrt{e^{2\mu} - 2e^\mu + 1}} = 1 \quad (2.2.6)$$

$$\overline{\left(\frac{ab(e^\mu - 1)}{ae^\mu - b} \right)} = \frac{\bar{a}\bar{b}(e^\mu - 1)}{\bar{a}e^\mu - \bar{b}} = \frac{a\bar{a}(1 - e^\mu)}{a - \frac{\bar{a}\bar{b}}{b}e^\mu} = \frac{1 - e^\mu}{a - \frac{1}{b}e^\mu} = \frac{1 - e^\mu}{a - be^\mu} \quad (2.2.7)$$

Thus, $C(z)$ is a disk automorphism preserving the unit circle. Now, since $C(z)$ is a Möbius transformation, the image of a circle is a circle. Further, since $C(z)$ is analytic except for a single simple pole in $\mathbb{C} \setminus \overline{\mathbb{D}}$, $C(z)$ is conformal in a neighborhood of each fixed point. Thus, any circle Γ passing through a and b must have as its image under $C(z)$ a circle through a and b meeting the unit circle in the same angle as Γ . This is sufficient to ensure that $C(\Gamma) = \Gamma$ for any circle Γ through a and b ; in particular, $C(L) = L$. Finally, to show that points on L are translated a fixed hyperbolic distance μ to the left along the geodesic (away from b and toward a) recall

[2] that the translation length $\rho(z, M(z))$ of a hyperbolic Möbius transformation of the form given in Equation 2.2.2 is given by the relation

$$\frac{1}{2} |\operatorname{tr}(M)| = \cosh \left(\frac{1}{2} \rho(z, M(z)) \right), \quad (2.2.8)$$

where

$$[\operatorname{tr}(M)]^2 = \frac{(\omega_1 + \omega_4)^2}{\omega_1\omega_4 - \omega_2\omega_3}. \quad (2.2.9)$$

Applying this relation to $C(z)$ we have

$$\cosh \left(\frac{1}{2} \rho(z, M(z)) \right) = \frac{e^\mu + 1}{\sqrt{2e^\mu}}, \quad (2.2.10)$$

and this reduces to

$$\rho(z, M(z)) = 2 \cosh^{-1} \left(\frac{e^\mu + 1}{\sqrt{2e^\mu}} \right) = \ln(e^\mu) = \mu. \quad (2.2.11)$$

This completes the proof. \square

Now, given a finite measured geodesic lamination (\mathcal{L}, σ) on \mathbb{D} , we use the hyperbolic Möbius transformation described in Proposition 2.2.1 to construct a discontinuous map $h_\sigma : \mathbb{D} \rightarrow \mathbb{D}$ (which extends to a continuous map on $\partial\mathbb{D}$) with the following properties.

1. $h_\sigma(\mathbb{D}) = \mathbb{D}$.
2. $h : S \rightarrow \partial\mathbb{D}$ defined by $h = h_\sigma|_S$ is a cyclic and order-preserving.
3. On the interior of any triangle induced by \mathcal{L} , h_σ is a hyperbolic isometry.
4. If $L \in \mathcal{L}$ is the common hyperbolic geodesic between neighboring triangles T_1 and T_2 , then the points of T_2 move to the left relative to the points of T_1 .

We will call the map h_σ a **finite left earthquake** on \mathbb{D} . Note that if we fix the orientation of the geodesics as given in the finite lamination \mathcal{L} (i.e., we continue to consider left and right endpoints as above) and globally replace the positive weights in the measured geodesic lamination with negative weights, we obtain a **finite right**

earthquake. All of the results and characteristics pertaining to left earthquakes also hold for these right earthquakes. In addition, if we relax the restriction that all weights be either positive (to induce a finite left earthquake) or negative (to induce a finite right earthquake) and allow both positive and negative weights, we have legitimate finite earthquake actions at the expense of uniqueness results to be given in Proposition 2.2.2. This more general class of finite “mixed” earthquakes will be the class we consider in constructing discrete conformal approximations (circle packing approximations) for the earthquake actions in Chapter IV.

We now explicitly construct the map h_σ . Let T_1 be any triangle induced by the finite measured geodesic lamination (\mathcal{L}, σ) . At least one side of T_1 must be a geodesic L_1 in \mathcal{L} with left and right endpoints a_1 and b_1 , respectively, as seen from the interior of T_1 , and having weight $\sigma(L_1) = \mu_1$. Using these parameters, construct the hyperbolic Möbius transformation C_1 , called the comparison map, defined in (2.2.1), and apply C_1 “down the tree of triangles.” That is, apply C_1 to all edges (geodesics) and nodes (triangles) below T_1 in the tree. In a sense, we apply the discontinuous, piecewise function

$$\tilde{C}_1(z) = \begin{cases} C_1(z) & \text{if } z \text{ is “below” } T_1 \text{ on the tree of triangles} \\ z & \text{otherwise} \end{cases} \quad (2.2.12)$$

to the closed unit disk.

Now, choose any triangle adjacent to T_1 . (If T_1 has more than one neighbor in the tree of triangles, choose one, follow the construction down that branch of the tree, return to T_1 , and continue down any other branches associated with those additional neighbors.) Call this neighbor T_2 . If T_2 is a border triangle, then the earthquake action is complete on this branch of the tree of triangles. If T_2 is not a border triangle, then one side of T_2 is a geodesic L_2 not equal to L_1 . Note that this is not necessarily a geodesic in the lamination \mathcal{L} ; it may, rather, be the image of one such geodesic under the action of C_1 . Since C_1 is a Möbius transformation, though, we are assured that L_2 is, in fact, a geodesic, and we may repeat the construction above. As

with L_1, L_2 has left and right endpoints a_2 and b_2 , as seen from the interior of T_2 , and weight $\sigma(L_2) = \mu_2$; the weights on our geodesics are not changed by the application of prior comparison maps. Note that exactly one of a_2 and b_2 is equal to exactly one of a_1 and b_1 , while the other of a_2 and b_2 is equal to either $C_1(a_1)$ or $C_1(b_1)$. As before, construct the hyperbolic disk automorphism C_2 defined in (2.2.1) from these parameters, and apply C_2 down the tree of triangles. Continue in this manner down every branch of the tree of triangles until reaching a border triangle, at each step constructing comparison maps from the images points in S under applications of the preceding comparison maps. Thus, if there are n points in S , there will be $n - 3$ comparison maps, one for each geodesic in the lamination \mathcal{L} .

When the tree of triangles has been exhausted, we have a map h_σ from the closed unit disk to the closed unit disk such that the restriction of h_σ to $\partial\mathbb{D}$ is a cyclic, order-preserving homeomorphism from the unit circle to itself. Clearly the map h_σ is discontinuous on the interior of \mathbb{D} , but our main concern will be the action of h_σ on the $\partial\mathbb{D}$.

In Example 2.2.1 we construct an explicit finite left earthquake from a given finite measured geodesic lamination.

Example 2.2.1. Let $S = \{s_1, s_2, s_3, s_4, s_5\} = \{1, e^{i\frac{\pi}{4}}, i, e^{i\frac{3\pi}{4}}, -1\}$. Let $\mathcal{L} = \{L_1, L_2\}$, and let T_1, T_2 , and T_3 be as shown in Figure 2.4a. Define σ by $\sigma(L_1) = \ln(2)$ and $\sigma(L_2) = \ln(3)$. These values for the weights on L_1 and L_2 may appear arbitrary, but they were chosen for reasons of computational convenience. Notice that in Figure 2.4a an additional dashed circle is drawn, and we have included two additional points on the geodesics L_1 and L_2 . These objects have no direct bearing on the action of the finite left earthquake; they do serve, however, as a reference and to illustrate that action. Using the triangle labeled T_1 as the “top” of the tree of triangles, we construct the map

$$C_1(z) = \frac{(2-i)z - i}{z + (1-2i)} \tag{2.2.13}$$

from the left and right endpoints and the weight associated with L_1 . We apply this

disk automorphism in the piecewise manner described above; the result is shown in Figure 2.4b. Note that the shaded portion of the closed disk is unchanged, while points in the unshaded portion have been translated to the left as seen from T_1 .

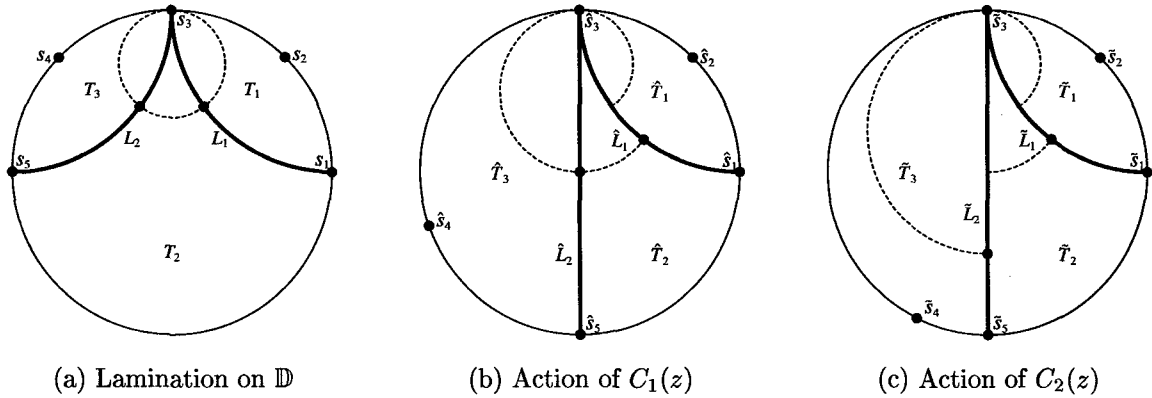


Figure 2.4: Finite Left Earthquake

Now, we construct a second map using the *new* endpoints of the geodesic L_2 . The explicit map thus constructed is given by

$$C_2(z) = \frac{-2iz - 1}{z - 2i}. \quad (2.2.14)$$

We apply this transformation down the tree of triangles to obtain the result shown in Figure 2.4c. Again, the shaded portion of the closed disk is unaffected by the piecewise application of the comparison map C_2 , and points in the unshaded region have been translated to the left relative to T_2 .

In Example 2.2.1 we illustrated the action of a simple finite left earthquake. In doing so, however, we chose a triangle from the lamination to act as the “first” in the tree of triangles induced by the lamination. Thereafter, the action of the earthquake was determined, but the requirement that we choose a starting point for the execution of a finite left earthquake raises the question of uniqueness. Would a different choice for the initial triangle result in a different earthquake? The answer is that the fundamental action of a finite left earthquake is independent of the choice of initial triangle. This result and an explanation of what is meant by “fundamental action” is given in Proposition 2.2.2.

Proposition 2.2.2. *The effect of a finite left earthquake on $S \subset \partial\mathbb{D}$ induced by a finite measured lamination (\mathcal{L}, σ) associated with S is uniquely determined, up to post-composition by a disk automorphism, by the measured lamination.*

For a proof of this result see the work of Gardiner, Hu, and Lakic [23, 24]. We do not include their proofs here since a concrete example of this property is perfectly illustrative and demonstrates beautifully the essential mechanism of their proofs, the explicit formulation of an appropriate Möbius transformation. As such, we rather include Example 2.2.2 as a illustration of the essentially unique determination of the action of a finite left earthquake on the points of S .

Example 2.2.2. Suppose that $S = \left\{ e^{\frac{2\pi(k-1)i}{16}} \right\}_{k=1}^{16}$, and let \mathcal{L} be the finite geodesic lamination associated with S as shown in Figure 2.5a. We have numbered the fourteen triangles induced by the lamination as T_1, T_2, \dots, T_{14} for reference, without necessarily implying any *a priori* decisions regarding the manner in which the finite left earthquake(s) are executed. Place a uniform weight of $\mu = \ln\left(\frac{3}{2}\right)$ on each geodesic of the lamination.

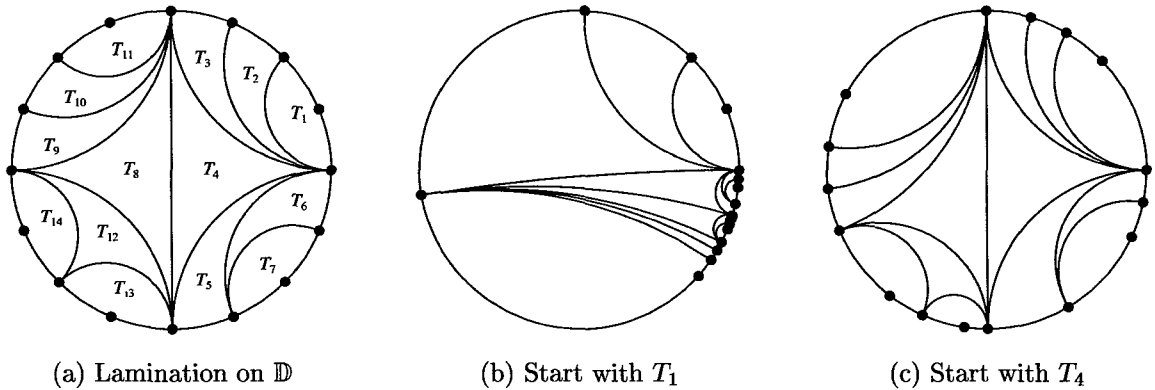


Figure 2.5: “Uniqueness” of Finite Left Earthquakes

In Figures 2.5b and 2.5c we show the action of the finite left earthquakes induced by placing T_1 and T_4 at the top of the tree of triangles, respectively. The action of the earthquake appears very different in each case. As Gardiner, Hu, and Lakic [23, 24] point out, however, if we construct a Möbius transformation by composing

the comparison maps associated with the unique sequence of geodesics separating the two triangles T_1 and T_4 as simple disk automorphisms rather than as piecewise functions, we obtain immediately the desired Möbius transformation. In this example, the desired maps are

$$C_1(z) \approx \frac{(.79 - .71i)z - (.35 + .35i)}{.5z - (.06 + 1.06i)}, \quad (2.2.15)$$

$$C_2(z) \approx \frac{(1.46 - i)z - (.02 + .5i)}{.5z + (.94 - 1.5i)}, \text{ and} \quad (2.2.16)$$

$$C_3(z) \approx \frac{(2.49 + .16i)z + (.49 + .08i)}{.5z + (2.48 + .24i)}. \quad (2.2.17)$$

Note that the Möbius transformations shown in (2.2.15), (2.2.16), and (2.2.17) are each created based on the images of their endpoints under the previous comparison maps applied in the application of the finite left earthquake induced by placing T_1 at the top of the tree of triangles. We do not use the endpoints of those geodesics in the original lamination, though any geodesic that forms a side of the initial triangle in the tree is always fixed by the action of a finite left earthquake, and we will thus use the initial values for the endpoints of those geodesics. Composing these three Möbius transformations we have

$$M(z) = (C_3 \circ C_2 \circ C_1)(z) \approx \frac{(1.95 - 5.57i)z - (4.28 + 1.19i)}{(2.64 - 3.57i)z - (4.97 + 3.19i)}. \quad (2.2.18)$$

A few routine calculations show that the image points of S under the two earthquake maps shown in Figure 2.5 differ only by post-composing the disk automorphism $M(z)$ given in (2.2.18) with the finite left earthquake action resulting from placing T_1 at the top of the tree of triangles. Note that should we wish to alter the order here, that is begin with the earthquake induced by placing T_4 at the top of the tree and post-compose by a Möbius transformation, then we do not simply reorder the maps C_1 , C_2 and C_3 ; rather, we must calculate a completely new set of maps based on the images of geodesics in that finite left earthquake.

Thus we have seen that given a finite measured geodesic lamination on \mathbb{D} , we can explicitly construct and describe the action of the (essentially) unique finite left

earthquake induced by that lamination. The next natural step is to ask whether or not given the action of a finite left earthquake we can determine the lamination which induced it. That is, given a finite set of points $S \subset \partial\mathbb{D}$ and their images under a finite left earthquake, can we find a finite measured geodesic lamination (\mathcal{L}, σ) that induces the given map on S ? The answer was given by Thurston [49].

Theorem 2.2.1 (Thurston’s Finite Earthquake Theorem). *Suppose that h is a given order-preserving map from a finite subset S of the unit circle into the unit circle. Then there exists a unique finite measured geodesic lamination (\mathcal{L}, σ) associated with S such that, up to post-composition by a Möbius transformation, h is the restriction to S of the finite left earthquake induced by (\mathcal{L}, σ) .*

Gardiner and Lakic [24] and Gardiner, Hu, and Lakic [23] give excellent proofs of this theorem. Their proofs are of particular value and interest in that they are especially constructive; their proofs suggest, inductively, a method to explicitly calculate the desired (unique) finite measured geodesic lamination given the sets S and $h(S)$. We do not describe the algorithm here, but we have implemented the algorithm in *Mathematica*, and the code used is provided in Appendix C.

Example 2.2.3. We take a “random” set of five points on the unit circle and another set of “random” points to act as their images under h . To say that the points used are random is somewhat misleading. In fact, the points in this example were chosen randomly within the constraints that we require that h is cyclic and order-preserving. The points used in this example are shown (to six significant figures) in Table 2.1. Using the *Mathematica* code given in Appendix C, we find the two appropriate geodesics and weights on each as shown in Figure 2.6.

Observe that any finite left earthquake on this finite measured geodesic lamination fixes the three points in the triangle placed at the top of the tree of triangles. Thus, the earthquake induced by the calculated lamination does not give the correct images in $h(s)$; in fact, no finite left earthquake can do so alone. The three points fixed by the earthquake point out a choice for the Möbius transformation which will map the

Table 2.1: The Points S and $h(S)$ Used to Compute a Lamination

	S		$h(S)$
s_1	$0.259205 + 0.965822i$	$h(s_1)$	$-0.485661 + 0.874147i$
s_2	$-0.294304 + 0.955712i$	$h(s_2)$	$-0.932807 + 0.360375i$
s_3	$-0.410866 - 0.911696i$	$h(s_3)$	$-0.171589 - 0.985169i$
s_4	$0.733058 - 0.680167i$	$h(s_4)$	$0.8436120 - 0.536941i$
s_5	$0.887984 - 0.459873i$	$h(s_5)$	$0.987219 - 0.159371i$

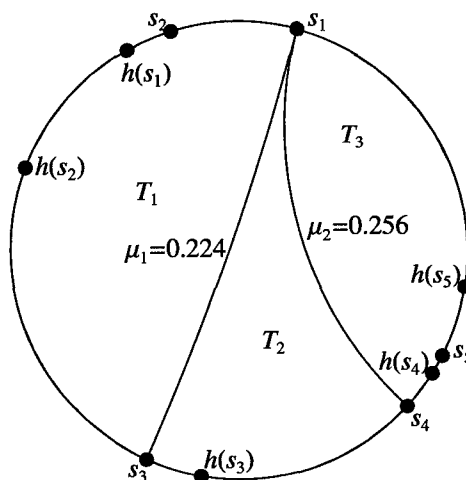


Figure 2.6: Measured Geodesic Lamination on S Given $h(s)$

points as desired. We calculate the unique Möbius transformation sending the three points in the first triangle to their images; in fact, the algorithm used to compute the lamination makes this the necessary choice of Möbius transformation. Thus, in this case we have three possible finite left earthquakes and three corresponding Möbius transformations given in (2.2.19), (2.2.20), and (2.2.21), corresponding to the finite left earthquakes induced by placing the triangles T_1 , T_2 , and T_3 , respectively, at the top of the tree of triangles, as shown in Figure 2.6.

$$M_1(z) = \frac{-(1.470 + 1.478i)z + (0.0489 + 0.496i)}{(0.472 - 1.580i)z - (1.950 + 0.738i)} \quad (2.2.19)$$

$$M_2(z) = \frac{(2.287 + 3.370i)z - (0.211 + 0.611i)}{(-0.628 + 0.152i)z + (3.571 + 1.957i)} \quad (2.2.20)$$

$$M_3(z) = \frac{(-0.807 + 0.640i)z + (0.107 - 0.189i)}{(0.173 - 0.132i)z - (0.524 - 0.886i)} \quad (2.2.21)$$

2.3 Grafting Maps and Complex Earthquakes

In geologic terms, earthquakes do not only involve lateral “shearing” along a fault line. Earthquakes may also involve a separation in which two tectonic plates move apart and new surface rises to fill the gap or a subduction in which one tectonic plate slides beneath another, and surface is lost. Just as we have maps which mimic a geologic shearing action, so we have maps which mimic these separation and subduction actions. We will consider these together as “grafting” actions which are positive or negative, respectively, in their behavior. Shearing and grafting maps, combined through composition, comprise what we will call **complex earthquakes**.

In this section we first revisit the shearing actions developed in Section 2.2, giving an alternate description through their local projective behavior. We then use this local projective structure to describe a new form of earthquake, a grafting action rather than a shearing action, introduced by McMullen [35], from whom much of the discussion below originates, and investigated by others [40, 41].

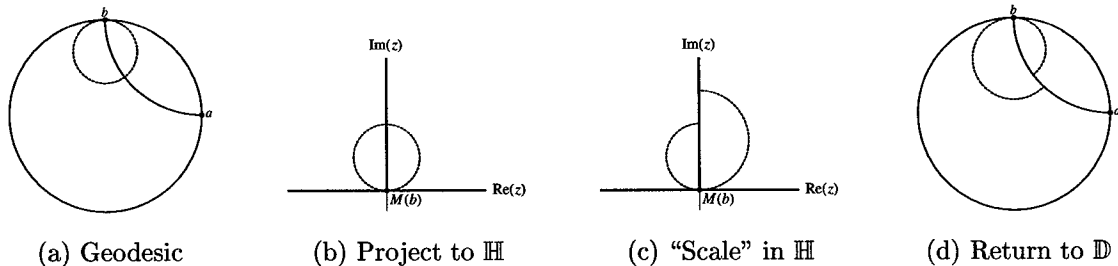


Figure 2.7: Local Projective Description of a Shearing Map

First, we revisit the action of a shearing map. Suppose $a, b \in \partial\mathbb{D}$ such that $a \neq b$, and $L \subset \mathbb{D}$ is the unique hyperbolic geodesic connecting a to b . Apply the Möbius transformation $M(z)$ which takes the unit disk \mathbb{D} to the upper half plane \mathbb{H} so that the image of L is the positive imaginary axis, the image of $\partial\mathbb{D}$ is the real axis,

$M(a) = \infty$, and $M(b) = 0$. Now, we apply a simple scaling, rz , where $r > 0$, in one quadrant of \mathbb{H} and the identity map on the other. Finally, we apply the inverse of the Möbius transformation M . As we can see in Figure 2.7, the effect of thus composing these maps is that of a hyperbolic shearing. In fact, should we perform this general composition and simplify the resulting function, we will find that the composition map is the comparison map given in (2.2.1).

Before we turn ourselves to the description of grafting maps and earthquakes, we need to recall some properties of the upper half plane \mathbb{H} as a model for the hyperbolic plane [2]. First, recall that the density we use to define a hyperbolic metric on $\mathbb{H} = \{z \in \mathbb{C} : \text{Im}(z) > 0\}$ is given by

$$\frac{1}{\text{Im}(z)}. \tag{2.3.1}$$

As a consequence, what we think of as a strip in a Euclidean sense may not be a strip in \mathbb{H} . Similarly, a strip in the upper half plane may not appear, to our Euclidean eye, as a strip at all. Specifically, we note that a Euclidean wedge in \mathbb{H} with its corner touching the real line, as shown in Figure 2.8, is a strip in the hyperbolic metric on \mathbb{H} , since the distance from edge to edge of the wedge is constant in the hyperbolic metric. The circular arcs shown in Figure 2.8 are all of equal length in the hyperbolic metric on \mathbb{H} .

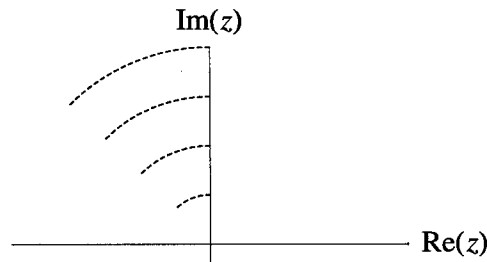


Figure 2.8: Hyperbolic Strip in \mathbb{H}

To define the grafting maps and imaginary earthquakes described by McMullen [35], we use the approach thus described. The difference is that rather than a piecewise scaling action given as multiplication by a real number, we apply a piecewise rotation

by some angle α given as multiplication by the complex number $e^{i\alpha}$. This piecewise rotation leaves a gap; we fill this gap by grafting in a hyperbolic cylinder, as shown in Figure 2.9c. Now, we can map the image of the upper half plane under the maps so far applied back to the upper half plane with a power map z^β , where

$$\beta = \frac{\pi}{\pi + \alpha}. \quad (2.3.2)$$

This map restores the real axis, and allows us to directly map the image region back to the unit disk and see the action of the earthquake on the disk. This is illustrated in Figure 2.9.

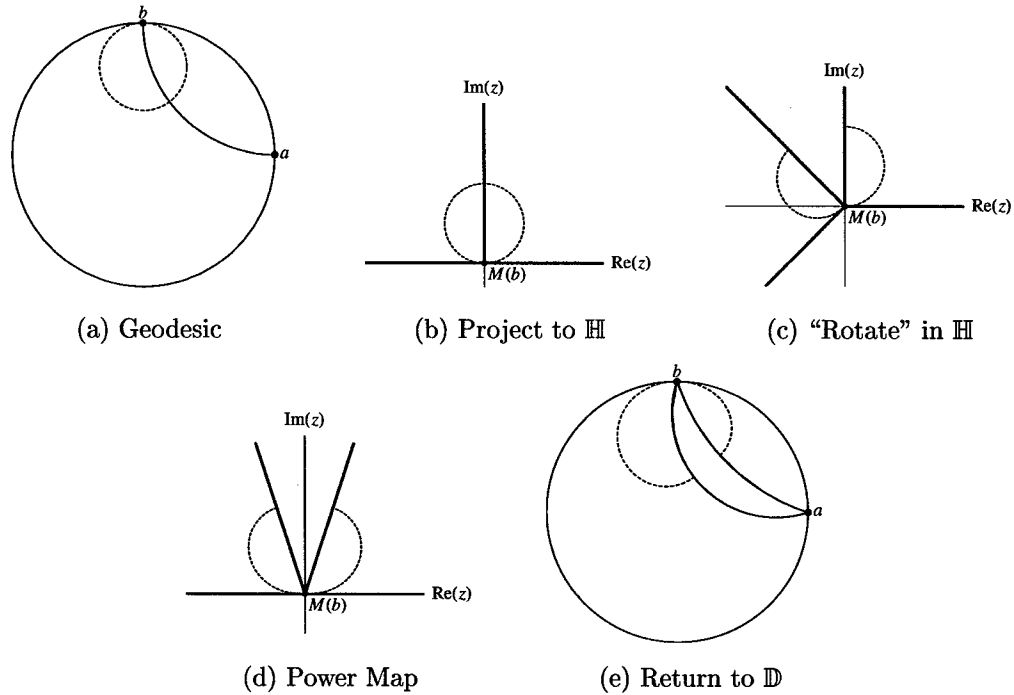


Figure 2.9: Local Projective Description of a Grafting Map

Note that in the application of the power map z^β , the arcs of circles and geodesics in Figure 2.9c are taken to curves which are no longer either geodesics or circles in Figure 2.9d. This is especially clear as we return to the unit disk \mathbb{D} in Figure 2.9e. The two curves connecting the points $a, b \in \partial\mathbb{D}$ are clearly not geodesics, and the two disjoint halves of the dashed reference circle shown in Figure 2.9a are no longer

circles. This failure to preserve geodesics and circles is key. Given a finite lamination of the disk, we may execute shearing maps on those geodesics sequentially since the maps involved are hyperbolic isometries and thus preserve the geodesics. In the case of grafting maps, however, we cannot perform the grafting actions in such a sequence, since the first application transforms the other geodesics of the lamination into curves which are no longer geodesics. To make the action of these grafting maps computable is the major motivation of this research.

Now we simply define a complex earthquake as the composition of shearing and grafting maps, applied in that order. Consider the shearing and grafting maps developed in Figure 2.7 and Figure 2.9. This composition is illustrated in Figure 2.10.

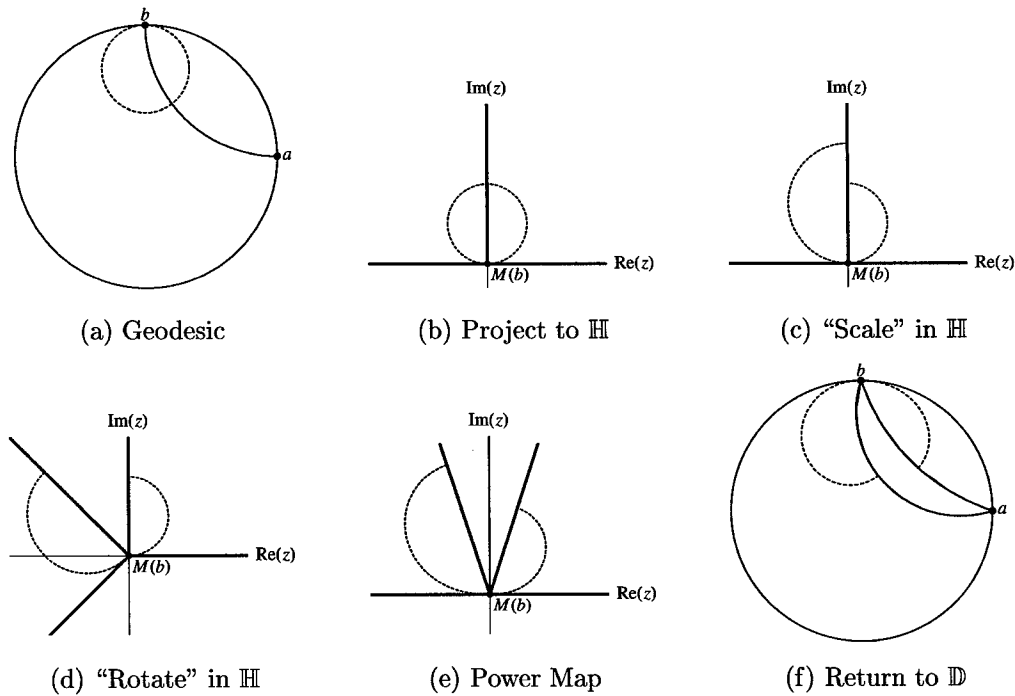


Figure 2.10: Local Projective Description of a Complex Earthquake Map

To call such a map a "complex" (as opposed to real or imaginary) earthquakes is quite natural. A real weight indicated a scaling, multiplication by a real number, and an imaginary weight indicated a rotation, multiplication by an imaginary number with unit modulus. Now, a complex weight $x + iy$ on the geodesic indicates that the

transformation applied to points in one quadrant of \mathbb{H} amounts to multiplication by a complex number $e^{x+iy} = e^x e^{iy}$. From this point, when we refer to measured geodesic laminations, we allow the measure to take complex values. We will, in the case of earthquakes on compact hyperbolic surfaces, restrict the imaginary part of complex measures to non-negative values. Otherwise, we place no *a priori* restriction on the weights in a measured geodesic lamination.

2.4 Riemann Surfaces and Teichmüller Theory

Our eventual goal is to define, discuss the properties of, and approximate the action of earthquakes, both grafting and shearing maps, on the Teichmüller spaces of Riemann surfaces. Here we review some of the important definitions and properties of Riemann surfaces and their Teichmüller spaces [14, 15, 24, 29, 30, 33, 48].

Definition 2.4.1. *A **Riemann surface** is a one complex-dimensional manifold with charts whose overlap maps are analytic. The maximal collection of charts on a Riemann surface is the **conformal structure** for that surface.*

The conformal structure for Riemann surface R (that is not the sphere) gives a convenient way of representing the surface in the complex plane \mathbb{C} , if R is Euclidean, or in the hyperbolic plane \mathbb{D} , if R is hyperbolic.

Definition 2.4.2. *Let R be a Riemann surface with fundamental group $\pi_1(R)$. A closed, connected subset P of \mathbb{C} (or \mathbb{D}) is called a **fundamental region** for R if*

1. *for each $z \in \mathbb{C}$ (or $z \in \mathbb{D}$) there exists at least one $\omega \in P$ such that $z = g(\omega)$, where $g \in \pi_1(R)$ (we say $z \sim \omega$); and*
2. *for every $\omega_1, \omega_2 \in P$, there does not exist an element $g \in \pi_1(R)$ such that $g(\omega_1) = \omega_2$.*

A torus T with fundamental group given by $\langle z+1, z+(1+i) \rangle$ has as a fundamental region the one shown in Figure 2.11. Here we have $z_i \sim \omega_2$ for each $i = 1, 2, 3, 4, 5$, and $\omega_1 \neq g(\omega_2)$ for any $g \in \langle z+1, z+(1+i) \rangle$.

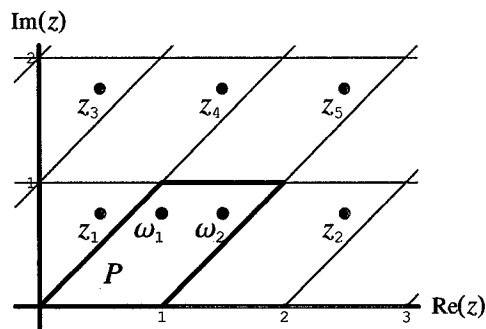


Figure 2.11: Fundamental Region for a Torus

Two Riemann surfaces R_1 and R_2 are said to be conformally equivalent if and only if there exists a conformal homeomorphism $f : R_1 \rightarrow R_2$. The set of equivalence classes of surfaces of the same topological type as R_1 under this equivalence relation is the **moduli space** of R_1 . The equivalence relation defined by conformal equivalence which determines the moduli space of R_1 is not adequate for our purposes. We will require that for surfaces R_1 and R_2 to be considered equivalent they must first be conformally equivalent (the same point in moduli space) and we will further require that the generators of their fundamental groups correspond.

Definition 2.4.3. Let R be a Riemann surface, and let Σ be a collection of canonical generators for $\pi_1(R)$. The collection Σ is called a **marking** for R . Two markings on R are equivalent if and only if they differ by the choice of their base point.

This now gives us a new equivalence relation which we use to describe another space of surfaces.

Definition 2.4.4. Two marked Riemann surfaces (R, Σ) and $(\hat{R}, \hat{\Sigma})$ are said to be equivalent if and only if there exists a conformal map $f : R \rightarrow \hat{R}$ for which the marking $f(\Sigma)$ is equivalent to $\hat{\Sigma}$. The **Teichmüller Space of R** is the set of these equivalence classes.

An illustration of how two surfaces may be conformally equivalent, and thus equivalent points in moduli space, while differing in their markings, making them different

points in Teichmüller space, is given in Figure 2.12. The tori (or fundamental regions and markings for the tori) T and \hat{T} shown in Figure 2.12a and Figure 2.12b, respectively, are conformally equivalent [30, 45]. As points in Teichmüller space, however, they differ in the choice of markings. The generator $z + 1$ corresponds to “going through” the hole in the torus once, and the generators $z + \omega$ and $z + \hat{\omega}$ each correspond to “going around” the hole in the torus once. Each of $z + \omega$ and $z + \hat{\omega}$, however, correspond to closed loops on the torus in different homotopy classes, since $z + \omega$ does not “go through” the hole and $z + \hat{\omega}$ “goes through” the hole once, as illustrated in Figure 2.12c.

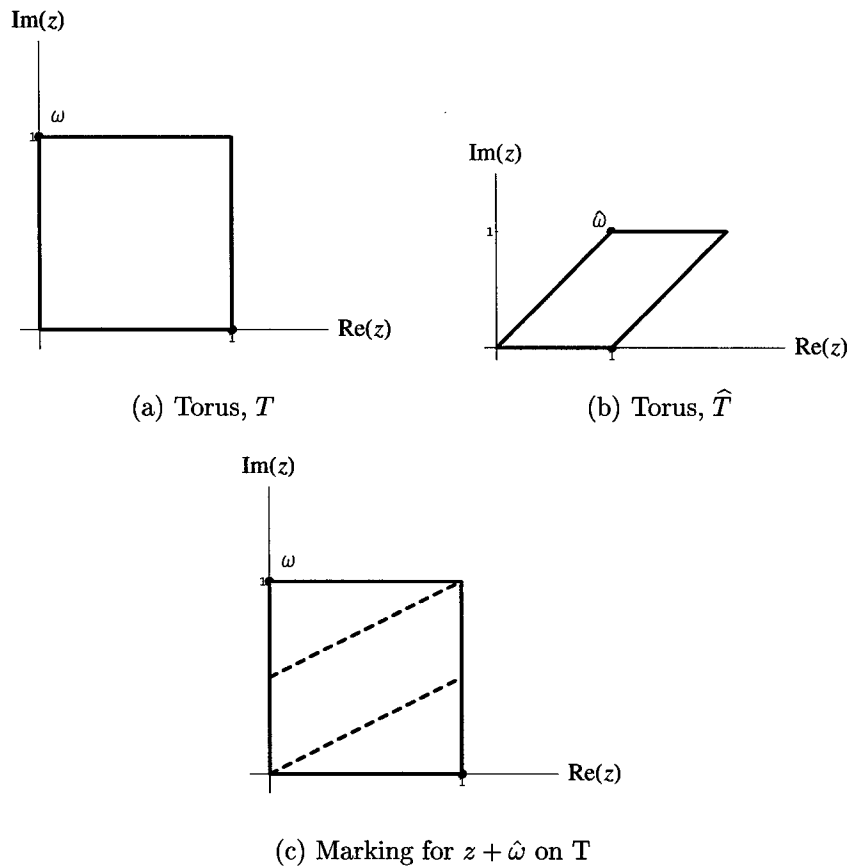


Figure 2.12: Moduli Space vs. Teichmüller Space

Another useful description of the Teichmüller space of a surface involves equivalence classes of maps from a reference or base surface. First we require a generalization

of the concept of a conformal map.

Definition 2.4.5. Let f be a continuous, orientation-preserving map from a domain $\Omega \subset \mathbb{C}$ into the complex plane, and fix $z_0 \in \Omega$. Define L_ε and ℓ_ε by

$$L_\varepsilon = \max \{|f(z) - f(z_0)| : |z - z_0| = \varepsilon\},$$

and

$$\ell_\varepsilon = \min \{|f(z) - f(z_0)| : |z - z_0| = \varepsilon\},$$

as shown in Figure 2.13. The **dilatation** of f at z_0 is

$$D_f(z_0) = \limsup_{\varepsilon \rightarrow 0} \left(\frac{L_\varepsilon}{\ell_\varepsilon} \right).$$

If $\sup_{z \in \Omega} \{D_f(z)\} \leq K$, then we say that $f : \Omega \rightarrow \mathbb{C}$ is **K -quasiconformal**.

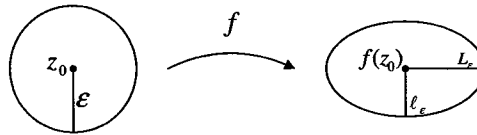


Figure 2.13: Action of a Map f with Dilatation $D_f(z_0) > 1$

Before moving on, we state as Lemma 2.4.1 a well-known and useful property of quasiconformal maps.

Lemma 2.4.1. If $f : \Omega \rightarrow \Delta$ is K_1 -quasiconformal and $g : \Delta \rightarrow \mathbb{C}$ is K_2 -quasiconformal, then their composition $g \circ f : \Omega \rightarrow \mathbb{C}$ is $(K_1)(K_2)$ -quasiconformal.

Note that the class of quasiconformal maps contains those maps which are conformal. Since a conformal map sends infinitesimal circles to infinitesimal circles [18], the limit of the ratios described in Definition 2.4.5 is 1. That is, a conformal map is 1-quasiconformal. Now, the class of quasiconformal maps allows us to define a new equivalence relation of the set of Riemann surfaces.

Definition 2.4.6. Quasiconformal maps f_1 and f_2 defined on a Riemann surface R are Teichmüller equivalent if and only if $f_2 \circ f_1^{-1}$ is homotopic to a conformal map.

Now, Proposition 2.4.1 establishes the equivalence of these two characterizations of points in Teichmüller space.

Proposition 2.4.1. *Fix a Riemann surface R , and suppose f_1 and f_2 are maps from R to Riemann surfaces R_1 and R_2 , respectively. R_1 and R_2 are equivalent in the Teichmüller space of R if and only if f_1 and f_2 are Teichmüller equivalent.*

Thus, points in the Teichmüller space of a Riemann surface R may be considered as either points or as functions. There is a natural metric on Teichmüller space as a function of how close to conformal (or how quasiconformal) maps which preserve the markings might be. If we fix a Riemann surface R and a marking Σ on R , the distance between two points $R_1 = f_1(R)$ and $R_2 = f_2(R)$ in the Teichmüller space of R is given by

$$d(R_1, R_2) = \frac{1}{2} \log(K^*),$$

where K^* is the infimum of the dilatation of $g_2 \circ g_1^{-1}$ where g_1 and g_2 are equivalent to f_1 and f_2 , respectively. This infimum is attained, by definition, by the unique **Teichmüller map**.

Remark 2.4.1. The Teichmüller maps on the space of tori are linear transformations. That is, the Teichmüller map from the torus T to the torus \hat{T} is affine.

2.5 Earthquakes on Surfaces

Now, we describe the action of earthquakes on compact Riemann surfaces with genus $g \geq 2$ (i.e., n -holed tori, $n \geq 2$) and their Teichmüller spaces. To do so, we must describe the constructions on these surfaces necessary to the earthquake actions. That is, we need measured geodesic laminations consisting of simple closed geodesics on the surface (though they will not necessarily be finite) and hyperbolic shearing and grafting maps.

Let R be a compact Riemann surface with genus $g \geq 2$, (i.e., R is a compact, hyperbolic Riemann surface). Just as in the disk, a finite geodesic lamination on R is a finite, pairwise disjoint collection of geodesics in the intrinsic metric on R , but

how do we define these geodesics? Well, we know that a geodesic in the Poincaré model of the hyperbolic plane is an arc of a circle which intersects $\partial\mathbb{D}$ orthogonally. Further, we know that for any hyperbolic Riemann surface, the universal cover for that surface is the hyperbolic plane where R is related to the universal cover through its conformal structure [14, 15, 29, 30, 45]. So, given a curve $\gamma \subset R$, γ is a geodesic on R if and only if γ lifts to a geodesic in the hyperbolic plane [45]. Thus, a lamination on the Riemann surface R lifts to a geodesic lamination in the hyperbolic plane, as illustrated in Figure 2.14, where we lift a geodesic lamination from a compact surface of genus 2 to the disk. The tiling is accomplished through the application of transition maps which, in this case, are hyperbolic isometries with axes perpendicular to corresponding sides of the fundamental region. The lift of geodesic segments are shown as dashed curves. For more detailed information on the structure of geodesics and laminations on surfaces, see the work of Bonahon [5, 7]. Take a collection of simple closed geodesics in R , and place on each geodesic in R a real (for shearing), imaginary (for grafting), or complex (for shearing then grafting) weight. This gives us a measured geodesic lamination (\mathcal{L}, σ) on R . Note, however, that while we began with a finite lamination on R , through the lift we obtain a countably infinite lamination on \mathbb{D} .

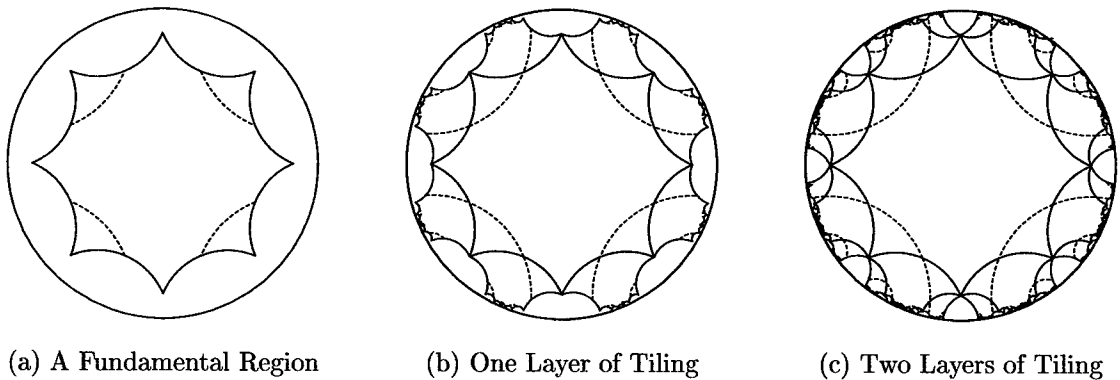
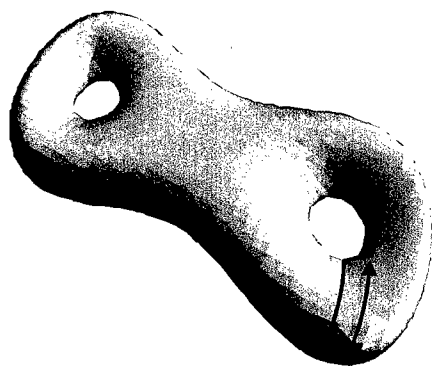


Figure 2.14: Geodesics on Surfaces Lift to Geodesics on \mathbb{D}

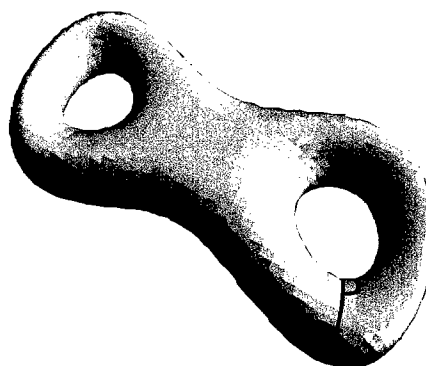
Now, we can define an earthquake on R in terms of the mechanisms already described in Section 2.2 and Section 2.3. A finite measured geodesic lamination on

R lifts to a measured geodesic lamination on \mathbb{D} comprising a sequence of geodesics $\{L_n\}_{n \in \mathbb{N}}$. To this point, we have only defined finite earthquakes on the disk, so how do we define an earthquake on a countably infinite set of geodesics? We do so just as a limit of finite earthquakes.

On the surface itself, this earthquake action has a nice geometric interpretation. Shearing along a geodesic in the disk induced by a geodesic on the hyperbolic Riemann surface R is equivalent to simply cutting open the surface along the geodesic, twisting by an amount prescribed by the weight on the geodesic, and gluing the two ends back together, as illustrated in Figure 2.15. Similarly, grafting along a geodesic in the disk induced by a geodesic on the surface R is equivalent to cutting open the surface along the geodesic, inserting a hyperbolic cylinder with a height prescribed by the weight on the geodesic, and gluing the ends together, as illustrated in Figure 2.16.



(a) Cut Along a Geodesic and Twist

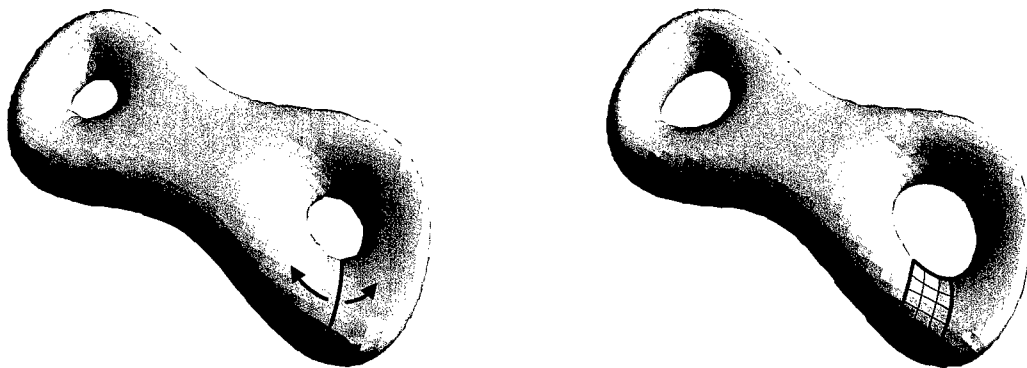


(b) Glue the Ends Together

Figure 2.15: Shearing Action on a Hyperbolic Surface

The question now becomes whether or not the resulting object is a Riemann surface. Are the objects illustrated in Figure 2.15b and Figure 2.16b Riemann surfaces? That is, is the action of an earthquake on a hyperbolic surface a map in the Teichmüller space of that surface?

To answer this question, we now turn to some technical definitions and results



(a) Cut Along a Geodesic and "Separate"

(b) Insert a Cylinder and Glue Together

Figure 2.16: Grafting Action on a Hyperbolic Surface

regarding the action of earthquakes, culminating, in Section 2.6, in the explicit construction of a conformal structure on the image of a Riemann surface under an earthquake (involving positive and negative shearing and positive grafting), demonstrating that earthquakes are maps in the Teichmüller space of the hyperbolic surface R .

Definition 2.5.1. *An orientation-preserving homeomorphism $\phi : \partial\mathbb{D} \rightarrow \partial\mathbb{D}$ is called a k -quasisymmetry if and only if*

$$\frac{1}{k} \leq \left| \frac{\varphi(e^{i(x+t)}) - \varphi(e^{ix})}{\varphi(e^{ix}) - \varphi(e^{i(x-t)})} \right| \leq k, \quad (2.5.1)$$

for all x and for all $t \in (-\frac{\pi}{2}, \frac{\pi}{2})$.

Quasisymmetries and quasiconformal maps are closely related in that the boundary values of a quasiconformal map give a quasisymmetry, and a quasisymmetry on $\partial\mathbb{D}$ induces a quasiconformal map on \mathbb{D} .

Definition 2.5.2. *Let (\mathcal{L}, σ) be a measured geodesic lamination, not necessarily finite, in \mathbb{D} ; say $\mathcal{L} = \{L_n\}$. Let I be a curve in \mathbb{D} with unit hyperbolic length such that $I \cap L_n$ contains no (non-empty) open subsets for every $L_n \in \mathcal{L}$, and I intersects any geodesic $L_n \in \mathcal{L}$ at most finitely many times. Define the quantity $m(I)$ as*

$$m(I) = \sum_{n \in \mathbb{N}_I} (k_n \bmod 2) |\sigma(L_n)|, \quad (2.5.2)$$

where $\mathbb{N}_I = \{n \in \mathbb{N} : I \cap L_n \neq \emptyset\}$ and k_n is the number of times I intersects L_n . The *transverse measure* of the measured geodesic lamination (\mathcal{L}, σ) is given by

$$m = \sup_{I \subset \mathbb{D}} \{m(I)\}. \quad (2.5.3)$$

In computing the quantity $m(I)$, the first time we cross a geodesic, we call that orientation positive, and for each successive crossing of the geodesic in that direction we add the associated weight. Crossing in the other direction is given a negative orientation, and such a crossing subtracts the associated weight from our measure. Thus, crossing a geodesic an odd number of times adds the associated weight to $m(I)$ and crossing an even number of times adds zero.

Now, we establish the intimate link between quasisymmetries and the transverse measure of a measured lamination on \mathbb{D} . One direction of Theorem 2.5.1 was proven by Thurston [49], and versions of the complete theorem have been proven independently by Gardiner, Hu, and Lakich [23], Gardiner and Lakic [24], Hu [25], and Šarić [40].

Theorem 2.5.1. *Let (\mathcal{L}, σ) be a measured geodesic lamination on \mathbb{D} and let E be the earthquake on \mathbb{D} induced by (\mathcal{L}, σ) . The continuous extension of E to $\partial\mathbb{D}$ is a quasisymmetry if and only if the transverse measure of (\mathcal{L}, σ) is bounded.*

Note that a single measured geodesic lamination may give rise to more than one earthquake, as illustrated in Example 2.2.2. As stated in Proposition 2.2.2, however, the extension of these earthquakes to their boundaries differ by a Möbius transformation. As a conformal map, this Möbius transformation has no effect of the nature, in terms of the quasisymmetry constant k , of the boundary quasisymmetry. That is, we are justified in speaking of the unique earthquake E in Theorem 2.5.1. Thus, an appropriately measured lamination gives an earthquake which induces a quasisymmetry on $\partial\mathbb{D}$. This quasisymmetry induces, in turn, a quasiconformal map on \mathbb{D} . Now, this is how we described the relationship between points in Teichmüller space.

2.6 A Conformal Structure on the Images of Hyperbolic Riemann Surfaces under Complex Earthquake Maps

Let R be a compact, hyperbolic Riemann surface, and suppose that we apply to R a finite complex earthquake E induced by a finite measured geodesic lamination (\mathcal{L}, σ) on R , where the lamination consists of n geodesics with complex weights $\sigma(L_i) = \mu_i + i\lambda_i$, $1 \leq i \leq n$, where $\mu_i \in \mathbb{R}$ and $\lambda_i \in \mathbb{R}$ such that $\lambda_i \geq 0$. This earthquake thus involves both shearing maps and (positive) grafting maps composed to form the complex earthquake.

Since R is a fixed Riemann surface, it has a conformal structure associated with it; say $\{\varphi_v\}_{v \in \Gamma}$ is the atlas for the conformal structure on R . Further, since each grafting map involves the insertion of a cylinder c_j , we have a conformal structure associated with each such cylinder such that the coordinate charts map c_j to subsets of a hyperbolic wedge. We do this by mapping first to an infinite strip and then applying the exponential map e^z to that strip. For each of c_j , $0 \leq j \leq m$, where m gives the number of geodesics in the lamination \mathcal{L} which have non-zero imaginary components for their weights, let $\{\phi_k^j\}_{k \in K}$ be the atlas associated with each such cylinder.

Define a pullback map P on \widehat{R} , the image of R under the complex earthquake E , so that the image of a point $r \in \widehat{R}$ under P is the unique point (on R or on one of the cylinders c_j) whose image under the complex earthquake E is r .

With this information we now define a conformal structure on the Riemann surface \widehat{R} . To define this conformal structure we need only describe a set of coordinate charts mapping open regions in the surface \widehat{R} to \mathbb{C} so that the transition maps associated with the coordinate charts are analytic. It is sufficient to construct for every point $r \in \widehat{R}$ a map from an open neighborhood $U \subset \widehat{R}$ to \mathbb{C} so that these maps satisfy the analyticity condition. It is sufficient to consider open sets of the following four classes.

1. U_A is the collection of all open sets $U_\alpha \subset \widehat{R}$ such that U_α does not intersect the

image under the earthquake E of any geodesic $L_i, 1 \leq i \leq n$, and is disjoint from every inserted cylinder $E(c_j), 1 \leq j \leq m$.

2. U_B is the collection of all open sets $U_\beta \subset \widehat{R}$ such that $U_\beta \subset E(c_j)$ for some $j, 1 \leq j \leq m$.
3. U_Γ is the collection of all open sets $U_\gamma \subset \widehat{R}$ such that U_γ intersects $E(L_i)$ for exactly one value $i, 1 \leq i \leq n$, where $\sigma(L_i) \in \mathbb{R}$, (i.e., the only map on that geodesic is a shearing operation).
4. U_Δ is the collection of all open sets $U_\delta \subset \widehat{R}$ such that U_δ intersects both $P^{-1}(R)$ and $E(c_j)$ for some $j, 1 \leq j \leq m$.

An illustration of representative sets from these classes is given in Figure 2.17.

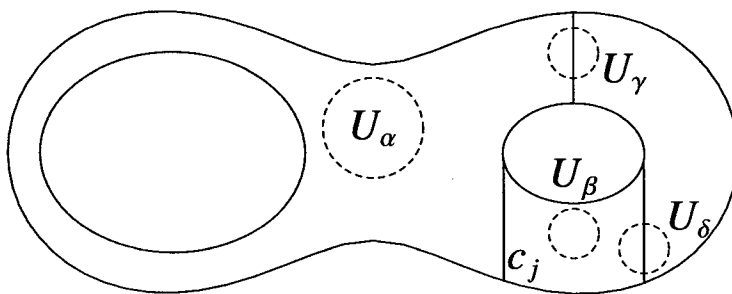


Figure 2.17: Open Sets to Define a Conformal Structure on \widehat{R}

Case I: Let $U_\alpha \in U_A$, and note that $P(U_\alpha)$ is an open set in R . From the conformal structure on R and corresponding to this open set $P(U_\alpha)$ we have a coordinate chart φ_α such that $\varphi_\alpha(P(U_\alpha)) \subset \mathbb{H} = \{z \in \mathbb{C} : \text{Im}(z) > 0\}$. We thus define a coordinate chart $\psi_\alpha : \widehat{R} \rightarrow \mathbb{C}$ on the open set U_α by $\psi_\alpha = \varphi_\alpha \circ P$. In this way we define a family of coordinate charts Ψ_A on \widehat{R} by $\Psi_A = \{\psi_\alpha\}_{\alpha \in A}$.

Case II: Let $U_\beta \in U_B$. In this case, $U_\beta \subset \text{Int}(E(c_j))$, for some $1 \leq j \leq m$, and the pullback map P takes this set to an open set on the finite cylinder c_j as shown in Figure 2.18a. Now, from the conformal structure on c_j we have a coordinate chart ϕ_β^j corresponding to $P(U_\beta)$ such that $\phi_\beta^j(P(U_\beta))$ is a subset of an infinite hyperbolic strip

of uniform width determined by the complex part of the weight on the appropriate geodesic in \mathcal{L} . We then have a grafting map g_β^j that opens the upper half-plane along the imaginary axis and glues in the hyperbolic strip as shown in Figure 2.18b. Following this with the conformal map M_j that transforms the result into the upper half-plane, we have a map $\psi_\beta : \widehat{R} \rightarrow \mathbb{C}$, shown in Figure 2.18c, on the open set U_β defined by $\psi_\beta = M_j \circ g_\beta^j \circ \phi_\beta^j \circ P$. In this way we define a family of coordinate charts Ψ_B on \widehat{R} by $\Psi_B = \{\psi_\beta\}_{\beta \in B}$.

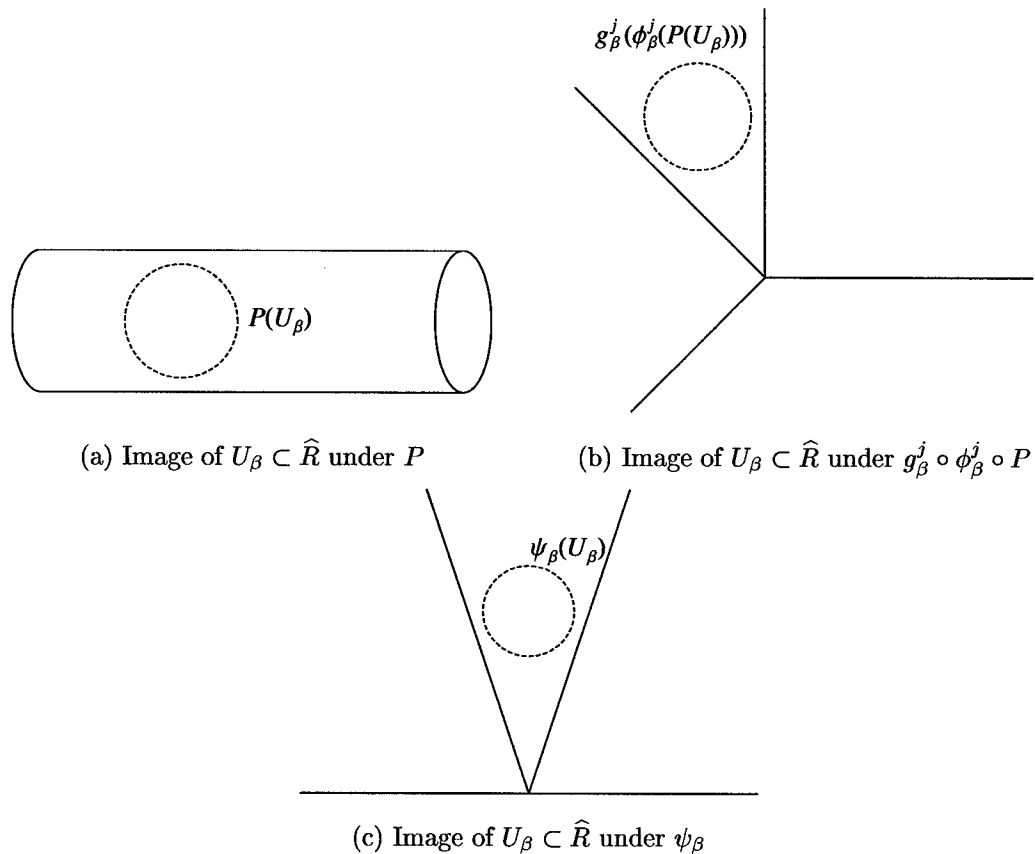


Figure 2.18: Construction of Coordinate Charts for Open Sets U_β

Case III: Let $U_\gamma \in U_\Gamma$, and note that $P(U_\gamma)$ is a set as shown in Figure 2.19a. From the conformal structure on R and corresponding to an open set containing $P(U_\gamma)$ we have a map φ_γ such that $\varphi_\gamma(P(U_\gamma)) \subset \mathbb{H}$. Now, we have disjoint sets that differ by the application of a hyperbolic shearing map, S_γ , along the vertical axis shown

in Figure 2.19b. We have thus defined a coordinate chart $\psi_\gamma : \widehat{R} \rightarrow \mathbb{C}$ on the open set U_γ by $\psi_\gamma = S_\gamma \circ \varphi_\gamma \circ P$. In this way, we define a family of coordinate charts $\Psi_\Gamma = \{\psi_\gamma\}_{\gamma \in \Gamma}$.

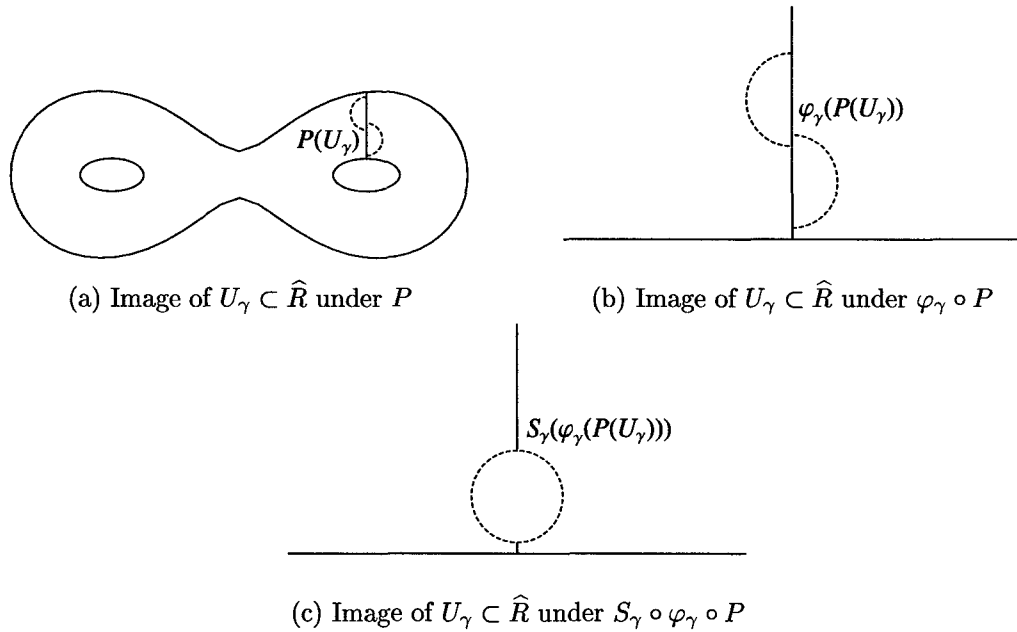


Figure 2.19: Construction of Coordinate Charts for Open Sets U_γ

Case IV: Let $U_\delta \in U_\Delta$, and note that $P(U_\delta)$ is divided between two distinct Riemann surfaces c_j , as shown in Figure 2.20a, and R , as shown in Figure 2.20b. To define coordinate charts on set of the form U_δ we define a pair of maps from these surfaces to the upper half-plane \mathbb{H} . Beginning with the cylinder, we have a map ϕ_δ^j such that $\phi_\delta^j(P(E(c_j) \cap U_\delta))$ is a hyperbolic strip of uniform width determined by the complex part of the weight on the appropriate geodesic in \mathcal{L} . We then have a grafting map g_δ^j that opens the upper half-plane along the imaginary axis and glues in the hyperbolic strip as shown in Figure 2.20c. At the same time, from the conformal structure on R we have a map φ_δ such that $\varphi_\delta(P((E(c_j))^c \cap U_\delta)) \subset \mathbb{H}$ as shown in Figure 2.20d. Applying the grafting map g_δ^j we put the pieces back together in \mathbb{C} . Now, we may need to shear along the hyperbolic geodesic whose image to this point is the imaginary axis in Figure 2.20d; this will depend upon whether or not the geodesic

associated with this grafting action had a weight with non-zero real part. Note that the shearing will take place along that portion of the set not intersecting $E(c_j)$, since we define complex earthquakes as the composition of shearing and grafting maps, in that order. Finally, we know that there exists a conformal map M_j that takes the opened half-plane to the upper half-plane.

$$\psi_\delta(r) = \begin{cases} M_j \circ g_\delta^j \circ \phi_\delta^j \circ P(r) & \text{if } r \in E(c_j) \cap U_\delta \subset \widehat{R} \\ M_j \circ S_\delta \circ g_\delta^j \circ \varphi_\delta \circ P(r) & \text{if } r \in (E(c_j))^C \cap U_\delta \subset \widehat{R} \end{cases} \quad (2.6.1)$$

This function now defines a map $\psi_\delta : \widehat{R} \rightarrow \mathbb{C}$ on the open set U_δ , as shown in Figure 2.20f. Taking all such functions over the set of possible sets $U_\delta \in U_\Delta$, we define a family of coordinate charts $\Psi_\Delta = \{\psi_\delta\}_{\delta \in \Delta}$.

Define a collection of open sets, $\widetilde{U} = U_A \cup U_B \cup U_\Gamma \cup U_\Delta$, and a collection of maps from \widehat{R} to \mathbb{C} , $\widetilde{\Psi} = \Psi_A \cup \Psi_B \cup \Psi_\Gamma \cup \Psi_\Delta$.

Proposition 2.6.1. *The transition maps in the structure $(\widetilde{U}, \widetilde{\Psi})$ are analytic.*

Proof. Let U be the intersection of two open sets in \widetilde{U} . We need only consider those intersections for which $U \in \mathbf{U}$. This gives four cases for the overlap region U in which we must verify the analyticity of the transition maps.

Case I: Suppose that $U \in U_A$. There are four possible ways in which U may occur as the result of intersections of sets in \widetilde{U} .

Case Ia: $U = U_{\alpha_1} \cap U_{\alpha_2}$, where $U_{\alpha_1}, U_{\alpha_2} \in U_A$. Associated with U_{α_1} and U_{α_2} we have coordinate charts $\psi_{\alpha_1}, \psi_{\alpha_2} \in \Psi_A$. Say $\psi_{\alpha_1} = \varphi_{\alpha_1} \circ P$ and $\psi_{\alpha_2} = \varphi_{\alpha_2} \circ P$. Now, consider the transition maps $\psi_{\alpha_2} \circ \psi_{\alpha_1}^{-1}$ and $\psi_{\alpha_1} \circ \psi_{\alpha_2}^{-1}$.

$$\begin{aligned} \psi_{\alpha_2} \circ \psi_{\alpha_1}^{-1} &= (\varphi_{\alpha_2} \circ P) \circ (\varphi_{\alpha_1} \circ P)^{-1} \\ &= \varphi_{\alpha_2} \circ P \circ P^{-1} \circ \varphi_{\alpha_1}^{-1} \\ &= \varphi_{\alpha_2} \circ \varphi_{\alpha_1}^{-1} \end{aligned}$$

Thus, $\psi_{\alpha_2} \circ \psi_{\alpha_1}^{-1} : \mathbb{C} \rightarrow \mathbb{C}$ is analytic, since $\varphi_{\alpha_i}, i = 1, 2$, were taken from the conformal structure on R , making $\varphi_{\alpha_2} \circ \varphi_{\alpha_1}^{-1}$ analytic. Similarly, $\varphi_{\alpha_1} \circ \varphi_{\alpha_2}^{-1}$ is analytic.

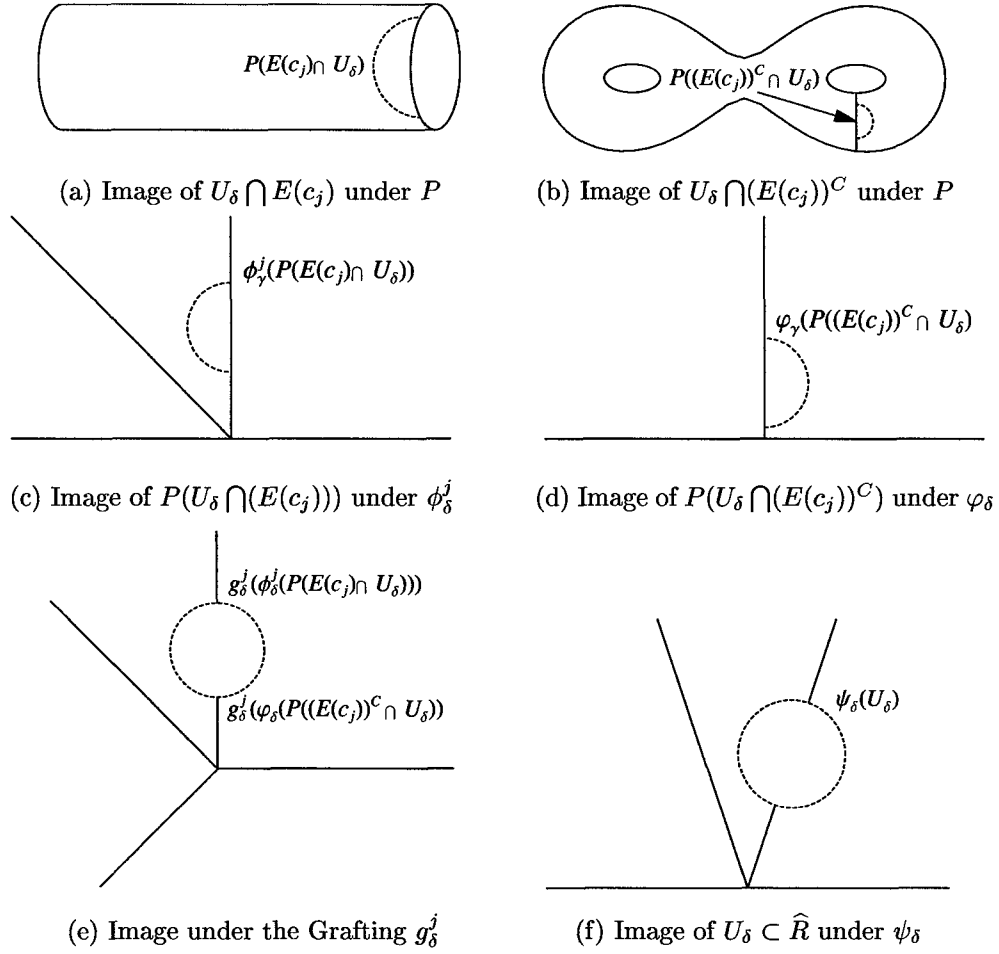


Figure 2.20: Construction of Coordinate Charts for Open Sets U_δ

Case Ib: $U = U_\alpha \cap U_\gamma$, where $U_\alpha \in U_A$ and $U_\gamma \in U_\Gamma$. Associated with U_α and U_γ we have coordinate charts $\psi_\alpha \in \Psi_A$ and $\psi_\gamma \in \Psi_\Gamma$, respectively. Say $\psi_\alpha = \varphi_\alpha \circ P$ and $\psi_\gamma = S_\gamma \circ \varphi_\gamma \circ P$. Now, consider the transition maps $\psi_\alpha \circ \psi_\gamma^{-1}$ and $\psi_\gamma \circ \psi_\alpha^{-1}$.

$$\begin{aligned}
 \psi_\alpha \circ \psi_\gamma^{-1} &= (\varphi_\alpha \circ P) \circ (S_\gamma \circ \varphi_\gamma \circ P)^{-1} \\
 &= \varphi_\alpha \circ P \circ P^{-1} \circ \varphi_\gamma^{-1} \circ S_\gamma^{-1} \\
 &= \varphi_\alpha \circ \varphi_\gamma^{-1} \circ S_\gamma^{-1}
 \end{aligned}$$

Note that the transition map $\psi_\alpha \circ \psi_\gamma^{-1}$ is defined only on the set U . Since the set U does not itself intersect the geodesic associated with the shearing map S_γ , on U the shearing map acts as either the identity map or a hyperbolic Möbius transformation.

In either case, the action of S_γ is (locally) analytic. Next, we note that since φ_α and φ_γ are taken from the conformal structure on R , $\varphi_\alpha \circ \varphi_\gamma^{-1}$ is analytic, where defined. Thus, the transition map $\psi_\alpha \circ \psi_\gamma^{-1}$ is the composition of analytic maps, and is therefore analytic. Similarly, $\psi_\gamma \circ \psi_\alpha^{-1}$ is also analytic.

Case Ic: $U = U_\alpha \cap U_\delta$, where $U_\alpha \in U_A$ and $U_\delta \in U_\Delta$. Associated with each of U_α and U_δ we have coordinate charts $\psi_\alpha \in \Psi_A$ and $\psi_\delta \in \Psi_\Delta$, respectively. Say $\psi_\alpha = \varphi_\alpha \circ P$ and ψ_δ of the form given in (2.6.1). We note that since U does not intersect the geodesic associated with the grafting of the cylinder, for every $r \in U$ we have $r \in (E(c_j))^c \cap U_\delta \subset \widehat{R}$, where j denotes the cylinder associated with the grafting. Thus, on U we have $\psi_\delta = M_j \circ S_\delta \circ g_\delta^j \circ \varphi_\delta \circ P$. Now, consider the transition maps $\psi_\alpha \circ \psi_\delta^{-1}$ and $\psi_\delta \circ \psi_\alpha^{-1}$.

$$\begin{aligned} \psi_\alpha \circ \psi_\delta^{-1} &= (\varphi_\alpha \circ P) \circ (M_j \circ S_\delta \circ g_\delta^j \circ \varphi_\delta \circ P)^{-1} \\ &= \varphi_\alpha \circ P \circ P^{-1} \circ \varphi_\delta^{-1} \circ (g_\delta^j)^{-1} \circ S_\delta^{-1} \circ M_j^{-1} \\ &= \varphi_\alpha \circ \varphi_\delta^{-1} \circ (g_\delta^j)^{-1} \circ S_\delta^{-1} \circ M_j^{-1} \end{aligned}$$

Note that we define the transition map $\psi_\alpha \circ \psi_\delta^{-1}$ only on the overlap region U . Since the set U does not itself intersect the inserted cylinder (or the boundary along which we weld the cylinder to the Riemann surface R via the grafting map $(g_\delta^j)^{-1}$), on U the inverse of the grafting map acts as either the identity map or as multiplication by an exponential map. In either case, the action of $(g_\delta^j)^{-1}$ is (locally) analytic. For the same reason, on U we have that S_δ^{-1} acts as either the identity map or a hyperbolic Möbius transformation, and is therefore (locally) analytic. Next, we note that since the maps φ_α and φ_δ were borrowed from the conformal structure on the original Riemann surface R , $\varphi_\alpha \circ \varphi_\delta^{-1}$ is analytic, where defined. Finally, the map M was chosen as the conformal map taking the region shown in Figure 2.20e to the upper half plane. Thus, the transition map $\psi_\alpha \circ \psi_\delta^{-1}$ is the composition of analytic maps on U , and is therefore analytic. Similarly, $\psi_\delta \circ \psi_\alpha^{-1}$ is also analytic.

Case Id: $U = U_\gamma \cap U_\delta$, where $U_\gamma \in U_\Gamma$ and $U_\delta \in U_\Delta$. Associated with each of U_γ and U_δ we have coordinate charts $\psi_\gamma \in \Psi_\Gamma$ and $\psi_\delta \in \Psi_\Delta$, respectively. Say

$\psi_\gamma = S_\gamma \circ \varphi_\gamma \circ P$ and ψ_δ of the form given in (2.6.1). We note that since U intersects neither the geodesic associated with the grafting of the cylinder nor the geodesic associated with the simple shearing, for every $r \in U$ we have $r \in (E(c_j))^c \cap U_\delta \subset \widehat{R}$, where j denotes the cylinder associated with the grafting. Thus, on U we have $\psi_\delta = M_j \circ S_\delta \circ g_\delta^j \circ \varphi_\delta \circ P$. Now, consider the transition maps $\psi_\gamma \circ \psi_\delta^{-1}$ and $\psi_\delta \circ \psi_\gamma^{-1}$.

$$\begin{aligned} \psi_\gamma \circ \psi_\delta^{-1} &= (S_\gamma \circ \varphi_\gamma \circ P) \circ (M_j \circ S_\delta \circ g_\delta^j \circ \varphi_\delta \circ P)^{-1} \\ &= S_\gamma \circ \varphi_\gamma \circ P \circ P^{-1} \circ \varphi_\delta^{-1} \circ (g_\delta^j)^{-1} \circ S_\delta^{-1} \circ M_j^{-1} \\ &= S_\gamma \circ \varphi_\gamma \circ \varphi_\delta^{-1} \circ (g_\delta^j)^{-1} \circ S_\delta^{-1} \circ M_j^{-1} \end{aligned}$$

Note that we define the transition map $\psi_\gamma \circ \psi_\delta^{-1}$ only on the overlap region U . Since the set U does not itself intersect the inserted cylinder (or the boundary along which we weld the cylinder to the Riemann surface R via the grafting map $(g_\delta^j)^{-1}$), on U the inverse of the grafting map acts as either the identity map or as multiplication by an exponential map. In either case, the action of $(g_\delta^j)^{-1}$ is (locally) analytic. For the same reason, on U we have that S_δ^{-1} and S_γ each act as either identity maps or hyperbolic Möbius transformations; they are thus (locally) analytic. Next, we note that since the maps φ_γ and φ_δ were borrowed from the conformal structure on the original Riemann surface R , $\varphi_\alpha \circ \varphi_\delta^{-1}$ is analytic, where defined. Finally, the map M was chosen as the conformal map taking the region shown in Figure 2.20e to the upper half plane. Thus, the transition map $\psi_\gamma \circ \psi_\delta^{-1}$ is the composition of analytic maps on U , and is therefore analytic. Similarly, $\psi_\delta \circ \psi_\alpha^{-1}$ is also analytic.

Case II: Suppose that $U \in U_B$. There are two ways in which U may occur as the result of intersections of sets in \widetilde{U} .

Case IIa: $U = U_{\beta_1} \cap U_{\beta_2}$, where $U_{\beta_1}, U_{\beta_2} \in U_B$. Associated with U_{β_1} and U_{β_2} we have coordinate charts $\psi_{\beta_1}, \psi_{\beta_2} \in \Psi_B$. Say $\psi_{\beta_1} = M_j \circ g_{\beta_1}^j \circ \phi_{\beta_1}^j \circ P$ and $\psi_{\beta_2} = M_j \circ g_{\beta_2}^j \circ \phi_{\beta_2}^j \circ P$. Note that since both U_{β_1} and U_{β_2} must necessarily lie in the same finite inserted cylinder, the grafting maps $g_{\beta_1}^j$ and $g_{\beta_2}^j$, are the same map. Now,

consider the transition maps $\psi_{\beta_2} \circ \psi_{\beta_1}^{-1}$ and $\psi_{\beta_1} \circ \psi_{\beta_2}^{-1}$.

$$\begin{aligned}
\psi_{\beta_2} \circ \psi_{\beta_1}^{-1} &= (M_j \circ g_{\beta_2}^j \circ \phi_{\beta_2}^j \circ P) \circ (M_j \circ g_{\beta_1}^j \circ \phi_{\beta_1}^j \circ P)^{-1} \\
&= M_j \circ g_{\beta_2}^j \circ \phi_{\beta_2}^j \circ P \circ P^{-1} \circ (\phi_{\beta_1}^j)^{-1} \circ (g_{\beta_1}^j)^{-1} \circ M_j^{-1} \\
&= M_j \circ g_{\beta_2}^j \circ \phi_{\beta_2}^j \circ (\phi_{\beta_1}^j)^{-1} \circ (g_{\beta_1}^j)^{-1} \circ M_j^{-1} \\
&= M_j \circ g_{\beta_2}^j \circ \left(\phi_{\beta_2}^j \circ (\phi_{\beta_1}^j)^{-1} \right) \circ (g_{\beta_1}^j)^{-1} \circ M_j^{-1}
\end{aligned}$$

Now, notice that the maps M_j and M_j^{-1} are analytic. Next, notice that the maps $g_{\beta_1}^j$ and $g_{\beta_2}^j$ have no effect on the analyticity of the maps involved, since both U_{β_1} and U_{β_2} are on the interior of the cylinder $E(c_j)$. These maps merely indicate that we consider the infinite hyperbolic strip in a different context. The action affecting analyticity takes place in the conformal structure on the cylinder c_j , and $\phi_{\beta_2}^j \circ (\phi_{\beta_1}^j)^{-1}$ is analytic since these maps were taken from this conformal structure. Thus, as a composition of analytic maps, $\psi_{\beta_2} \circ \psi_{\beta_1}^{-1}$ is analytic. Similarly, $\psi_{\beta_1} \circ \psi_{\beta_2}^{-1}$ is analytic.

Case IIb: $U = U_\beta \cap U_\delta$, where $U_\beta \in U_B$ and $U_\delta \in U_\Delta$. Associated with each of U_β and U_δ we have coordinate charts $\psi_\beta \in \Psi_B$ and $\psi_\delta \in \Psi_\Delta$, respectively. Say $\psi_\beta = M_j \circ g_\beta^j \circ \phi_\beta^j \circ P$ and ψ_δ of the form given in (2.6.1). Note that since U does not intersect any geodesic associated with the grafting of the cylinder, for every $r \in U$ we have $r \in E(c_j) \cap U_\delta \subset \widehat{R}$, where j denotes the cylinder associated with the grafting. Thus, on U we have $\psi_\delta = M_j \circ g_\delta^j \circ \phi_\delta^j \circ P$. Now, consider the transition maps $\psi_\beta \circ \psi_\delta^{-1}$ and $\psi_\delta \circ \psi_\beta^{-1}$.

$$\psi_\beta \circ \psi_\delta^{-1} = (M_j \circ g_\beta^j \circ \phi_\beta^j \circ P) \circ (M_j \circ g_\delta^j \circ \phi_\delta^j \circ P)^{-1}$$

This case, thus reduces to Case IIa, and the transition maps $\psi_\beta \circ \psi_\delta^{-1}$ and $\psi_\delta \circ \psi_\beta^{-1}$ are analytic.

Case III: Suppose that $U \in U_\Gamma$. Then, $U = U_{\gamma_1} \cap U_{\gamma_2}$, where $U_{\gamma_1}, U_{\gamma_2} \in U_\Gamma$. Associated with each of U_{γ_1} and U_{γ_2} we have coordinate charts $\psi_{\gamma_1}, \psi_{\gamma_2} \in \Psi_\Gamma$. Say $\psi_{\gamma_1} = S_\gamma \circ \varphi_{\gamma_1} \circ P$ and $\psi_{\gamma_2} = S_\gamma \circ \varphi_{\gamma_2} \circ P$. Note that the earthquake (shearing) map in each of these coordinate charts is the same, since this earthquake is defined by intersection with a particular weighted geodesic rather than a particular set U . Now,

consider the transition maps $\psi_{\gamma_2} \circ \psi_{\gamma_1}^{-1}$ and $\psi_{\gamma_1} \circ \psi_{\gamma_2}^{-1}$.

$$\begin{aligned} \psi_{\gamma_2} \circ \psi_{\gamma_1}^{-1} &= (S_\gamma \circ \varphi_{\gamma_2} \circ P) \circ (S_\gamma \circ \varphi_{\gamma_1} \circ P)^{-1} \\ &= S_\gamma \circ \varphi_{\gamma_2} \circ P \circ P^{-1} \circ \varphi_{\gamma_1}^{-1} \circ S_\gamma^{-1} \\ &= S_\gamma \circ \varphi_{\gamma_2} \circ \varphi_{\gamma_1}^{-1} \circ S_\gamma^{-1} \end{aligned}$$

The action of the transition map here reduces to a hyperbolic isometry, and is thus analytic.

Case IV: Suppose that $U \in U_\Delta$. $U = U_{\delta_1} \cap U_{\delta_2}$, where $U_{\delta_1}, U_{\delta_2} \in U_\Delta$. Associated with each of U_{δ_1} and U_{δ_2} we have coordinate charts $\psi_{\delta_1}, \psi_{\delta_2} \in \Psi_\Delta$. Say ψ_{δ_1} and ψ_{δ_2} are each of the form given in (2.6.1). The set U can now be decomposed into three disjoint sets, $U = U_\alpha \cup L \cup U_\beta$, where $U_\alpha \in U_A$, $U_\beta \in U_B$, and $L = \partial U_\alpha \cap \partial U_\beta$, as shown in Figure 2.21. We have already shown that the transition maps $\psi_{\delta_1} \circ \psi_{\delta_2}^{-1}$ and $\psi_{\delta_2} \circ \psi_{\delta_1}^{-1}$ are analytic on each of the sets U_α and U_β . These transition maps, though, are also clearly continuous on all of U . Since the image of $L \subset U$ in the plane has measure zero, any map which is K -quasiconformal on the image of $U \setminus L$ is also K -quasiconformal on L [33]; special cases of this result are often given in texts on complex analysis [18]. Thus, since the transition maps are analytic (1-quasiconformal) on the images of U_α and U_β , the transition maps are analytic on all of U .

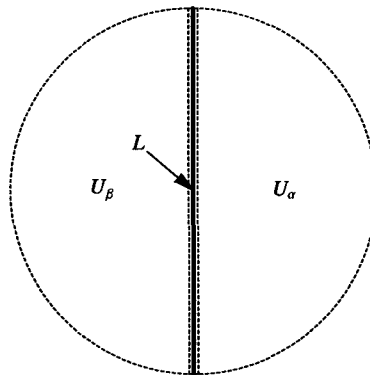


Figure 2.21: Partition of U into U_α , U_β , and L

Thus, the transition maps in the structure $(\tilde{U}, \tilde{\Psi})$ are analytic. \square

Since the structure defined above describes a cover for the surface \widehat{R} and a set of maps on that cover so that the transition maps are analytic, we have defined a sufficient conformal structure on the surface \widehat{R} ; we simply include any other sets and maps compatible with this structure.

CHAPTER III

CIRCLE PACKING

3.1 Preliminaries and Definitions

A circle packing is a configuration of circle with a prescribed pattern of tangencies. William Thurston conjectured in 1985 that these circle packings might be used to approximate the action of conformal maps [50]. These circle packings have since been widely studied, with applications in many different areas of mathematics. We begin here with some basic definitions and a general discussion of circle packing. Several excellent resources are available with much greater detail [20, 42, 45, 46].

Definition 3.1.1. *A vertex is called a **0-simplex**. An edge is called a **1-simplex**. A face is called a **2-simplex**.*

We use these simplexes to describe a combinatorial object called a **2-complex**.

Definition 3.1.2. *A **simplicial 2-complex** \mathcal{K} is a topological space represented as a countable (possibly finite) union of 0-, 1-, and 2-simplexes with the following properties.*

1. *Every face of a simplex in \mathcal{K} is itself a simplex in \mathcal{K} .*
2. *2-simplexes of \mathcal{K} intersect either in the empty set or in a simplex of \mathcal{K} .*
3. *No 0-simplex (vertex) of \mathcal{K} is in more than a finite number of simplexes of \mathcal{K} .*
4. *\mathcal{K} is connected.*

We will consider a subset of all possible simplicial 2-complexes in which the 2-simplexes (faces) are combinatorial triangles.

Definition 3.1.3. *A **bounded degree abstract triangulation** \mathcal{K} is an abstract simplicial 2-complex which triangulates an orientable topological surface such that*

1. the set of interior vertices (vertices such that every incident edge belongs to two faces) is non-empty and edge-connected;
2. no interior edge (an edge belonging to two faces) in \mathcal{K} has both vertices on the boundary;
3. no vertex in \mathcal{K} belongs to more than two boundary edges;
4. there is an upper bound on the degree of vertices in \mathcal{K} .

It is this combinatorial object, the abstract triangulation, which encapsulates the “prescribed pattern of tangencies” in our circle packing. We refer to these triangulations as abstract to emphasize the fact that in the definition we have implied no concrete geometric realization. A 2-complex and, by extension, the associated abstract triangulation are purely combinatorial objects; they have no inherent geometric structure until they are realized as a circle packing.

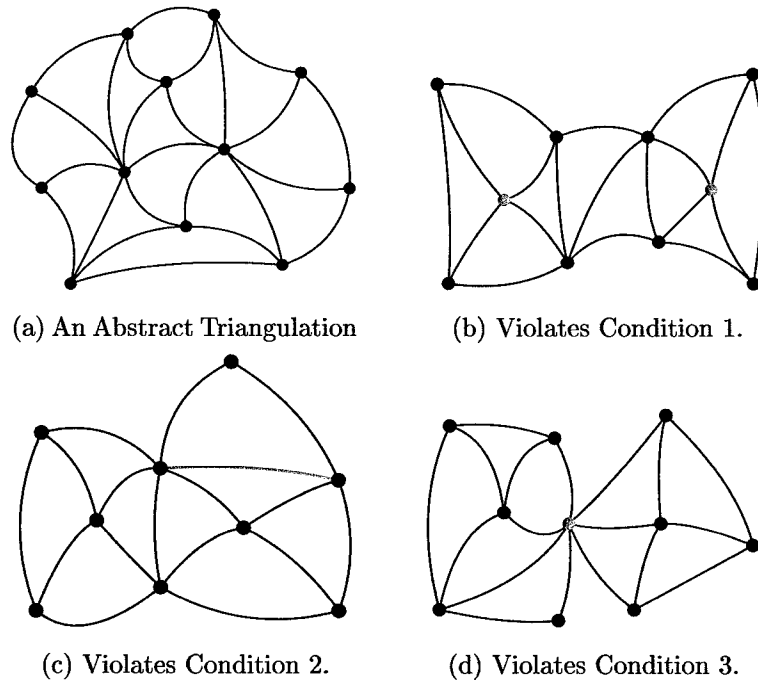


Figure 3.1: An Abstract Triangulation and Pathological Triangulations

An example of a simple valid abstract triangulation is shown in Figure 3.1; we also

show how triangulations may fail to meet conditions (1) through (3) from Definition 3.1.3. In Figure 3.1b we see two interior vertices which are not edge connected; in Figure 3.1c we see an edge whose endpoints are both boundary vertices; and in Figure 3.1d we see a vertex belonging to four boundary edges. Note that since the triangulations shown are all finite, they must also satisfy the bounded degree condition.

Definition 3.1.4. *A **circle packing** is a configuration of circles with a specified pattern of tangencies. In particular, if \mathcal{K} is an abstract triangulation of a topological surface, then a circle packing P for \mathcal{K} is a configuration of circles such that*

1. *P contains a circle C_v for every vertex $v \in \mathcal{K}$;*
2. *if $[u, v]$ is an edge of \mathcal{K} , then C_v is externally tangent to C_u ;*
3. *if $\langle v, u, w \rangle$ is a positively oriented face of \mathcal{K} , then $\langle C_v, C_u, C_w \rangle$ forms a positively oriented mutually tangent triple of circles in P .*

Realizing such a configuration is, at its most essential, a problem in computing the necessary radii of each circle in the packing. Examples of such algorithms are given by Collins and Stephenson [17, 42] and Mohar [37]. A simple example of an algorithm implemented in *Mathematica* for computing the radii is also given in Appendix D. All of these algorithms amount to numerically solving a boundary value problem in which the radii of the boundary circles are fixed and the remaining radii are computed algorithmically. A circle packing is called **univalent** if the circles in the packing have mutually disjoint interiors. That is, the packing is univalent if no two circles intersect in more than one point. This univalent circle packing represents a geometric realization of the underlying abstract triangulation \mathcal{K} . Vertices in the triangulation may be realized in this packing as the centers (in some particular geometry, hyperbolic, Euclidean, or spherical) of the circles, and the edges as geodesic segments connecting the centers. This embedding is called the **carrier** of the circle packing.

If \mathcal{K} is embedded in \mathbb{C} in two different ways (e.g., by giving two different sets of values for the radii of the boundary circles), there is a natural piecewise map from the carrier associated with one packing to the other achieved by sending triangles of one packing to their counterparts in the other using affine maps. These piecewise affine maps are referred to as **discrete conformal maps**.

In Figure 3.2 we have a graphic description of a bounded degree abstract triangulation, \mathcal{K} . This triangulation comprises 27 vertices, with edges between vertices indicating tangencies.

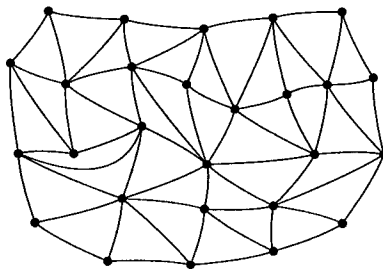


Figure 3.2: An Abstract Triangulation \mathcal{K}

We can produce a geometric realization (as a circle packing) of this combinatorial structure in any number of ways. Two different circle packings, obtained using the algorithm in Appendix D and displayed using the *Mathematica* code in Appendix E, are shown in Figure 3.3. In each of Figure 3.3a and Figure 3.3b, a triangle is shaded for reference; the triangle in each case corresponds to a face determined by the same three vertices from the triangulation shown in Figure 3.2.

The packings P_1 and P_2 in Figure 3.3 are embedded in \mathbb{C} and are normalized by placing the center of a circle (Circle 1) in each packing at the origin and placing the center of an adjacent circle (Circle 2) on the real axis. The shaded triangles illustrate how the discrete conformal map from P_1 to P_2 is described. The map which takes the shaded triangle in 3.3a to the shaded triangle in 3.3b is given by

$$f(z) = f(x + iy) = 1.67628x + 0.808753y. \quad (3.1.1)$$

It is easy to verify that this map is k -quasiconformal with $k = 2.07267$, since it

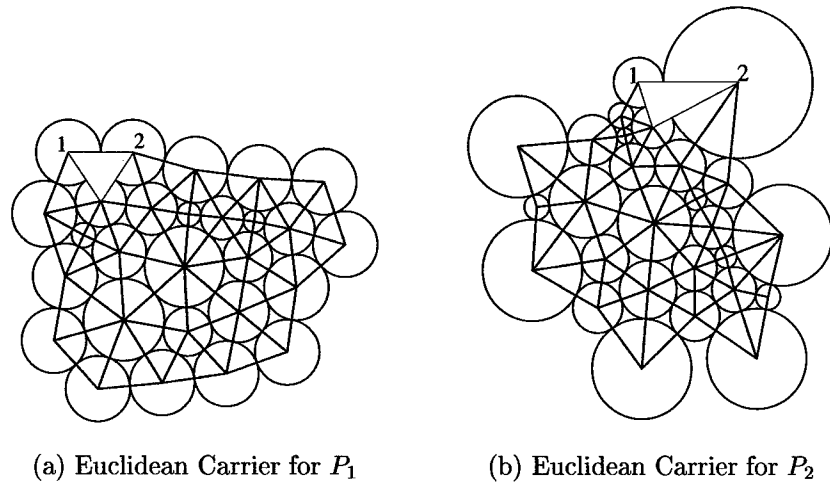


Figure 3.3: The Carriers of Two Different Circle Packings of \mathcal{K}

maps gross circles, not just infinitesimal circles, to ellipses with $k = 2.07267$ the ratio between their major and minor axes.

Definition 3.1.5. A **chain of circles** in a packing P for an abstract triangulation \mathcal{K} is a collection of circles $(C_{v_1}, C_{v_2}, \dots, C_{v_n})$ in P such that v_i and v_{i+1} share an edge in \mathcal{K} for $i = 1, 2, \dots, n - 1$, and $v_i \neq v_j$, if $i \neq j$. Thus, a chain of circles describes a non-self-intersecting edge path in \mathcal{K} . Similarly, a **closed chain** is a collection of circles corresponding to a closed non-self-intersecting edge path in \mathcal{K} .

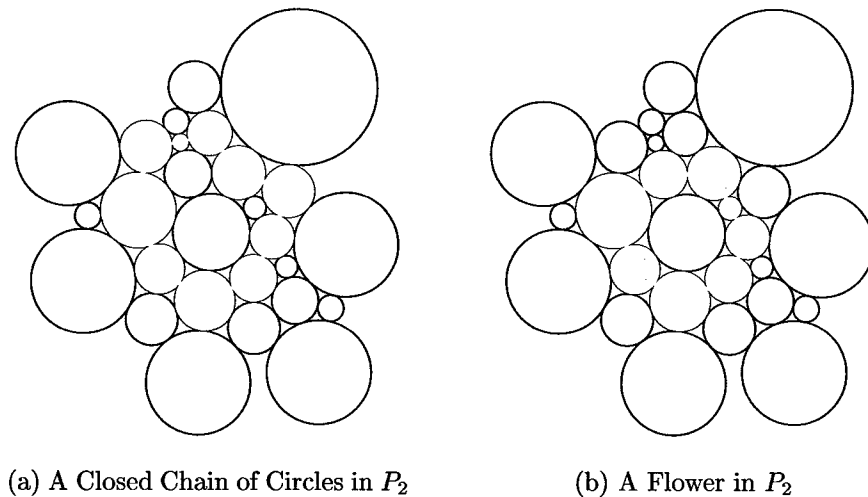


Figure 3.4: Chains of Circles and Flowers

Examples of closed chains of circles in the packing P_2 are shown (as shaded circles) in Figure 3.4. A special category of chains leads to a building-block for our circle packings. A **flower** consists of a central circle and some number of **petal** circles, the closed chain of successively tangent neighbors surrounding the central circle. An example of a flower from the packing P_2 is shown (as shaded circles) in Figure 3.4b.

One particularly useful circle packing is the **regular hexagonal packing**, a packing in which every interior vertex has degree 6 and each circle has the same radius. An example of a regular hexagonal packing, sometimes also referred to as a penny packing, is shown in Figure 3.5a. Another packing commonly seen is the **ball-bearing packing**, shown in Figure 3.5b.

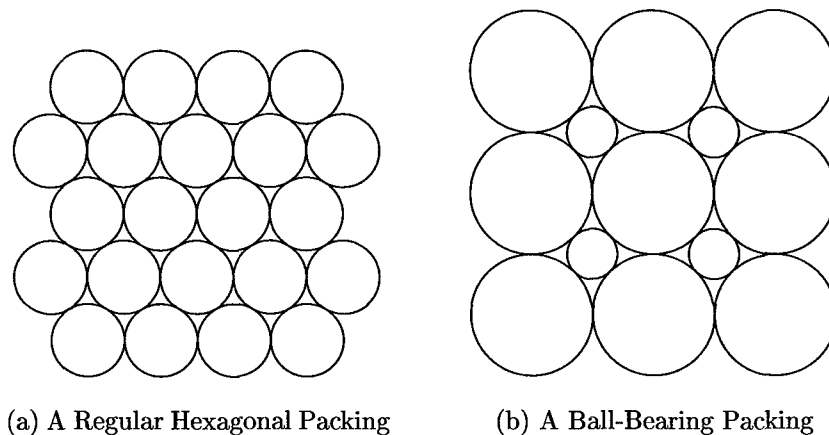


Figure 3.5: Two Important Types of Circle Packings

3.2 Discrete Function Theory

The important characteristic of the discrete conformal maps induced by circle packings is not that they are quasiconformal; the key fact, suggested by Thurston [51] and proven by Rodin and Sullivan [39], is that these maps are “nearly conformal.” This is the result given in Theorem 3.2.1, the Rodin-Sullivan Theorem. Before we state this theorem, however, we first state some geometric results associated with circle packing that are interesting in themselves and required for the proof of Theorem 3.2.1.

Lemma 3.2.1 (Length-Area Lemma). *Let P be a univalent packing in \mathbb{D} and C_v a circle in P with Euclidian radius r . Assume there exist m disjoint chains of circles in P having combinatorial lengths n_1, n_2, \dots, n_m , such that each chain separates C_v from 0 and a point on $\partial\mathbb{D}$. Then*

$$r < \frac{4}{\sqrt{\sum_{i=1}^m \frac{1}{n_i}}}. \quad (3.2.1)$$

As the number of generations separating a circle in a packing from the boundary increases Lemma 3.2.1, the Length-Area Lemma, has the effect of forcing the radius of this circle to zero (in the limit). For a more detailed discussion of Lemma 3.2.1, the Length-Area Lemma, see [39, 42].

Lemma 3.2.2 (Ring Lemma). *Given a univalent flower $(C_{v_0}; C_{v_1}, C_{v_2}, \dots, C_{v_n})$ in \mathbb{C} there is a lower bound C_n , depending only on n , on the ratio of the radius r_i of C_{v_i} to the radius r_0 of C_{v_0} for each $i = 1, 2, \dots, n$; that is*

$$C_n < \frac{r_i}{r_0}, \quad (3.2.2)$$

$i = 1, 2, \dots, n$.

Lemma 3.2.2, the Ring Lemma, guarantees that central angles in the carrier on a flower are bounded away from zero and π . That is, suppose we are given a complex \mathcal{K} in which the **degree** of each vertex, the number of adjacent vertices, is bounded; also suppose we have two (different) packings P_1 and P_2 associated with \mathcal{K} . The Ring Lemma guarantees that the quasiconformality of the induced conformal map from P_1 to P_2 is bounded.

Lemma 3.2.3 (Hexagonal Packing Lemma). *There is a sequence $\{s_n\}_n \in \mathbb{N}$, decreasing to zero, with the following property. Let c_1 be a circle in a univalent Euclidean circle packing P , and suppose the first n generations of circles about c_1 are combinatorially equivalent to n generations of the regular hexagonal packing around one of its circles. Then for any circle $c \in P$ tangent to c_1 ,*

$$\left| 1 - \frac{r_c}{r_{c_1}} \right| \leq s_n, \quad (3.2.3)$$

where r_c is the radius of the circle c in P and r_{c_1} is the radius of the circle c_1 in P .

The immediate value of Lemma 3.2.1, Lemma 3.2.2, and Lemma 3.2.3 is their use in proving Theorem 3.2.1, the Rodin-Sullivan Theorem, one of the fundamental results in the study of circle packing.

Theorem 3.2.1 (Rodin-Sullivan Theorem). *Fix a simply connected domain $\Omega \subsetneq \mathbb{C}$ and points $p, q \in \Omega$. Let P_k be the portion lying in Ω of the infinite regular hexagonal packing whose circles all have radius $\frac{1}{k}$, and let \mathcal{K}_k be the underlying complex for the packing P_k . Suppose \tilde{P}_k is a packing in \mathbb{D} for \mathcal{K}_k with all boundary circles tangent to $\partial\mathbb{D}$, and let $f_k : \text{carr}(P_k) \rightarrow \text{carr}(\tilde{P}_k)$ be the induced discrete conformal map. If each \tilde{P}_k has been normalized so that $f_k(p) = 0$ and $f_k(q) > 0$, then $\{f_k\}$ converges locally uniformly to the unique Riemann map $f : \Omega \rightarrow \mathbb{D}$ satisfying $f(p) = 0$ and $f(q) > 0$.*

An illustration of the use of circle packing to approximate the action of the unique Riemann map from a simply connected domain to the disk is shown in Example 3.2.1.

Example 3.2.1. Let $\Omega = \{z \in \mathbb{C} : |z| < 1 \text{ and } \text{Re}(z) > 0\}$. That is, Ω is the upper half unit disk. We wish to map Ω to the unit disk \mathbb{D} with the unique Riemann map f , normalized so that $f(i(\sqrt{2}-1)) = 0$ and f maps the imaginary axis to the imaginary axis. In this case, we may explicitly construct the desired map: $f(z) = -i \left(\frac{z^2 + 2iz + 1}{z^2 - 2iz + 1} \right)$.

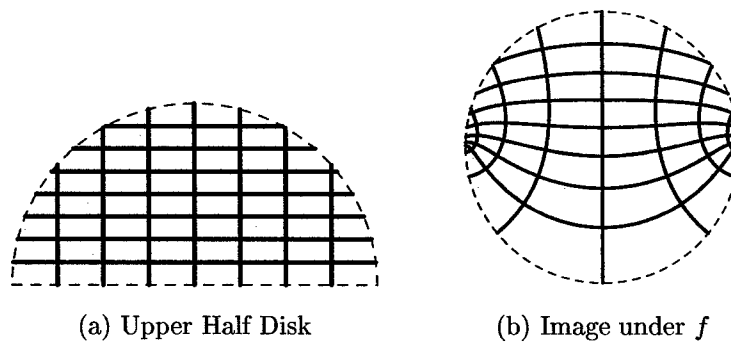


Figure 3.6: Unique Riemann Map $f : \Omega \rightarrow \mathbb{D}$

The action of this map is illustrated in Figure 3.6. For reference, we have included an

orthogonal grid on Ω , shown in Figure 3.6a, and the image of this grid in \mathbb{D} , shown in Figure 3.6b.

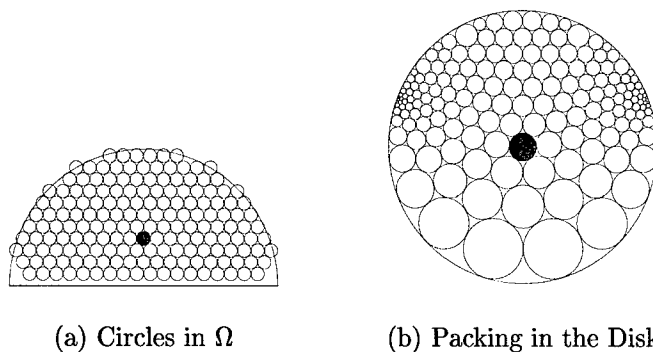


Figure 3.7: Approximate Riemann Map with Circle Packing (171 Circles)

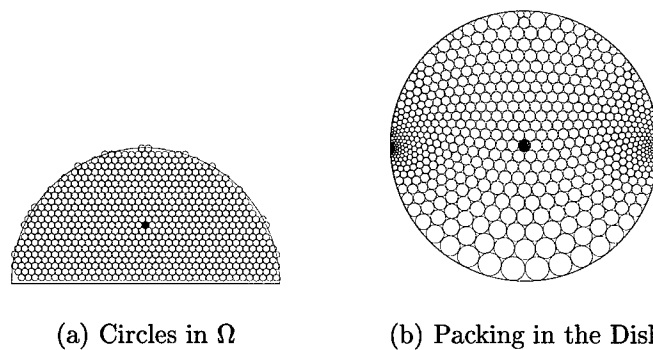


Figure 3.8: Approximate Riemann Map with Circle Packing (342 Circles)

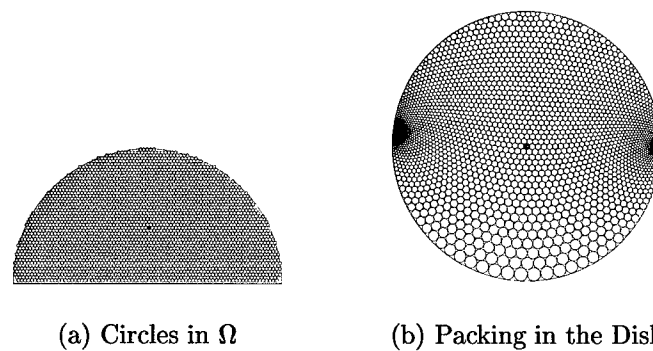


Figure 3.9: Approximate Riemann Map with Circle Packing (684 Circles)

We now illustrate, in Figure 3.7, Figure 3.8, and Figure 3.9, the approximation of this map through successively finer circle packings, showing the result given by Theorem 3.2.1, the Rodin-Sullivan Theorem. Clearly, the action of the explicit map described in Figure 3.6 is emerging; the image of the orthogonal grid in Figure 3.6 appears in chains of circles. The shaded circle in each of Figure 3.7a, Figure 3.8a, and Figure 3.9a represents the point mapped to the origin. In the images under f shown in Figure 3.7b, Figure 3.8b, and Figure 3.9b, the shaded circles are centered at the origin.

The requirement that the packings used in Theorem 3.2.1, the Rodin-Sullivan Theorem, all be of uniformly degree 6 is quite restrictive. Since the initial proof of Theorem 3.2.1, however, Stephenson [43] relaxed the degree 6 condition using techniques of random walks, and He and Rodin [27] showed that only a uniform bound on the degree is necessary. To thus relax the requirement on the combinatorics of the packing, we require Lemma 3.2.4, sometimes referred to as the Packing Lemma.

Lemma 3.2.4 (Packing Lemma). *Let $\{K_n\}_{n \in \mathbb{N}}$ be a sequence of combinatorial closed disks such that*

1. *there exists a uniform bound on the degree of the vertices in K_n for each $n \in \mathbb{N}$, and*
2. *the sequence $\{K_n\}_{n \in \mathbb{N}}$ is either a nested sequence which exhausts a parabolic combinatorial disk or is asymptotically parabolic.*

There exists a sequence $\{s_m\}_{m \in \mathbb{N}} \subset \mathbb{R}$, decreasing to zero, with the following property. Suppose that for some n , u and v are adjacent interior vertices of K_n whose combinatorial distance from ∂K_n are both at least m , and suppose that P_n and \tilde{P}_n are two univalent, Euclidean circle packings for K_n . Then

$$\left| \frac{\tilde{r}_u}{\tilde{r}_v} - \frac{r_u}{r_v} \right| \leq s_m, \quad (3.2.4)$$

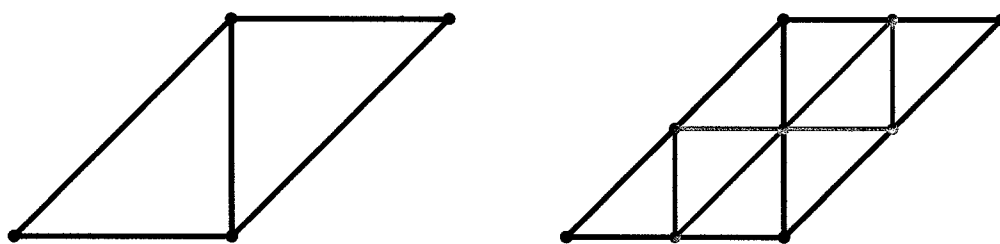
where r_u and r_v are the radii of the circle in P_n corresponding to u and v , and \tilde{r}_u and \tilde{r}_v are the radii of the circle in \tilde{P}_n corresponding to u and v .

Essentially, Lemma 3.2.4, the Packing Lemma, states that for a circle “deep” in a packing, the ratio of its radius to any given neighbor is nearly the same in the packings P_n and \tilde{P}_n ; in other words, the triangles in P_n and \tilde{P}_n are nearly similar triangles. This gives us that away from the boundary, the induced discrete conformal map between P_n and \tilde{P}_n is nearly conformal. This fact will play an important role in the proof of our main result in Chapter IV.

3.3 Hex Refinement

In order to obtain the various approximation results for circle packing and discrete analytic function theory, we need a method to refine given circle packings. The primary requirement in any such refinement is that we maintain some uniform control over the degree of the complexes generated by the refinement algorithm since we require that Lemma 3.2.2, the Ring Lemma, applies at each successive level of refinement. The hex refinement method developed by Bowers and Stephenson [11] is especially nice.

Definition 3.3.1. *If \mathcal{K} is a 2-complex, the **hex refinement** of \mathcal{K} is the complex formed by adding a vertex to each edge and adding an edge between any two vertices lying on the same face, as shown in Figure 3.10.*



(a) Two Triangles Before Hex Refinement

(b) Two Triangles After Hex Refinement

Figure 3.10: Hex Refinement

Note that hex refinement, and refinement in general, is really a combinatorial process, refining the combinatorics of the complex \mathcal{K} ; one must repack the new complex

obtained by refining \mathcal{K} in order to realize the effect of the refinement in a circle packing. Hex refinement has a number useful characteristics described by Bowers and Stephenson [11] and summarized in Proposition 3.3.1.

Proposition 3.3.1 (Bowers and Stephenson). *Any new interior vertices added to a 2-complex \mathcal{K} by hex refinement have degree 6, while the degree of the original vertices remain unchanged. If \mathcal{K} is embedded in \mathbb{C} in such a way that the edges correspond to Euclidean line segments, then its hex refinement may be realized by adding line segments joining the midpoint of each edge within every face. In this case, each face in \mathcal{K} is subdivided into four new faces, each similar to the original face in which it is contained and having edges one-half as long.*

Notice that refining only one edge in a complex is not permitted, since this would result in a complex that is not a triangulation; the faces bordering the refined face will have an extra vertex along the common edge they share with the refined face, giving combinatorial quadrilaterals rather than triangles. We can, however, locally refine only those triangles in the complex which present some difficulty with respect to desired characteristics of the complex, then correct the introduced problems on adjacent faces by adding a single edge from a vertex to the midpoint of the opposite side, as shown in Figure 3.11.

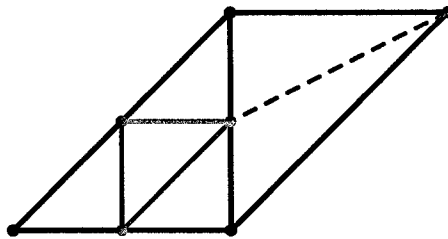


Figure 3.11: Hex Refinement and Correction on Adjacent Triangle

This process of hex refinement of individual faces (or subsets of the triangles in a triangulation) and the addition of edges to absorb extra vertices can be used to locally refine an abstract triangulation in order to improve the discrete conformal

approximation in troublesome areas. Local refinement will play a key role in the discrete conformal approximation of earthquakes in Chapter IV.

3.4 Combinatorial Welding

We now describe the process of combinatorial welding developed by Williams [53, 54]. Suppose two abstract triangulations \mathcal{K}_1 and \mathcal{K}_2 are embedded in a surface S and suppose $h : B_1 \subset \partial\mathcal{K}_1 \rightarrow B_2 \subset \partial\mathcal{K}_2$ is a homeomorphism. The map h will be used to attach the triangulations \mathcal{K}_1 and \mathcal{K}_2 along the subsets of their respective boundaries B_1 and B_2 and form a new triangulation \mathcal{K} . In Chapter IV, h will be taken as a discrete version of the map defining an earthquake along a geodesic, and the attaching described here will act as a combinatorial shearing and/or combinatorial grafting in the construction of combinatorial earthquakes.

If the map h respects the combinatorial structures of \mathcal{K}_1 and \mathcal{K}_2 , that is, if h sends vertices and edges in B_1 and B_2 to vertices and edges, respectively, the combinatorial welding process is trivial. We simply identify vertices and edges in $B_1 \subset \partial\mathcal{K}_1$ with their images in $B_2 \subset \partial\mathcal{K}_2$, as shown in Figure 3.12. Note that the action of h on the vertices in B_1 is sufficient to determine the combinatorial action of h on all of B_1 .

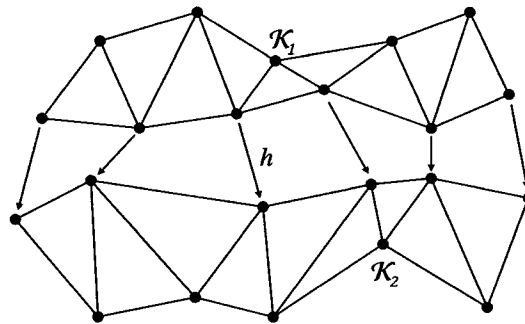


Figure 3.12: Welding Action when h Respects the Combinatorics of \mathcal{K}_1 and \mathcal{K}_2

Much more interesting is the case in which h does not respect the combinatorics of \mathcal{K}_1 and \mathcal{K}_2 in this way. In general, the images of vertices in B_1 under that action of h will not be vertices in B_2 . In order that the map h be well-defined in these cases, it is necessary to modify the triangulations \mathcal{K}_1 and \mathcal{K}_2 so that h will respect the modified

combinatorial structure. This modification is accomplished using a refinement similar to that shown in Figure 3.11. Specifically, for each boundary vertex $v \in B_1$ we refine B_2 by adding a vertex to B_2 embedded at the point $h(v)$. Likewise, for each boundary vertex $w \in B_2$ we refine B_1 by adding a vertex to B_1 embedded at the point $h^{-1}(w)$. When vertices are thus inserted, however, \mathcal{K}_1 and \mathcal{K}_2 will not necessarily remain triangulations. To maintain the characteristics of a triangulation, we must further refine each of \mathcal{K}_1 and \mathcal{K}_2 . If we add a vertex $h(v)$ or $h^{-1}(w)$ to an edge $[a, b]$ of a triangle $\langle a, b, c \rangle$, we refine the original complex (of \mathcal{K}_1 or \mathcal{K}_2) by adding an edge from c to the new vertex. An example of this process is shown in Figure 3.13.

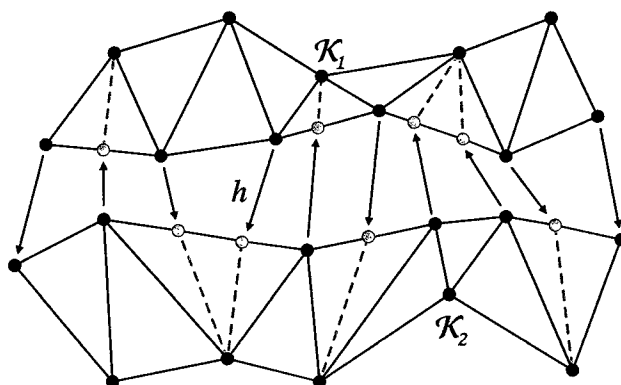


Figure 3.13: Welding Action with Combinatorial Refinement of \mathcal{K}_1 and \mathcal{K}_2

Note that this refinement process is well-defined and produces new triangulations since, by definition, each face in the triangulations may have at most one edge contained in the boundary. We therefore add vertices to only one edge in any given face which might interfere with the refinement process.

It is important that in the course of executing these combinatorial weldings and then embedding the resulting combinatorics in a circle packing to realize a geometry that we maintain control over the combinatorial and geometric characteristics of the process. Specifically, we must ensure that

1. the degree of the complex resulting from the combinatorial welding is bounded,
and

2. the new edges added to the carriers of \mathcal{K}_1 and \mathcal{K}_2 do not result in triangles with arbitrarily small angles.

Condition (1) will then guarantee that we can apply Lemma 3.2.2, the Ring Lemma, to the packing associated with the new complex which results from the combinatorial welding, thus giving bounds on the angles in the new packing. Condition (2) will ensure the existence of similar bounds for the packing prior to welding and repacking; when we artificially insert edges in the carrier of the initial packing so that there is a bijection between triangles in the two carriers, we must not create triangles with arbitrarily small angles. Thus, with these two conditions satisfied we may construct quasiconformal discrete maps between the carriers in the surfaces associated with the initial packing and the post-welding packing. These technical considerations are easily overcome through the use of local hex refinement (Condition (1)) and through “rounding off” the refinement to existing vertices if the new vertex added in the welding refinement is too close to an existing vertex (Condition (2)). The details of these processes, and verification of their validity, are given in [53, 54]. Once we have welded the two sides of the complex together in this way, we may pack the resulting complex. Now, we have a bijection between the triangles in the carrier of the original packing (after it has been suitably refined) and the new packing which results once the shearing operation is completed; we use these triangles to construct a piecewise affine, and thus quasiconformal, map from the original packing to the new packing. Thus, the discretization of the map along the boundary leads to a discretization of the map on the entire surface. This now leads us to Proposition 3.4.1, proven in [54].

Proposition 3.4.1 (Williams). *Combinatorial attachment by h induces a piecewise linearization \hat{h} of h . If h is bilipschitz, then the linearization \hat{h} will be bilipschitz as well.*

3.5 Density of Packable Surfaces

Demonstrations of the existence of circle packings have been given variously by Thurston [51], Minda and Rodin [36], and Beardon and Stephenson [4]. Brooks [12] showed that compact packable surfaces are dense in moduli space, and Bowers and Stephenson [8, 10] extended this result to include surfaces of finite analytic type. Other results on the density of packable surfaces have been given by Barnard and Williams [1] and Williams [54]. The results thus demonstrated which are germane to this research are summarized in Theorem 3.5.1.

Theorem 3.5.1. *Let \mathcal{K} be an abstract triangulation of a surface of type (g, n, m) . There exists a unique surface in moduli space which supports a packing for \mathcal{K} . A complex, along with a choice of marking, then determines a unique point in Teichmüller space. Moreover, the collection of all packable surfaces is dense in Teichmüller space.*

The density of merely packable surfaces as given in Theorem 3.5.1 is extremely useful and powerful. Of equal interest is the density of other subsets of packable surfaces and the characteristics of convergent sequences of packable surfaces.

Proposition 3.5.1. *Let R be a compact Riemann surface that is not packable. If $\{R_n\}_{n=1}^{\infty}$ is any sequence of compact, packable Riemann surfaces such that $R_n \rightarrow R$ in the Teichmüller metric where each admits a packing P_n with degree uniformly bounded through the sequence, then the radii in the circle packings $\{P_n\}_{n=1}^{\infty}$ tend to zero as $n \rightarrow \infty$.*

Proof. First note that since the circle packings $\{P_n\}_{n=1}^{\infty}$ are assumed to be of bounded degree, Lemma 3.2.1 guarantees that the radius of one circle in a packing is arbitrarily small if and only if the radii of all circles in that packing are small. Proceeding by way of contraposition, suppose that the radii of circles in P_n are bounded away from zero by some fixed positive constant for each $n \in \mathbb{N}$. For every $n \in \mathbb{N}$, R_n is a compact Riemann surface, and therefore has finite area. Since $R_n \rightarrow R$ and R is compact, there exists a uniform upper bound on the area of the Riemann surfaces R_n . Hence, there

exists a uniform bound on the total number of circles in each packing P_n . There are thus only a finite number of abstract triangulations possible among the circle packings $\{P_n\}_{n=1}^\infty$. By the pigeonhole principle, there exists a subsequence $\{R_{n_k}\}_{k=1}^\infty \subseteq \{R_n\}_{n=1}^\infty$ such that for each $k \in \mathbb{N}$ the circle packing realized in P_{n_k} corresponds to a single abstract triangulation \mathcal{K} , (i.e., there exists a subsequence of packings each having the same combinatorial structure). Since the abstract triangulation uniquely determines a surface for which that triangulation is realized as a packing, we find that $\{R_{n_k}\}_{k=1}^\infty$ is a constant sequence of Riemann surfaces. Now, $R_n \rightarrow R$ as $n \rightarrow \infty$, so every subsequence of $\{R_n\}_{n=1}^\infty$ must likewise converge to R ; that is $R_{n_k} \rightarrow R$ as $k \rightarrow \infty$. Thus R is an element of the sequence $\{R_n\}_{n=1}^\infty$; in fact, R is equivalent to infinitely many elements of this sequence. Therefore, R is a compact, packable Riemann surface. Thus, by our contrapositive argument, if a sequence of packable surfaces, R_n , with degree uniformly bounded through the sequence converge to a Riemann surface that is not, itself, packable, then the mesh of the packings on the surfaces goes to zero. \square

We now introduce another class of compact Riemann surfaces called **equilateral surfaces** which will be useful in constructing sequences of packable Riemann surfaces while maintaining control over the combinatorics of their underlying complexes.

Definition 3.5.1. *Suppose S denotes a compact, orientable topological surface and let K denote a triangulation of the surface S . If we paste together equilateral triangles (triangles conformally equivalent to equilateral triangles) in the pattern of K to impose a piecewise affine structure on S , this affine structure defines a conformal structure on S , guaranteeing that S is a Riemann surface. Riemann surfaces thus constructed are called **equilateral surfaces**.*

Just as has been shown for compact surfaces by Brooks [12] and for surfaces of finite analytic type by Bowers and Stephenson [8, 10], if we fix a genus $g > 0$ this seemingly very restrictive class of (compact) equilateral surfaces of genus g is dense in Teichmüller space of genus g , as shown by Belyĭ [3]. We state this result as Theorem 3.5.2.

Theorem 3.5.2 (Belyĭ). *If S is a Riemann surface of genus $g > 0$, the set of equilateral surfaces of genus g is countable and dense in the Teichmüller space of S .*

This result guarantees the existence of sequences of packable Riemann surfaces with underlying combinatorial structures over which we may exercise a significant degree of control. This ability to control the underlying combinatorics allows us the ability to manipulate the geometry of our packings in that we may force the circles in a sequence of packable (and packed) surfaces to decrease in size.

Corollary 3.5.1. *Let S be a Riemann surface and let R be an arbitrary point in the Teichmüller space of S . There exists a sequence of points $\{R_n\}$ in the Teichmüller space of S such that $R_n \rightarrow R$ in the Teichmüller metric as $n \rightarrow \infty$, R_n is packable for every n , and the radii of the circles in P_n go to zero as $n \rightarrow \infty$, where P_n is the unique packing on the surface R_n for every n .*

Proof. First note that since the set of equilateral surfaces on S is dense in the Teichmüller space of S , there exists a sequence of equilateral surfaces $\{E_n^1\}$ in the Teichmüller space of S such that $E_n^1 \rightarrow R$ as $n \rightarrow \infty$. Corresponding to the equilateral surface E_1^1 we have a triangulation K_1^1 . This triangulation corresponds to a unique packable surface R_1^1 , distinct from E_1^1 . An example of an equilateral surface and the packable surface it induces is shown in Figure 3.14. (This figure appeared in [11] and is used with permission of the authors.)

Now, refine the triangulation K_1^1 using hex refinement to create a new triangulation K_1^2 . Note that refining this triangulation has no effect on the structure of the surface E_1^1 ; that is, the equilateral surface E_1^2 corresponding to K_1^2 is the same as E_1^1 , since hex refinement on an equilateral triangle divides that face into 4 new equilateral triangles. So, K_1^2 corresponds to a unique packable surface R_1^2 , distinct from E_1^2 (and E_1^1). Continuing in this manner, we construct a sequence of packable surfaces $\{R_1^m\}_{m=1}^\infty$. As $m \rightarrow \infty$, the triangles in the carrier of the packing P_1^m on R_1^m converge to equilateral triangles, and the sequence $\{R_1^m\}_{m=1}^\infty$ converges to a surface conformally equivalent to E_1^1 . Thus, $R_1^m \rightarrow E_1^1$ as $m \rightarrow \infty$ in the Teichmüller metric. Note,

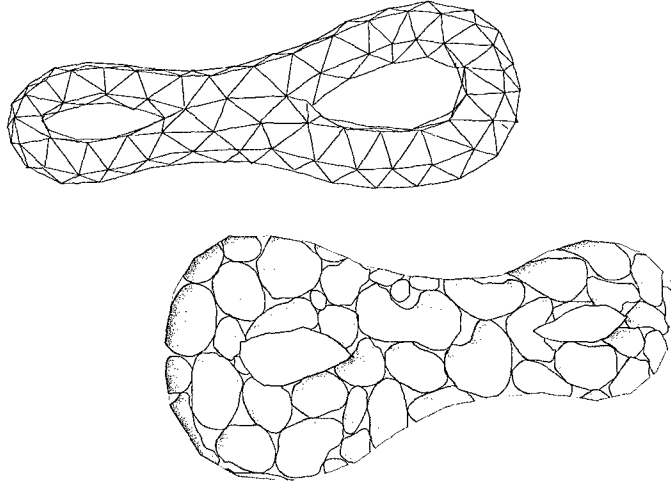


Figure 3.14: An Equilateral Surface and the Induced Packable Surface

however, that the degree of each packing in the sequence $\{P_1^m\}_{m=1}^\infty$ is bounded by the same constant, since the hex packing does not change the degree of any vertex in the initial packing and every new vertex has degree 6 since all vertices in the packing are interior vertices. Now, a standard application of Lemma 3.2.1, the Length-Area Lemma, guarantees that the radii of the circles in the sequence $\{P_1^m\}_{m=1}^\infty$ go to zero as $k \rightarrow \infty$. We repeat this process for each equilateral surface E_n^1 , generating for each a sequence of packable surfaces $\{R_n^m\}_{m=1}^\infty$ such that $R_n^m \rightarrow E_n^1$ in the Teichmüller metric and the radii of the circles in the sequence of packings $\{P_n^m\}_{m=1}^\infty$ corresponding the packable surfaces go to zero as $m \rightarrow \infty$.

$$\begin{array}{cccc}
 R_1^1 & R_2^1 & \cdots & \cdots \\
 R_1^2 & R_2^2 & \cdots & \cdots \\
 \vdots & \vdots & \ddots & \vdots \\
 E_1^1 & E_2^1 & \cdots & R
 \end{array}$$

Now, for each $n \in \mathbb{N}$, choose a surface R_n from the sequence $\{R_n^m\}_{m=1}^\infty$ such that the Teichmüller distance from R_n to E_n^1 is less than 2^{-n} and the maximum radius of any circle in the packing on R_n (in the intrinsic metric on the surface) is similarly less than 2^{-n} . We now have a sequence $\{R_n\}_{n=1}^\infty$ such that $R_n \rightarrow R$ in the Teichmüller

metric as $n \rightarrow \infty$, R_n is packable for every n , and the radii of the circles in P_k go to zero as $n \rightarrow \infty$, where P_n is the unique packing on the surface R_n for every n . \square

CHAPTER IV

PACKING EARTHQUAKES

Throughout this chapter let (\mathcal{L}, σ) be a finite measured geodesic lamination of \mathbb{D} associated with a set of points $S \subset \mathbb{D}$. Suppose \mathcal{L} consists of n disjoint, simple, closed geodesics $\{L^i\}_{i=1}^n$. Note that throughout this chapter we suppose that the real (shearing) part of the weight on any geodesic L^i may assume any real value, while the imaginary (grafting) part may assume only non-negative real values. This indicates that the shearing maps we consider may shear to either the left or the right, and the grafting maps we consider involve only the insertion of cylinders of positive height. Much of the construction below is taken from [54]; we reproduce it here in the interest of making this exposition as self-contained as possible.

4.1 Discrete Laminations

Let $\{P_n\}_{k=1}^\infty$ be a sequence of packings in \mathbb{D} with uniformly bounded degree and mesh decreasing to zero. Let D_k denote the Euclidean carrier of P_k for each $k \in \mathbb{N}$. Note that the construction of a “combinatorial” earthquake E_k of this Euclidean carrier as an approximation of the finite earthquake E is complicated by the fact that D_k is not equal to \mathbb{D} for any fixed $k \in \mathbb{N}$.

Note that any given geodesic in the lamination \mathcal{L} will pass indiscriminately through the points and triangles of the Euclidean carrier D_k . Thus, shearing and grafting D_k along the geodesics of the lamination is not directly possible. In order to approximate the action of the earthquake E , therefore, we construct a combinatorial lamination of D_k that respects the combinatorial structure and converges to the finite geodesic lamination \mathcal{L} as $k \rightarrow \infty$. This combinatorial lamination comprises combinatorial “geodesics” $\{\ell_k^i\}_{i=1}^n$ corresponding to the true hyperbolic geodesics $\{L^i\}_{i=1}^n$, constructed in the following manner.

We consider packings that are hyperbolic in \mathbb{D} ; that is, we consider packings that fill the disk. Let a_k^i and b_k^i be the endpoint of the geodesic $L^i \subset \partial\mathbb{D}$. We construct ℓ_k^i

as an edge path which, in the limit, connects a_k^i and b_k^i , whose Hausdorff distance to L^i is minimal, and which satisfies the following three conditions.

1. Every vertex in ℓ_k^i must have a neighbor in both components of $D_k \setminus \ell_k^i$.
2. The combinatorial geodesics $\{\ell_k^i\}$ are disjoint, except possibly at their common endpoints.
3. Any hyperbolic geodesic perpendicular to L^i intersects ℓ_k^i in exactly one point.

It is not immediately clear that we can in general construct such a rigidly characterized edge path through the combinatorics of D_k . Lemma 4.1.1 guarantees that such constructions are, in fact, possible.

Lemma 4.1.1 (Williams). *By taking k sufficiently large and possibly modifying D_n near L^i , we can find paths ℓ_k^i so that conditions (1) through (3) are satisfied. Moreover, $\ell_k^i \rightarrow L^i$ uniformly as $k \rightarrow \infty$.*

In Figure 4.1 we see successively finer packings in the disk and increasingly more accurate piecewise linear combinatorial approximations of the hyperbolic geodesic L .

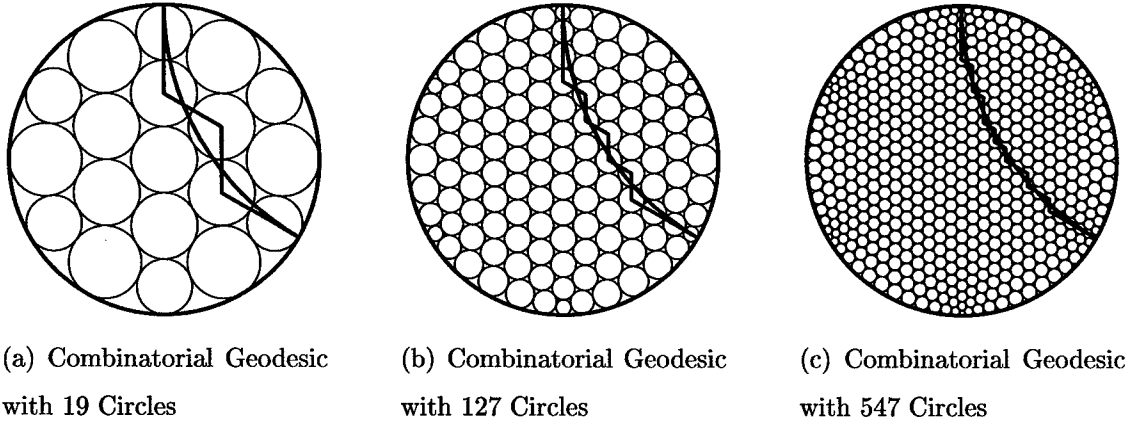


Figure 4.1: Approximating a Geodesic L with Combinatorial Geodesics ℓ_k

4.2 Hyperbolic Projections

Having described a discrete analog of the finite measured geodesic lamination (\mathcal{L}, σ) , we now must describe discrete analogs for the hyperbolic shearing maps and grafting maps associated with each geodesic. We cannot, of course, use the shearing and grafting maps associated with the lamination (\mathcal{L}, σ) directly; rather, we construct hyperbolic projections p_k^i which take the combinatorial geodesic ℓ_k^i to L^i . Thus, by pre-and post-composition with the map p_k^i , we may construct an appropriate transformation to give a discrete shearing and/or grafting along ℓ_k^i using the shearing and/or grafting map on L^i .

Notice that the collection of hyperbolic geodesics perpendicular to the geodesic L^i in the lamination fill \mathbb{D} . By the construction of the discrete geodesic ℓ_k^i , each such perpendicular geodesic η intersects ℓ_k^i exactly once. We may thus define a map $p_k^i : D_k \cap \mathbb{D} \rightarrow \mathbb{D}$ by the requirement that $p_k^i|_\eta$ be the unique hyperbolic Möbius transformation with axis η and translation length equal to the hyperbolic distance from $\ell_k^i \cap \eta$ to $L^i \cap \eta$. The action of such a map on a segment of a discrete geodesic in \mathbb{D} corresponding to the geodesic between 1 and i is shown in Figure 4.2. Note that this map is clearly a quasismetry.

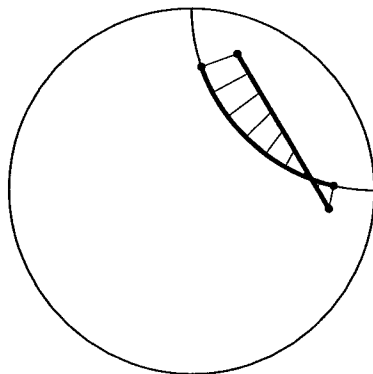


Figure 4.2: Action of a Hyperbolic Projection p_k^i

We have constructed discrete geodesic approximations ℓ_k^i to the geodesic L^i and the corresponding hyperbolic projections p_k^i , and Lemma 4.1.1 guarantees that $\ell_k^i \rightarrow$

L^i as $k \rightarrow \infty$. We now ask how the hyperbolic projections p_k^i behave as $k \rightarrow \infty$. The answer is given by Proposition 4.2.1.

Proposition 4.2.1 (Williams). *The sequence $\{p_k^i\}$ is uniformly bilipschitz on $\overline{\mathbb{D}}$ and converges uniformly to the identity map on $\overline{\mathbb{D}}$.*

4.3 Discrete Shearing Maps

With the hyperbolic projections $\{p_k^i\}$ we now define discrete shearing operations $\{h_k^i\}$ which approximate the hyperbolic shearing maps $\{h^i\}$ such that $h_k^i \rightarrow h^i$ as $k \rightarrow \infty$. For each $k \in \mathbb{N}$, define h_k^i by

$$h_k^i = (p_k^i)^{-1} \circ h^i \circ (p_k^i). \quad (4.3.1)$$

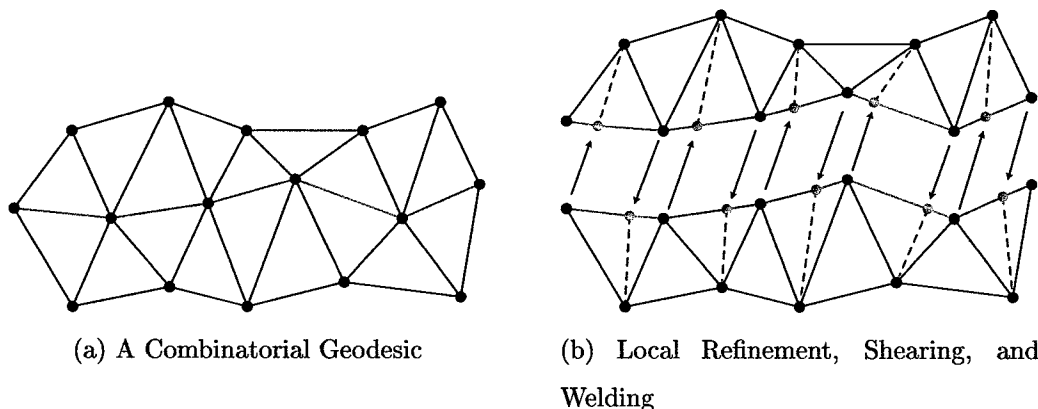


Figure 4.3: Combinatorial Shearing and Welding

By Lemma 4.3.1, this map behaves in the manner we require, simulating the action of a hyperbolic shearing and converging to that hyperbolic shearing.

Proposition 4.3.1 (Williams). *The discretized maps h_k^i are bilipschitz on ℓ_k^i with bilipschitz constants bounded independently of i and k , and h_k^i converges uniformly to the hyperbolic shearing map h^i on \mathbb{D} as $k \rightarrow \infty$.*

4.4 Discrete Grafting Maps

As we did for discrete shearing maps in Section 4.3, we may use the hyperbolic projections $\{p_k^i\}$ to define discrete grafting operations $\{g_k^i\}$ which approximate the

hyperbolic grafting maps $\{g^i\}$ such that $g_k^i \rightarrow g^i$ as $k \rightarrow \infty$. First, we need to understand the action of the grafting map, g^i . The action of this map is to open the disk along the geodesic L^i , creating two copies of the geodesic. We then parameterize each copy of the geodesic and the boundary of an infinite hyperbolic strip by arc length and identify corresponding points in the parameterizations. The only difference in the discrete grafting is that the discrete geodesic ℓ_k^i and L^i do not agree. So, for each $k \in \mathbb{N}$, define g_k^i by

$$g_k^i = (p_k^i)^{-1} \circ g^i \circ (p_k^i). \quad (4.4.1)$$

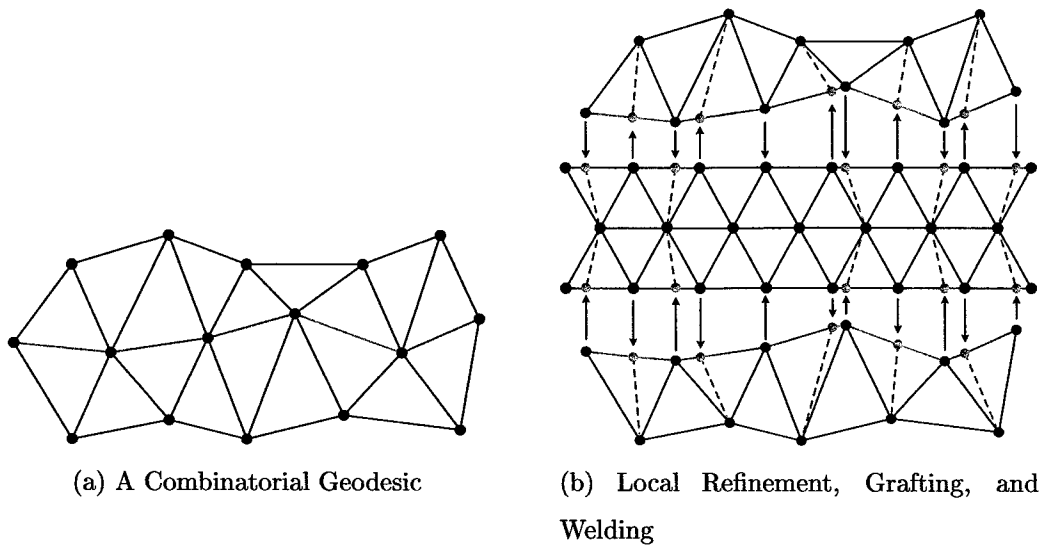


Figure 4.4: Combinatorial Grafting and Welding

Proposition 4.4.1. *The discretized maps g_k^i are bilipschitz on ℓ_k^i with bilipschitz constants bounded independently of i and k , and g_k^i converges uniformly to the hyperbolic grafting map g^i on \mathbb{D} as $k \rightarrow \infty$.*

Proof. The fact that the maps g_k^i are bilipschitz on ℓ_k^i follows directly from Proposition 3.4.1. As for convergence, Proposition 4.2.1 guarantees that p_k^i converges uniformly to the identity. Thus, g_k^i converges uniformly to g^i as $k \rightarrow \infty$. \square

We now define a combinatorial earthquake as the composition of a discrete grafting

map with a discrete shearing map, $E_k = g_k \circ h_k$, just as we defined continuous earthquakes as the composition of grafting and shearing maps, $E = g \circ h$.

4.5 Convergence of Discrete Earthquake Maps on Hyperbolic Riemann Surfaces

Thus far, we have described a family of transformations on the Teichmüller space of a hyperbolic Riemann surface and a process whereby we may discretely mimic the action of those transformations through circle packing. In Theorem 4.5.1 we show that this "mimicry" is in fact a convergent numerical method.

Theorem 4.5.1. *Let R be a compact hyperbolic Riemann surface with a finite measured geodesic lamination (\mathcal{L}, σ) . Let $\{P_k\}$ be a sequence of finite bounded degree packings with mesh decreasing to zero corresponding to Riemann surfaces $\{R_k\}$ such that $R_k \rightarrow R$ as $k \rightarrow \infty$ in the Teichmüller metric. Then the surfaces $E_k(R_k) = \widehat{R}_k$ induced by the discrete earthquake maps E_k converge to the surface $E(R) = \widehat{R}$ under the earthquake map E induced by (\mathcal{L}, σ) .*

Proof. Let R be a compact hyperbolic Riemann surface, and let (\mathcal{L}, σ) be a finite measured geodesic lamination on R . In a sense, the proof of this result reduces to showing that the diagram (4.5.1) commutes.

$$\begin{array}{ccc}
 \{R, c_1, c_2, \dots, c_m\} & \xrightarrow{E} & \widehat{R} \\
 f_k \uparrow f_{j_k} & & \uparrow \hat{f}_k \\
 \{R_k, c_{1_k}, c_{2_k}, \dots, c_{m_k}\} & \xrightarrow{E_k} & \widehat{R}_k
 \end{array} \tag{4.5.1}$$

Note that requiring the mesh of the sequence of bounded degree packings $\{P_k\}$ to approach zero as $k \rightarrow \infty$ is equivalent to requiring that the radii of the circles in the packings approach zero. Thus, we are guaranteed the existence of such a sequence by Corollary 3.5.1. Further, the construction of the surfaces in the proof of Corollary 3.5.1 allows the freedom to control the degree of vertices adjacent to the geodesics along which we shear and graft.

The Teichmüller distance between the packable surfaces R_k and R is going to zero, so for each $k \in \mathbb{N}$ there exists a map $f_k : R_k \rightarrow R$ that respects the markings on R_k and R and is $1 + \varepsilon_k$ -quasiconformal, where $\varepsilon_k \rightarrow 0$ as $k \rightarrow \infty$, (i.e., as $k \rightarrow \infty$, $f_k \rightarrow f$, where f is conformal). More precisely, the map f_k consists of a map from the disk (or other model of the hyperbolic plane) to the disk through a map between the surfaces and their respective conformal structures. Where no ambiguity arises, however, we will speak about the map as $f_k : R_k \rightarrow R$.

Let $\{c_j\}_{j=1}^m$, be the cylinders grafted into the Riemann surface R by the finite earthquake E . For each $j = 1, 2, \dots, m$, let $\{c_{j_k}\}_{k \in \mathbb{N}}$ be a sequence of cylinders admitting a circle packing of finite, uniformly bounded degree so that $c_{j_k} \rightarrow c_j$ as $k \rightarrow \infty$ in the Teichmüller metric. Further, require that the mesh of the packing on c_{j_k} goes to zero as $k \rightarrow \infty$ for each $j = 1, 2, \dots, m$. Thus, for each $k \in \mathbb{N}$ there exists a map $f_{j_k} : c_{j_k} \rightarrow c_j$ that is $1 + \varepsilon_{j_k}$ -quasiconformal, where $\varepsilon_{j_k} \rightarrow 0$ as $k \rightarrow \infty$, $j = 1, 2, \dots, m$, (i.e., as $k \rightarrow \infty$, $f_{j_k} \rightarrow f_j$, where f_j is conformal).

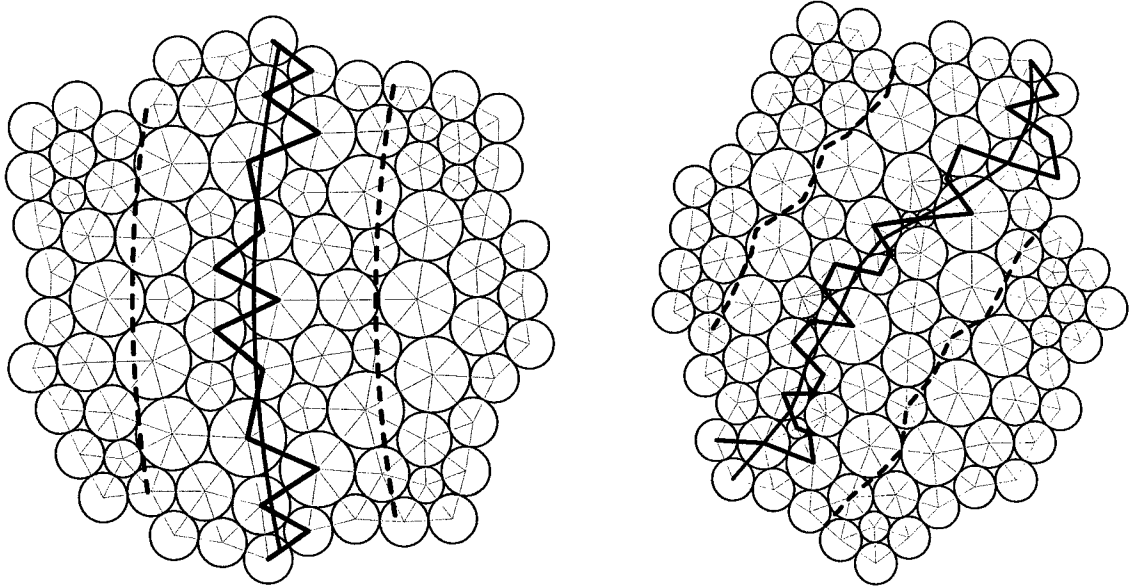
Let \widehat{R} be the image of R under the action of the earthquake E , and for each $k \in \mathbb{N}$ let \widehat{R}_k be the image of R_k under the action of a combinatorial earthquake E_k . We construct these combinatorial earthquakes by describing laminations on the surfaces R_k corresponding to the lamination on R . Since on a hyperbolic Riemann surface there is exactly one simple closed geodesic in each non-zero homotopy class [14, 29], corresponding to each geodesic in the lamination \mathcal{L} on R there is a unique geodesic on R_k in the corresponding homotopy class. Taking the collection of these geodesics, we have a finite measured geodesic lamination (\mathcal{L}_k, σ) on R_k . Notice that we have left the weights σ unchanged; we simply assign to each geodesic in \mathcal{L}_k the weight on the corresponding geodesic in R . Now, we have finite measured geodesic laminations on each $R_k, k \in \mathbb{N}$, and we may carry out the discrete shearing and welding operations of combinatorial earthquakes.

Around each geodesic $L^i, i = 1, 2, \dots, n$, in the lamination \mathcal{L} on R we place a collar, a neighborhood of uniform width isometric to a cylinder, so that no two such neighborhoods intersect. Call this collar C^i . Since the geodesics in the finite lamina-

tion are disjoint by construction, the Collar Theorem [14] guarantees that there exists such a collar about each geodesic. Similarly, about each geodesic $L_k^i, i = 1, 2, \dots, n$ in the lamination \mathcal{L}_k on R_k there exists a collar C_k^i such that the collection of collars on R_k is disjoint. We require that the collar C_k^i on R_k have width less than $\frac{1}{2}$ the width of the corresponding C^i on R . Now, since $R_k \rightarrow R$ in the Teichmüller metric, the maps between R_k and R are going to conformal maps and the markings on R_k are converging to the markings on R . Thus, for k sufficiently large, the image of the collar C_k^i under the map f_k is contained in the collar C^i , and, by construction, this containment is proper, (i.e., $f_k(C_k^i) \subsetneq C^i$ for all k sufficiently large). Further, since the mesh of the packings on R_k goes to zero, for k sufficiently large, the discrete geodesic ℓ_k^i corresponding to $L_k^i, i = 1, 2, \dots, n$, lies strictly within the interior of the collar C_k^i .

Consider the images of the collars C_k^i under the action of the discrete earthquake E_k . If the geodesic L_k^i about which we built the collar C_k^i has real weight, and thus induces only a discrete shearing action on the discrete geodesic, then there is no difficulty in defining what we will call a **quasicollar** on \widehat{R}_k as the image of C_k^i under E_k . The image of the discrete geodesic ℓ_k^i and the image of the geodesic L_k^i are contained in this quasicollar. This is shown in Figure 4.5, where the geodesic L_k^i is shown as a solid gray curve, the discrete geodesic ℓ_k^i is shown as a solid black, piecewise linear curve, and the collar C_k^i is denoted by dashed curves.

The case in which the weight on L_k^i has non-zero imaginary part is somewhat more problematic. The action of the earthquake in this case will divide the collar into two disjoint sets. Since the grafting (imaginary) component of the earthquake involves the insertion of a non-trivial cylinder, however, we may extend these disjoint regions at least one generation of triangles deep into the interior of the cylinder to create quasicollars about the ends of the inserted cylinder. (Note that since the mesh of the packing is going to zero, the region occupied by one generation of triangles is getting arbitrarily small.) Since the inserted cylinder has non-zero height, we may construct these quasicollars so that they are disjoint.



(a) Geodesic, Discrete Geodesic, and Collar on R_k

(b) Images under a Discrete Shearing Map

Figure 4.5: Geodesics, Discrete Geodesics, and Quasicollars

Define a pullback map $P_k : \widehat{R}_k \rightarrow \{R_k, c_{1_k}, \dots, c_{m_k}\}$ by letting $P_k(\hat{r})$ be the unique pre-image $r \in R_k$ of the point $\hat{r} \in \widehat{R}_k$ under the combinatorial earthquake E_k . Note that since the degree of the vertices in the complex on \widehat{R}_k is bounded and since, by construction, the angles in the packing on R_k are bounded away from zero, the map P_k is $1 + \hat{\varepsilon}_k$ -quasiconformal. Further, at any point isolated from the combinatorial geodesics, as $k \rightarrow \infty$ the number of generations of circles on the packed surfaces between that point and the combinatorial geodesics goes to infinity; thus, at any such point, Lemma 3.2.4, the Packing Lemma, guarantees that the dilatation of the maps P_k goes to 1 as $k \rightarrow \infty$, (i.e., as $k \rightarrow \infty$, on points isolated from the combinatorial geodesics, $P_k \rightarrow \widehat{P}$, where \widehat{P} is conformal).

Since each of R , R_k , and \widehat{R}_k are Riemann surfaces, they each have a conformal structure; in the case of R_k and \widehat{R}_k , they inherit their conformal structures from their packings. Let $\{\varphi_\nu\}_{\nu \in \Upsilon}$, $\{\psi_\nu\}_{\nu \in N}$, $\{\varphi_{k_\nu}\}_{\nu \in \Upsilon_k}$, and $\{\psi_{k_\nu}\}_{\nu \in N_k}$ be the collection of coordinate charts in the conformal structure on R , \widehat{R} , R_k , and \widehat{R}_k , respectively. Note that the structure on \widehat{R} will be the structure described in Section 2.6. Now,

we consider a collection of maps $\hat{f}_k : \hat{R}_k \rightarrow \hat{R}$, each defined on open sets in \hat{R}_k . Let $U \subset \hat{R}_k$.

Case I: Suppose $U \subset \hat{R}_k$ is an open set such that U does not intersect the interior of any quasicollar, and U does not intersect any cylinder inserted by the earthquake E_k . Associated with this open set in \hat{R}_k we have a coordinate chart $\psi_{k\nu}$. Now, the map $P^{-1} \circ f_k \circ P_k \circ \psi_{k\nu}^{-1}$ takes an open subset of the unit disk \mathbb{D} corresponding to the pair $(U, \psi_{k\nu})$ to an open subset $U_\alpha \subset \hat{R}$ so that $U_\alpha \in U_A$, as described in Section 2.6. Corresponding to U_α , we take from the conformal structure on \hat{R} described in Section 2.6 a coordinate chart ψ_α . Thus we have the following:

$$\begin{aligned} \psi_\alpha \circ P^{-1} \circ f_k \circ P_k \circ \psi_{k\nu}^{-1} &= \varphi_\alpha \circ P \circ P^{-1} \circ f_k \circ P_k \circ \psi_{k\nu}^{-1} \\ &= \varphi_\alpha \circ f_k \circ P_k \circ \psi_{k\nu}^{-1}. \end{aligned}$$

Since φ_α and $\psi_{k\nu}^{-1}$ are conformal (or 1-quasiconformal) and the maps f_k and P_k are $(1 + \varepsilon_k)$ -quasiconformal and $(1 + \hat{\varepsilon}_k)$ -quasiconformal, respectively, the map thus described is $(1 + \varepsilon_k)(1 + \hat{\varepsilon}_k)$ -quasiconformal, by Lemma 2.4.1. Note that ε_k and $\hat{\varepsilon}_k$ are independent of the set U , since they depend only on the maps f_k and P_k , which are globally $(1 + \varepsilon_k)$ -quasiconformal and $(1 + \hat{\varepsilon}_k)$ -quasiconformal, respectively. By construction, U is isolated in \hat{R}_k from the images of the geodesics defining the earthquake E_k , and $\varepsilon_k, \hat{\varepsilon}_k \rightarrow 0$ as $k \rightarrow \infty$. Thus, as $k \rightarrow \infty$, the map $\psi_\alpha \circ P^{-1} \circ f_k \circ P_k \circ \psi_{k\nu}^{-1} : \hat{R}_k \rightarrow \hat{R}$ approaches a conformal map.

Case II: Suppose $U \subset \hat{R}_k$ is an open set such that U does not intersect the interior of any quasicollar, and U is contained in the interior of some cylinder inserted by the earthquake E_k . Associated with this open set in \hat{R}_k we have a coordinate chart $\psi_{k\nu}$. Now, the map $P^{-1} \circ f_k \circ P_k \circ \psi_{k\nu}^{-1}$ takes an open subset of the unit disk \mathbb{D} corresponding to the coordinate pair $(U, \psi_{k\nu})$ from the conformal structure on R_k to an open subset $U_\beta \subset \hat{R}$ so that $U_\beta \in U_B$, as described in Section 2.6. Corresponding to U_β , we take from the conformal structure on \hat{R} described in Section 2.6 a coordinate chart ψ_β .

Thus we have the following:

$$\begin{aligned}\psi_\beta \circ P^{-1} \circ f_{j_k} \circ P_k \circ \psi_{k_\nu}^{-1} &= M_j \circ g_\beta^j \circ \phi_\beta^j \circ P \circ P^{-1} \circ f_{j_k} \circ P_k \circ \psi_{k_\nu}^{-1} \\ &= M_j \circ g_\beta^j \circ \phi_\beta^j \circ f_{j_k} \circ P_k \circ \psi_{k_\nu}^{-1}.\end{aligned}$$

Since $M_j \circ g_\beta^j \circ \phi_\beta^j$ and $\psi_{k_\nu}^{-1}$ are conformal (or 1-quasiconformal) and the maps f_{j_k} and P_k are $(1 + \varepsilon_{j_k})$ -quasiconformal and $(1 + \hat{\varepsilon}_k)$ -quasiconformal, respectively, the map thus described is $(1 + \varepsilon_{j_k})(1 + \hat{\varepsilon}_k)$ -quasiconformal. Again, we note that the constants describing the deviation from conformality, ε_{j_k} and $\hat{\varepsilon}_k$, are independent of the choice of U . By construction, U is isolated in \widehat{R}_k from the images of the geodesics defining the earthquake E_k , and $\varepsilon_{j_k}, \hat{\varepsilon}_k \rightarrow 0$ as $k \rightarrow \infty$. Thus, as $k \rightarrow \infty$, the map $\psi_\beta \circ P^{-1} \circ f_{j_k} \circ P_k \circ \psi_{k_\nu}^{-1} : \widehat{R}_k \rightarrow \widehat{R}$ approaches a conformal map.

Case III: Suppose that U is a small open subset of \widehat{R}_k such that U intersects $E_k(\ell_k^i)$ for some $i = 1, 2, \dots, n$, and U intersects the boundary of the quasicollar \widehat{C}_k^i associated with L_k^i . Corresponding to U we have a coordinate chart ψ_{k_ν} . Now, we have two cases to consider depending on whether the weight on the geodesic L^i has non-zero imaginary part.

Case IIIa: Suppose $\text{Im}(\sigma(L^i)) = 0$; that is, the earthquake action on the geodesic L^i involves only a shearing action. This gives that the map P_k takes U to a subset of R_k such that $P_k(U) \not\subseteq C_k^i$ and $P_k(U) \cap \ell_k^i \neq \emptyset$, as shown in Figure 4.6.

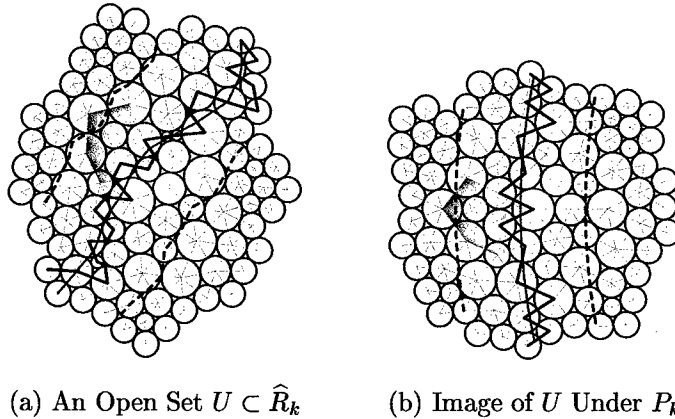


Figure 4.6: Pullback of Geodesics, Discrete Geodesics, and Quasicollars

Note that in Figure 4.6b we have included the refining edges associated with the shearing so that there is a bijection between individual triangles in Figure 4.6a and Figure 4.6b.

Now, we wish to send this set $P_k(U)$ to a subset of R , but there is a geometric difficulty to be resolved. The “halves” of $P_k(U)$ have as one portion of their boundaries a segment of the discrete geodesic ℓ_k^i . We need these segments of their boundaries to lie on the actual geodesic L_k^i in R_k . The problem is easily resolved, at the expense of admitting some quasiconformality in our eventual transformation, by the application of the hyperbolic projection p_k^i described in Section 4.2, as illustrated in Figure 4.7.

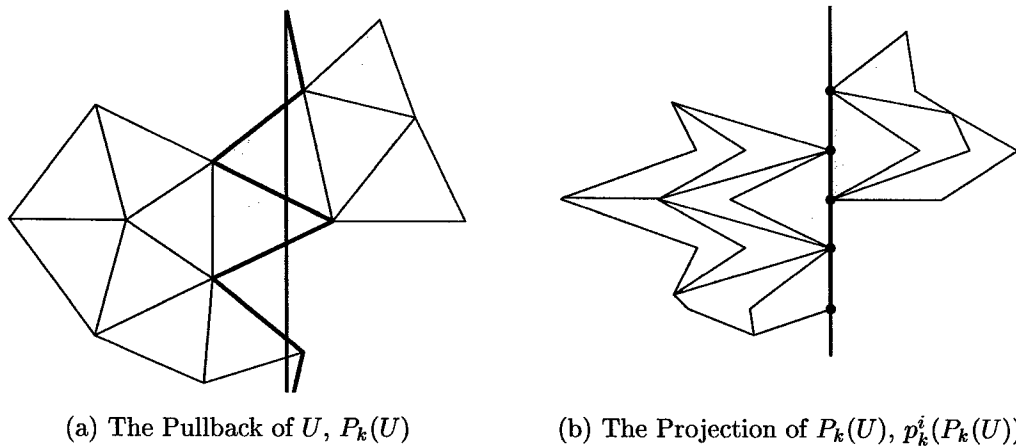


Figure 4.7: Projection of Geodesics, Discrete Geodesics, and Quasicollars

This p_k^i map on the set $P_k(U)$ is $1 + \tilde{\varepsilon}_k$ -quasiconformal, but Proposition 4.2.1 guarantees that p_k^i converges uniformly to the identity; so $\tilde{\varepsilon}_k \rightarrow 0$ as $k \rightarrow \infty$. Further, the constant $\tilde{\varepsilon}_k$ is independent of the choice of U . This independence is a result of two facts. First, the projection associated with any given geodesic L^i and the accompanying discrete geodesic ℓ_k^i has a quasiconformality constant uniform across the entire geodesic. Second, there are only finitely many geodesics for which we must use these projections. Taking the maximum such quasiconformal constant as $\tilde{\varepsilon}_k$, we have independence of the choice for U .

Corresponding to the set $p_k^i(P_k(U)) \subset R_k$, or more precisely to some open subset of R_k containing $p_k^i(P_k(U)) \subset R_k$, we have a coordinate chart φ_{k_v} which takes $p_k^i(P_k(U))$

to a subset of a fundamental region for R_k in the Poincaré unit disk, \mathbb{D} . The image of $p_k^i(P_k(U)) \cap L_k^i$ under this map is thus an arc of a hyperbolic geodesic in \mathbb{D} . There exists a disk automorphism $M_k^U : \mathbb{D} \rightarrow \mathbb{D}$ such that $M_k^U(\varphi_{k_v}(p_k^i(P_k(U))) \cap L_k^i)$ is a small arc of a hyperbolic geodesic in \mathbb{D} that is the projection of the geodesic L^i in R . We may choose this arc of the projection of L^i sufficiently small that the set $M_k^U(\varphi_{k_v}(p_k^i(P_k(U))))$ is contained in a single fundamental region for R .

Now, a second difficulty arising from the projection operation must be addressed. If we were to apply a shearing map on the lift of the geodesic L^i which separates the “halves” of $M_k^U(\varphi_{k_v}(p_k^i(P_k(U))))$ using the weight associated with L^i , the sides will not necessarily match along the geodesic, as illustrated in Figure 4.8.

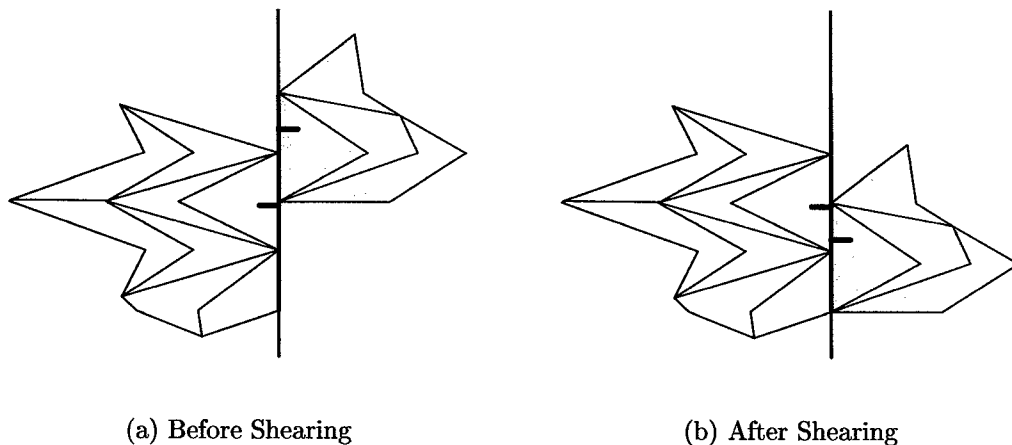


Figure 4.8: Misalignment under Pullback, Projection, and Shearing

The difference along the geodesic is a quasismetry on one half of the intersection with L^i , however, and extends to a $1 + \bar{\varepsilon}_k$ -quasiconformal map, Q_k^U , in the corresponding half of $M_k^U(\varphi_{k_v}(p_k^i(P_k(U))))$ [24, 33]. Recall, however, that the quasismetry and associated quasiconformal map arise as a result of the need for a hyperbolic projection p_k^i to correct the difference between the geodesic L_k^i and the discrete geodesic ℓ_k^i . Lemma 4.1.1 guarantees that $\ell_k^i \rightarrow L_k^i$ uniformly as $k \rightarrow \infty$. Thus, $\bar{\varepsilon}_k \rightarrow 0$ as $k \rightarrow \infty$. Further, since the quasiconformality of M_k^U depends only on the quasismetry associated with the projection p_k^i , $\bar{\varepsilon}_k$ is independent of the choice of U .

Corresponding to the set $Q_k^U(M_k^U(\varphi_{k_v}(p_k^i(P_k(U)))) \subset \mathbb{D}$, we have a map from the

conformal structure on R , φ_v^{-1} , taking this set to an open set on R intersecting the geodesic L^i . (Again, the coordinate chart really comes from an open set containing the set of interest.) Notice that as a result of applying the correction Q_k^U , the two halves of this image (on either side of the lift to \mathbb{D} of the geodesic L^i) now match the action of the shearing caused by P^{-1} . We now apply P^{-1} , to obtain a set $V \subset \widehat{R}$. Corresponding to this open set we have a coordinate chart from the conformal structure on \widehat{R} defined in Section 2.6. Since $V \in U_\Gamma$, as described in Section 2.6, we have a coordinate chart ψ_γ corresponding to V . This gives the following:

$$\begin{aligned} & \psi_\gamma \circ P^{-1} \circ \varphi_v^{-1} \circ Q_k^U \circ M_k^U \circ \varphi_{k_v} \circ p_k^i \circ P_k \circ \varphi_{k_v}^{-1} \\ = & S_\gamma \circ \varphi_\gamma \circ P \circ P^{-1} \circ \varphi_v^{-1} \circ Q_k^U \circ M_k^U \circ \varphi_{k_v} \circ p_k^i \circ P_k \circ \varphi_{k_v}^{-1} \\ = & S_\gamma \circ \varphi_\gamma \circ \varphi_v^{-1} \circ Q_k^U \circ M_k^U \circ \varphi_{k_v} \circ p_k^i \circ P_k \circ \varphi_{k_v}^{-1}. \end{aligned}$$

This map is $(1 + \bar{\varepsilon}_k)(1 + \tilde{\varepsilon}_k)(1 + \hat{\varepsilon}_k)$ -quasiconformal, where this quasiconformality is independent of the choice for U . Now, consider the dilatation at a point $u \in U$. If u is not contained in the set $E_k(\ell_k^i)$, then Lemma 3.2.4, the packing Lemma, guarantees that the dilatation at u goes to 1 since each of $\bar{\varepsilon}_k, \tilde{\varepsilon}_k, \hat{\varepsilon}_k \rightarrow 0$ as $k \rightarrow \infty$. Thus, this map from \widehat{R}_k to \widehat{R} converges to a conformal map, except perhaps on the image of the discrete geodesic ℓ_k^i under the earthquake E_k . But this set has measure zero, and the map is continuous. Thus, the limit map is conformal on all of U [33].

Case IIIb: Suppose $\text{Im}(\sigma(L^i)) > 0$; that is, the earthquake action on the geodesic L^i is a grafting action (and potentially a shearing action as well). The situation here is somewhat more complicated than the previous case since the map P_k takes the portion of U on the inserted cylinder to a cylinder c_{j_k} and the remaining points of U to a subset of R_k . We will deal with the maps on these two subsets of U separately.

First, consider that subset of U which is taken to R_k . Call this subset U_1 . $P_k(U_1) \not\subset C_k^i$ and $P_k(U_1) \cap \ell_k^i \neq \emptyset$. We wish to send this set $P_k(U_1)$ to a subset of R , but there is a geometric difficulty to be resolved. $P_k(U_1)$ has as one portion of its boundary a segment of the discrete geodesic ℓ_k^i ; we need this segment of the boundary to lie on the actual geodesic L_k^i in R_k . As before, this problem is easily addressed, at the

expense of admitting some quasiconformality into our eventual transformation, by the application of the hyperbolic projection p_k^i described in Section 4.2. This map on the set $P_k(U_1)$ is $1 + \tilde{\varepsilon}_k$ -quasiconformal, but Proposition 4.2.1 guarantees that p_k^i converges uniformly to the identity; so $\tilde{\varepsilon}_k \rightarrow 0$ as $k \rightarrow \infty$. As in Case IIIa, $\tilde{\varepsilon}_k$ is independent of the choice of U .

Corresponding to the set $p_k^i(P_k(U_1)) \subset R_k$, or more precisely to some open subset of R_k containing $p_k^i(P_k(U_1)) \subset R_k$, we have a coordinate chart φ_{k_v} which takes $p_k^i(P_k(U_1))$ to a subset of a fundamental region for R_k in the Poincaré unit disk, \mathbb{D} . The image of $p_k^i(P_k(U_1)) \cap L_k^i$ under this map is thus an arc of a hyperbolic geodesic in \mathbb{D} . There exists a disk automorphism $M_k^U : \mathbb{D} \rightarrow \mathbb{D}$ such that $M_k^U(\varphi_{k_v}(p_k^i(P_k(U_1)))) \cap L_k^i$ is a small arc of the hyperbolic geodesic in \mathbb{D} that results from the lift of the geodesic L^i in R . We may choose M_k^U such that the set $M_k^U(\varphi_{k_v}(p_k^i(P_k(U_1))))$ is an open set intersecting this geodesic in a fundamental region for R .

Again, we will require a correction to compensate for the effect of the hyperbolic projection p_k^i . Call this correction Q_k^U , and note that this map is a quasisymmetry on the intersection with the lift of the geodesic L^i and is $(1 + \bar{\varepsilon}_k)$ -quasiconformal, as in Case IIIa. Again, the quasiconformality constant $\bar{\varepsilon}_k$ is independent of the choice for U .

Corresponding to the set $Q_k^U(M_k^U(\varphi_{k_v}(p_k^i(P_k(U_1)))) \subset \mathbb{D}$, we have a map from the conformal structure on R , φ_v^{-1} , taking this set to an open set on R intersecting the geodesic L^i . (Again, the coordinate chart really comes from an open set containing the set of interest.) We now apply P^{-1} , to obtain a set $V_1 \subset \widehat{R}$ adjoining the edge of an inserted cylinder c_j .

Now, consider that subset of U which is taken into c_{j_k} . Call this subset U_2 . $P_k(U_2) \subset c_{j_k}$ and $P_k(U_2)$ intersects the boundary of the cylinder c_{j_k} . We take this set into the cylinder c_j via the $1 + \tilde{\varepsilon}_k$ -quasiconformal map f_{j_k} , where $\tilde{\varepsilon}_k$ is independent of the choice of U , since we may choose $\tilde{\varepsilon}_k$ as the maximum of the constants associated with the finitely many cylinders $\{c_j\}$. We then apply the map P^{-1} to obtain a set $V_2 \subset \widehat{R}$.

The way we have constructed these maps, in particular the application of the map p_k^i , ensures that the set $V = V_1 \cup V_2 \subset \widehat{R}$ is an element of the collection U_Δ as described in Section 2.6. Corresponding to this set V we have a coordinate chart ψ_δ from the conformal structure on \widehat{R} given in Section 2.6. This gives the following piecewise map $\Pi_k : \widehat{R}_k \rightarrow \widehat{R}$:

$$\Pi_k(u) = \begin{cases} \psi_\delta \circ P^{-1} \circ \varphi_v^{-1} \circ Q_k^U \circ M_k^U \circ \varphi_{k_v} \circ p_k^i \circ P_k \circ \psi_{k_v}^{-1}(u) & \text{if } u \in U_1 \subset \widehat{R}_k \\ \psi_\delta \circ P^{-1} \circ f_{j_k} \circ P_k \circ \psi_{k_v}^{-1}(u) & \text{if } u \in U_2 \subset \widehat{R}_k. \end{cases}$$

The first of these maps, for $u \in U_1$, is $(1 + \bar{\varepsilon}_k)(1 + \tilde{\varepsilon}_k)(1 + \hat{\varepsilon}_k)$ -quasiconformal. The second map, for $u \in U_2$, is $(1 + \varepsilon_{j_k})(1 + \hat{\varepsilon}_k)$ -quasiconformal. As we have shown, each of these constants is independent of the choice of U . Now, consider the dilatation at a point $u \in U$. If u is not contained in the set $E_k(\ell_k^i)$, then Lemma 3.2.4, the packing Lemma, guarantees that the dilatation at u goes to 1 since each of $\bar{\varepsilon}_k, \tilde{\varepsilon}_k, \hat{\varepsilon}_k, \varepsilon_{j_k} \rightarrow 0$ as $k \rightarrow \infty$. Thus, this piecewise map Π_k from \widehat{R}_k to \widehat{R} converges to a conformal map Π , except perhaps on the image of the discrete geodesic ℓ_k^i under the earthquake E_k . But this set has measure zero, and the map is continuous. Thus, the map Π is conformal on all of U [33].

Thus, as $k \rightarrow \infty$ the maps from \widehat{R}_k to \widehat{R} are becoming conformal, and, by construction, the markings on surfaces \widehat{R} and \widehat{R}_k are consistent. Therefore, the surfaces \widehat{R}_k converge to a surface conformally equivalent to \widehat{R} with equivalent markings; but this is equivalent to saying $\widehat{R}_k \rightarrow \widehat{R}$ (in the Teichmüller metric) as $k \rightarrow \infty$, and the result is shown. \square

CHAPTER V

EARTHQUAKES ON EUCLIDEAN SURFACES

In the work of Thurston [51], McMullen [35], and others [16, 21, 23, 24, 25, 40, 54], earthquake maps are confined to hyperbolic Riemann surfaces. To this point, we have similarly limited the scope of our attention, examining only the approximation of these complex earthquakes, shearing and grafting maps on hyperbolic Riemann surfaces. We now turn our attention to the question of whether or not we can meaningfully define earthquake maps on the Teichmüller space of Euclidean Riemann surfaces. In this chapter we address four basic issues related to earthquakes on tori. Initially, we have a question of definition; we must define those earthquakes. Given this definition, we have three problems we must address. First, we must determine whether or not the earthquakes thus defined are transformations of points in the Teichmüller space of tori. That is, is the image of a torus under a Euclidean earthquake another torus? Second, we must determine whether or not the Euclidean earthquakes thus defined exhibit properties similar to those of the hyperbolic earthquakes. Finally, can we approximate the action of these Euclidean earthquakes using circle packing?

5.1 Defining Earthquakes on the Torus

From the perspective of shearing and grafting maps on the Riemann surface, we define (Euclidean) earthquakes on tori in a manner analogous to the manner in which those maps were defined on hyperbolic surfaces. That is, we define a shearing by opening the torus along a geodesic, twisting by a prescribed amount, and gluing the surface back together along the seam of the geodesic. Similarly, we define a grafting by opening the torus along a geodesic, inserting a cylinder of some prescribed height, and gluing the surface together.

To define such an action, we first need to discuss finite measured geodesic laminations of tori. Recall that in constructing earthquakes on hyperbolic surfaces we used the Poincaré unit disk and the upper half plane (with appropriate metrics) to

describe the earthquake action. We have a similar construction here, where we use the Euclidean (rather than hyperbolic) upper half-plane \mathbb{H} as a lifting cover for the Euclidean surface, the torus. We restrict ourselves to the upper half-plane so that each point in the Teichmüller space of tori is uniquely defined (after normalization) by a single point $\omega \in \mathbb{H}$ [29, 30]. We now define a finite Euclidean geodesic lamination on a torus.

Definition 5.1.1. *A finite geodesic lamination \mathcal{L} of the Euclidean torus T is a collection of finitely many disjoint geodesics on T which lifts to a collection of disjoint (and thus parallel) Euclidean lines in the upper half-plane \mathbb{H} .*

Note that the structure of the Euclidean plane dictates that in a finite geodesic lamination of the plane consisting of more than a single geodesic, those geodesics must all be parallel (in a Euclidean sense). This limits substantially the forms that such a lamination may take in the Euclidean case; we have less freedom in constructing these laminations than in the hyperbolic case since we have only one “point at infinity.” Just as in the hyperbolic case, we place a measure on the lamination \mathcal{L} .

Definition 5.1.2. *A finite geodesic lamination \mathcal{L} of the Euclidean plane \mathbb{C} is a collection of finitely many disjoint Euclidean lines (geodesics). In this way, \mathcal{L} divides \mathbb{H} into disjoint strips.*

Recall that the construction of complex earthquakes on hyperbolic surfaces required the use of hyperbolic isometries. In the Euclidean complex plane, the isometries we need are simply translations $z + \alpha, \alpha \in \mathbb{C}$. A shearing map arises from a translation with axis parallel to the geodesic along which we wish to shear, and a grafting map arises from a translation with axis perpendicular to the geodesic along which we intend to graft. In grafting, we insert finite cylinders, and in the plane this is represented by the insertion of a finite strip into the gap created by the piecewise application of the grafting translation (with axis perpendicular to the geodesic). Note that we may select this finite strip (essentially a Euclidean parallelogram) so that its

generators (and thus the marking) are consistent with the generators (and thus the marking) that defines the Teichmüller space under examination.

We model the actions of shearing and grafting on a torus on the fundamental regions for the tori in the upper half-plane, just as we used the upper half-plane (and the Poincaré unit disk) to model hyperbolic earthquakes. These four actions, left and right shearing and positive and negative grafting, are illustrated in Figure 5.1. We then define complex Euclidean earthquakes, earthquakes with complex weights, as the composition of Euclidean shearing and then Euclidean grafting operations. Recall that in the hyperbolic case we claimed that the term complex earthquake was illustrative in that the earthquake action was described as multiplication by a complex number in the local model on \mathbb{H} . A similar idea holds in the case of Euclidean earthquakes; rather than multiplication by a complex number, we now transform defining points in the fundamental region through the addition of a complex number.

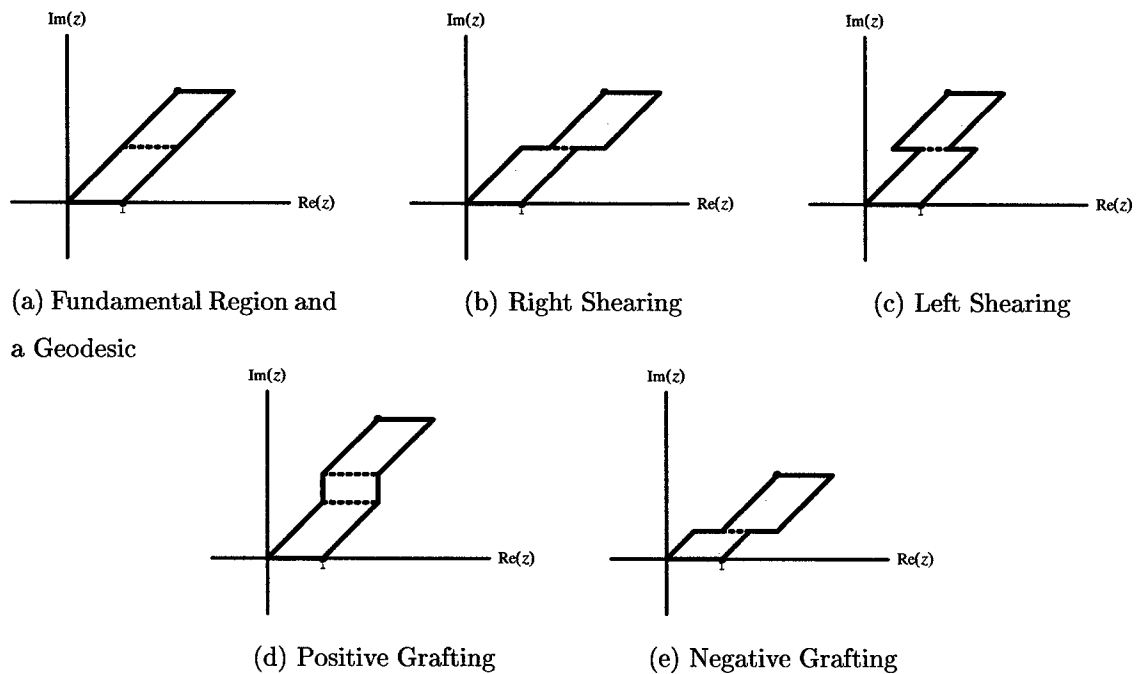


Figure 5.1: Earthquake Actions on the Fundamental Region of a Torus

Note that in constructing these Euclidean earthquake maps, we place some restrictions on the weights. First, consider the imaginary part (grafting component) of

the complex weights. In [35], positive grafts of any size were permitted, but negative grafts (amounting to removal of portions of the surface) required some restrictions for obvious geometric reasons. We must restrict negative grafting weights similarly in the Euclidean case. There are two reasons for this restriction. First, we do not want to remove so much in a negative graft along a particular geodesic that we remove another geodesic. Second, we must not remove all of the torus remaining in one direction.

5.2 A Conformal Structure on the Images of Tori under Complex Earthquake Maps

We can now turn to the first of our outstanding problems, Problem 5.2.1.

Problem 5.2.1. *Do earthquakes on Euclidean surfaces, and in particular compact tori, result in Riemann surfaces? That is, are shearing and grafting maps defined on tori transformations in the Teichmüller space of tori?*

Suppose that we apply a finite complex Euclidean earthquake E induced by a finite measured geodesic lamination (\mathcal{L}, σ) to the torus T (a compact Euclidean Riemann surface), where the lamination consists of n geodesics with complex weights $\sigma(L_i) = \mu_q + i\lambda_q, 1 \leq q \leq n$, where $\mu_q \in \mathbb{R}$ and $\lambda_q \in \mathbb{R}$ such that λ_q , if negative, is sufficiently small so that the execution of the negative grafting operation does not remove another geodesic in the lamination and does not reduce the torus to a degenerate surface. This earthquake thus involves both shearing maps and grafting maps composed to form the complex earthquake.

Since T is a fixed Riemann surface, it has a conformal structure associated with it; say $\{\varphi_v\}_{v \in \Upsilon}$ is the atlas for the conformal structure on T . Further, since each grafting map with positive imaginary weight involves the insertion of a cylinder c_j , we have a conformal structure associated with each such cylinder so that the coordinate charts map c_j to subsets of a Euclidean strip. For each of $c_j, 0 \leq j \leq m$, where m gives the number of geodesics in the lamination \mathcal{L} which have positive imaginary components

for their weights, let $\{\phi_k^j\}_{k \in K}$ be the atlas associated with each such cylinder.

Define a pullback map P on \widehat{T} so that the image of a point $\tau \in \widehat{T}$ under P is the unique point (on T or on one of the cylinders c_j) whose image under the complex earthquake E is τ .

With this information we now define a conformal structure on the Riemann surface \widehat{T} , the image of T under the complex earthquake E . To define this conformal structure we need only describe a set of coordinate charts mapping open regions in the surface \widehat{T} into \mathbb{C} so that the transition maps associated with the coordinate charts are analytic. It is sufficient to construct for every point $\tau \in \widehat{T}$ a map from an open neighborhood $U \subset \widehat{T}$ into \mathbb{C} so that these maps satisfy the analyticity condition. We consider open sets of the following five classes.

1. U_A is the collection of all open sets $U_\alpha \subset \widehat{T}$ such that U_α does not intersect the image under the earthquake E of any geodesic $L_i, 1 \leq i \leq n$, and is disjoint from every inserted cylinder $c_j, 1 \leq j \leq m$.
2. U_B is the collection of all open sets $U_\beta \subset \widehat{T}$ such that $U_\beta \subset E(c_j)$ for some $j, 1 \leq j \leq m$.
3. U_Γ is the collection of all open sets $U_\gamma \subset \widehat{T}$ such that U_γ intersects $E(L_i)$ for exactly one value $i, 1 \leq i \leq n$, where $\sigma(L_i) \in \mathbb{R}$, (i.e., the only map on that geodesic is a shearing operation).
4. U_Δ is the collection of all open sets $U_\delta \subset \widehat{T}$ such that U_δ intersects both $P^{-1}(R)$ and $E(c_j)$ for some $j, 1 \leq j \leq m$.
5. U_Ξ is the collection of all open sets $U_\xi \subset \widehat{T}$ such that U_ξ intersects the image of the boundary of some cylinder removed by the action of a negative grafting action.

An illustration of representative sets from these classes is given in Figure 5.2.

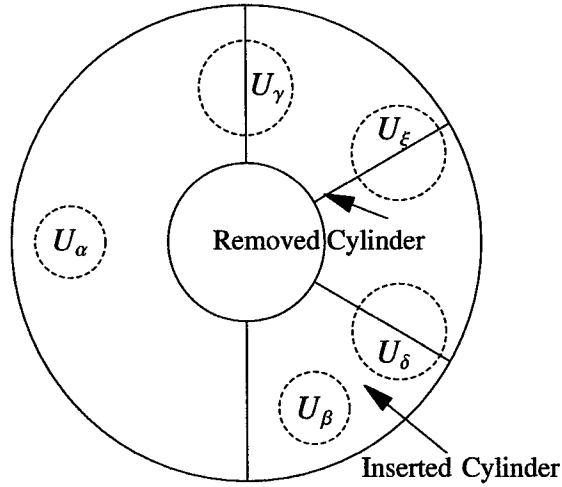
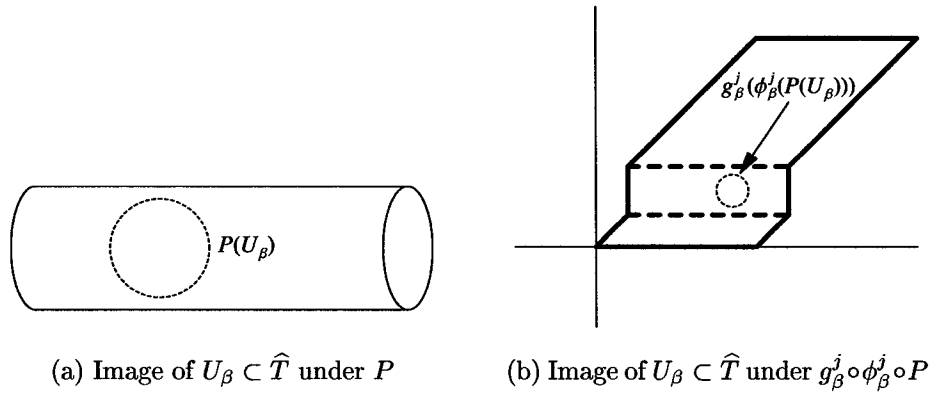


Figure 5.2: Open Sets to Define a Conformal Structure on the Torus \hat{T}

Case I: Let $U_\alpha \in U_A$, and note that $P(U_\alpha)$ is an open set in T . From the conformal structure on T and corresponding to this open set $P(U_\alpha)$ we have a coordinate chart φ_α such that $\varphi_\alpha(P(U_\alpha)) \subset \mathbb{C}$. We thus define a coordinate chart $\psi_\alpha : \hat{T} \rightarrow \mathbb{C}$ on the open set U_α by $\psi_\alpha = \varphi_\alpha \circ P$. In this way we define a family of coordinate charts Ψ_A on \hat{T} by $\Psi_A = \{\psi_\alpha\}_{\alpha \in A}$.



(a) Image of $U_\beta \subset \hat{T}$ under P

(b) Image of $U_\beta \subset \hat{T}$ under $g_\beta^j \circ \phi_\beta^j \circ P$

Figure 5.3: Construction of Coordinate Charts for Open Sets U_β

Case II: Let $U_\beta \in U_B$. In this case, $U_\beta \subset \text{Int}(E(c_j))$, for some $1 \leq j \leq m$, and the pullback map P takes this set to an open set on the finite cylinder c_j as shown in Figure 5.3a. Now, from the conformal structure on c_j we have a coordinate chart ϕ_β^j

corresponding to $P(U_\beta)$ such that $\phi_\beta^j(P(U_\beta))$ is a subset of an infinite Euclidean strip of uniform width determined by the complex part of the weight on the appropriate geodesic in \mathcal{L} . We then have a grafting map g_β^j that opens the plane along the corresponding geodesic in \mathcal{C} and glues in the strip as shown in Figure 5.3b. This gives us a map $\psi_\beta : \widehat{T} \rightarrow \mathbb{C}$ on the open set U_β defined by $\psi_\beta = g_\beta^j \circ \phi_\beta^j \circ P$. In this way we define a family of coordinate charts Ψ_B on \widehat{T} by $\Psi_B = \{\psi_\beta\}_{\beta \in B}$.

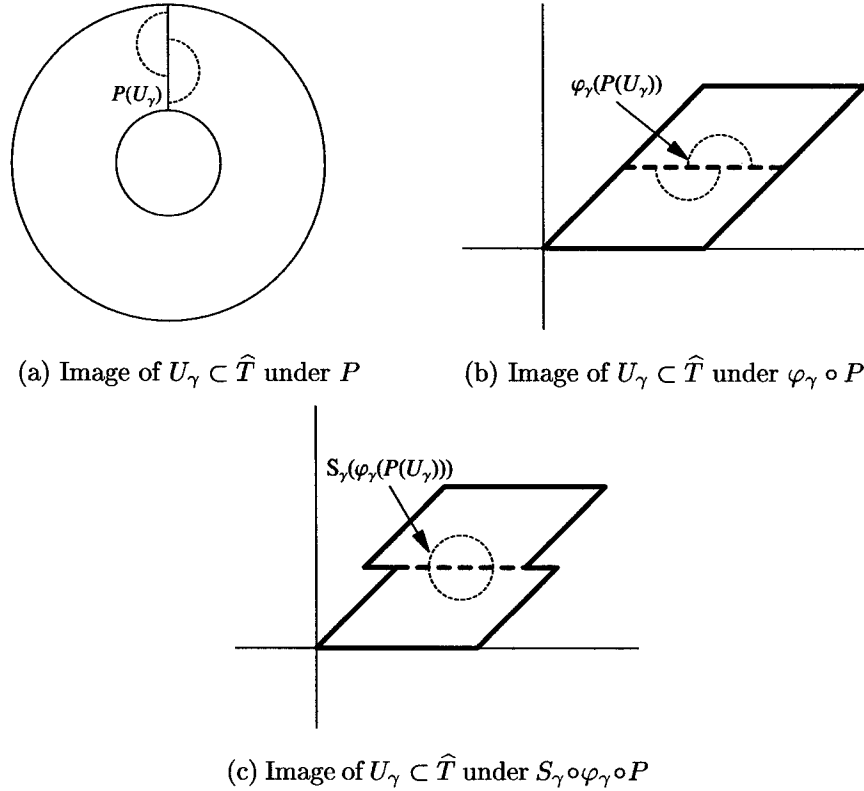


Figure 5.4: Construction of Coordinate Charts for Open Sets U_γ

Case III: Let $U_\gamma \in U_\Gamma$, and note that $P(U_\gamma)$ is a set as shown in Figure 5.4a. From the conformal structure on T and corresponding to an open set containing $P(U_\gamma)$ we have a map φ_γ such that $\varphi_\gamma(P(U_\gamma)) \subset \mathbb{C}$. Now, we have disjoint sets that differ by the application of a Euclidean shearing map (a piecewise translation), S_γ , along the axis determined by the geodesic shown in Figure 5.4b. We have thus defined a coordinate chart $\psi_\gamma : \widehat{T} \rightarrow \mathbb{C}$ on the open set U_γ by $\psi_\gamma = S_\gamma \circ \varphi_\gamma \circ P$. In this way, we

define a family of coordinate charts $\Psi_\Gamma = \{\psi_\gamma\}_{\gamma \in \Gamma}$.

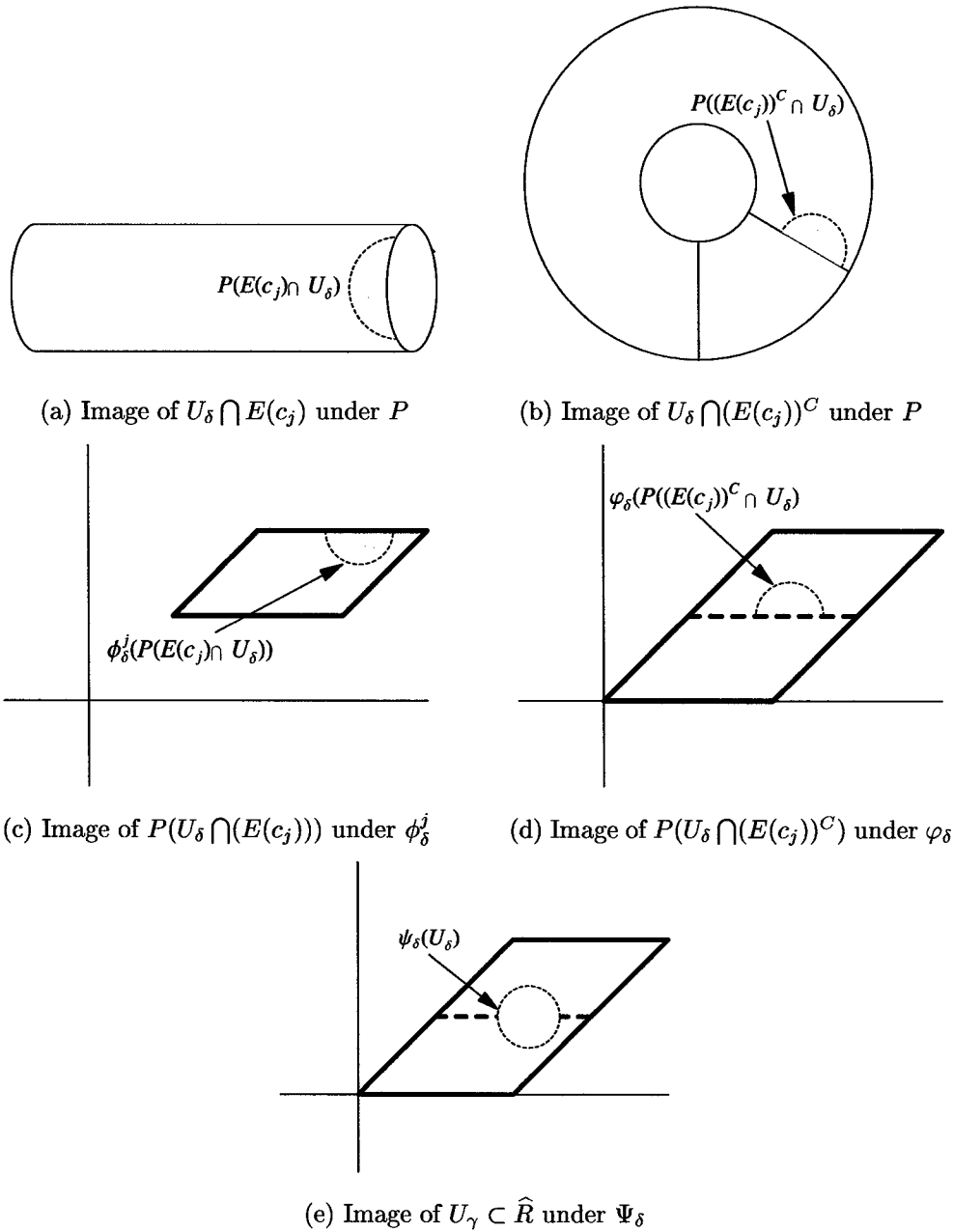


Figure 5.5: Construction of Coordinate Charts for Open Sets U_δ

Case IV: Let $U_\delta \in U_\Delta$, and note that $P(U_\delta)$ is divided between two distinct Riemann surfaces c_j , as shown in Figure 5.5a, and T , as shown in Figure 5.5b. To define coordinate charts on set of the form U_δ we define a pair of maps from these

surfaces to the upper half-plane \mathbb{H} . Beginning with the cylinder, we have a map ϕ_δ^j such that $\phi_\delta^j(P(E(c_j) \cap U_\delta))$ is a Euclidean strip of uniform width determined by the complex part of the weight on the appropriate geodesic in \mathcal{L} as shown in Figure 5.5c. At the same time, from the conformal structure on T we have a map φ_δ such that $\varphi_\delta(P((E(c_j))^C \cap U_\delta)) \subset \mathbb{H}$ as shown in Figure 5.5d. Applying the grafting map g_δ^j we put the pieces back together in \mathbb{H} . Now, we may need to shear along the hyperbolic geodesic whose image to this point is the imaginary axis in Figure 5.5d; this will depend upon whether or not the geodesic associated with this grafting action had a weight with non-zero real part. Note that the shearing will take place along that portion of the set not intersecting $E(c_j)$, since we define complex earthquakes as the composition of shearing and grafting maps, in that order.

$$\psi_\delta(\tau) = \begin{cases} g_\delta^j \circ \phi_\delta^j \circ P(\tau) & \text{if } \tau \in E(c_j) \cap U_\delta \subset \widehat{T} \\ S_\delta \circ g_\delta^j \circ \varphi_\delta \circ P(\tau) & \text{if } \tau \in (E(c_j))^C \cap U_\delta \subset \widehat{T} \end{cases} \quad (5.2.1)$$

This function now defines a map $\psi_\delta : \widehat{T} \rightarrow \mathbb{C}$ on the open set U_δ , as shown in Figure 5.5e. Taking all such functions over the set of possible sets $U_\delta \in U_\Delta$, we define a family of coordinate charts $\Psi_\Delta = \{\psi_\delta\}_{\delta \in \Delta}$.

Case V: Let $U_\xi \in U_\Xi$, and note that $P(U_\xi)$ is a set as shown in Figure 5.6a. From the conformal structure on T and corresponding to an open set containing $P(U_\xi)$ we have a map φ_ξ such that $\varphi_\xi(P(U_\xi)) \subset \mathbb{C}$. Now, we have disjoint sets that differ by the application of a negative Euclidean grafting map (a piecewise translation), g_ξ , along the axis perpendicular to the geodesic shown in Figure 5.6b and a negative Euclidean shearing map (piecewise translation) along the axis shown in Figure 5.6b. We have thus defined a coordinate chart $\psi_\xi : \widehat{T} \rightarrow \mathbb{C}$ on the open set U_ξ by $\psi_\xi = S_\xi \circ g_\xi \circ \varphi_\xi \circ P$. In this way, we define a family of coordinate charts $\Psi_\Xi = \{\psi_\xi\}_{\xi \in \Xi}$.

Define a collection of open sets, $\widetilde{U} = U_A \cup U_B \cup U_\Gamma \cup U_\Delta \cup U_\Xi$, and a collection of maps from \widehat{T} to \mathbb{C} , $\widetilde{\Psi} = \Psi_A \cup \Psi_B \cup \Psi_\Gamma \cup \Psi_\Delta \cup \Psi_\Xi$. Given this collection of open sets and corresponding coordinate charts on the image \widehat{T} , Proposition 5.2.1 provides

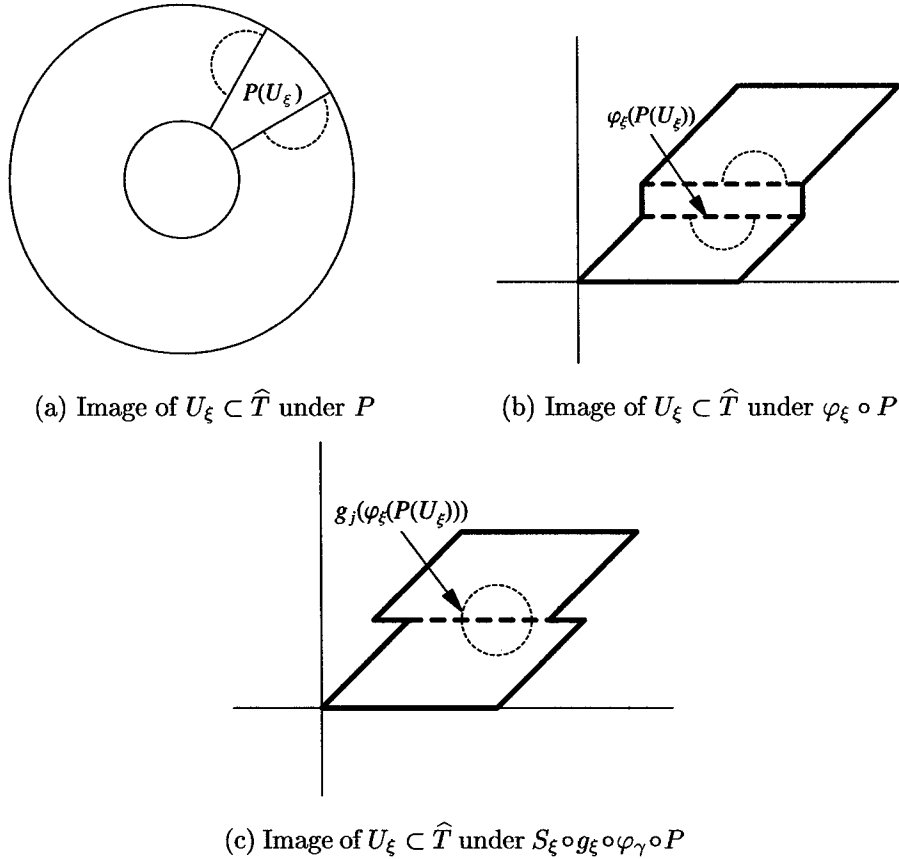


Figure 5.6: Construction of Coordinate Charts for Open Sets U_ξ

an answer to Problem 5.2.1; we prove that \hat{T} is, in fact a Riemann surface. This leads us immediately to Corollary 5.2.1, that Euclidean earthquakes are transformations on the Teichmüller space of tori.

Proposition 5.2.1. *The transition maps in the structure $(\tilde{U}, \tilde{\Psi})$ are analytic.*

Proof. Let U be the intersection of two open sets in \tilde{U} . We need only consider those intersections for which $U \in \tilde{U}$. This gives five cases for the overlap region U in which we must verify the analyticity of the transition maps.

Case I: Suppose that $U \in U_A$. There are nine ways in which U may occur as the result of intersections of sets in \tilde{U} .

Case Ia: $U = U_{\alpha_1} \cap U_{\alpha_2}$, where $U_{\alpha_1}, U_{\alpha_2} \in U_A$. Associated with U_{α_1} and U_{α_2} we have coordinate charts $\psi_{\alpha_1}, \psi_{\alpha_2} \in \Psi_A$. Say $\psi_{\alpha_1} = \varphi_{\alpha_1} \circ P$ and $\psi_{\alpha_2} = \varphi_{\alpha_2} \circ P$. Now,

consider the transition maps $\psi_{\alpha_2} \circ \psi_{\alpha_1}^{-1}$ and $\psi_{\alpha_1} \circ \psi_{\alpha_2}^{-1}$.

$$\begin{aligned}\psi_{\alpha_2} \circ \psi_{\alpha_1}^{-1} &= (\varphi_{\alpha_2} \circ P) \circ (\varphi_{\alpha_1} \circ P)^{-1} \\ &= \varphi_{\alpha_2} \circ P \circ P^{-1} \circ \varphi_{\alpha_1}^{-1} \\ &= \varphi_{\alpha_2} \circ \varphi_{\alpha_1}^{-1}\end{aligned}$$

Thus, $\psi_{\alpha_2} \circ \psi_{\alpha_1}^{-1} : \mathbb{C} \rightarrow \mathbb{C}$ is analytic, since $\varphi_{\alpha_i}, i = 1, 2$, were taken from the conformal structure on T , making $\varphi_{\alpha_2} \circ \varphi_{\alpha_1}^{-1}$ analytic. Similarly, $\varphi_{\alpha_1} \circ \varphi_{\alpha_2}^{-1}$ is analytic.

Case Ib: $U = U_\alpha \cap U_\gamma$, where $U_\alpha \in U_A$ and $U_\gamma \in U_\Gamma$. Associated with U_α and U_γ we have coordinate charts $\psi_\alpha \in \Psi_A$ and $\psi_\gamma \in \Psi_\Gamma$, respectively. Say $\psi_\alpha = \varphi_\alpha \circ P$ and $\psi_\gamma = S_\gamma \circ \varphi_\gamma \circ P$. Now, consider the transition maps $\psi_\alpha \circ \psi_\gamma^{-1}$ and $\psi_\gamma \circ \psi_\alpha^{-1}$.

$$\begin{aligned}\psi_\alpha \circ \psi_\gamma^{-1} &= (\varphi_\alpha \circ P) \circ (S_\gamma \circ \varphi_\gamma \circ P)^{-1} \\ &= \varphi_\alpha \circ P \circ P^{-1} \circ \varphi_\gamma^{-1} \circ S_\gamma^{-1} \\ &= \varphi_\alpha \circ \varphi_\gamma^{-1} \circ S_\gamma^{-1}\end{aligned}$$

Note that the transition map $\psi_\alpha \circ \psi_\gamma^{-1}$ is defined only on the set U . Since the set U does not itself intersect the geodesic associated with the shearing map S_γ , on U the shearing map acts as either the identity map or as a translation. In either case, the action of S_γ is (locally) analytic. Next, we note that since φ_α and φ_γ are taken from the conformal structure on T , $\varphi_\alpha \circ \varphi_\gamma^{-1}$ is analytic, where defined. Thus, the transition map $\psi_\alpha \circ \psi_\gamma^{-1}$ is the composition of analytic maps, and is therefore analytic. Similarly, $\psi_\gamma \circ \psi_\alpha^{-1}$ is also analytic.

Case Ic: $U = U_\alpha \cap U_\delta$, where $U_\alpha \in U_A$ and $U_\delta \in U_\Delta$. Associated with each of U_α and U_δ we have coordinate charts $\psi_\alpha \in \Psi_A$ and $\psi_\delta \in \Psi_\Delta$, respectively. Say $\psi_\alpha = \varphi_\alpha \circ P$ and ψ_δ of the form given in (5.2.1). We note that since U does not intersect the geodesic associated with the grafting of the cylinder, for every $\tau \in U$ we have $\tau \in (E(c_j))^C \cap U_\delta \subset \hat{T}$, where j denotes the cylinder associated with the grafting. Thus, on U we have $\psi_\delta = S_\delta \circ g_\delta^j \circ \varphi_\delta \circ P$. Now, consider the transition

maps $\psi_\alpha \circ \psi_\delta^{-1}$ and $\psi_\delta \circ \psi_\alpha^{-1}$.

$$\begin{aligned}
\psi_\alpha \circ \psi_\delta^{-1} &= (\varphi_\alpha \circ P) \circ (S_\delta \circ g_\delta^j \circ \varphi_\delta \circ P)^{-1} \\
&= \varphi_\alpha \circ P \circ P^{-1} \circ \varphi_\delta^{-1} \circ (g_\delta^j)^{-1} \circ S_\delta^{-1} \\
&= \varphi_\alpha \circ \varphi_\delta^{-1} \circ (g_\delta^j)^{-1} \circ S_\delta^{-1}
\end{aligned}$$

Note that we define the transition map $\psi_\alpha \circ \psi_\delta^{-1}$ only on the overlap region U . Since the set U does not itself intersect the inserted cylinder (or the boundary along which we weld the cylinder to the Riemann surface T via the grafting map $(g_\delta^j)^{-1}$), on U the inverse of the grafting map acts as either the identity map or as a translation. In either case, the action of $(g_\delta^j)^{-1}$ is (locally) analytic. For the same reason, on U we have that S_δ^{-1} acts as either the identity map or a translation, and is therefore (locally) analytic. Next, we note that since the maps φ_α and φ_δ were borrowed from the conformal structure on the original Riemann surface T , $\varphi_\alpha \circ \varphi_\delta^{-1}$ is analytic, where defined. Thus, the transition map $\psi_\alpha \circ \psi_\delta^{-1}$ is the composition of analytic maps on U , and is therefore analytic. Similarly, $\psi_\delta \circ \psi_\alpha^{-1}$ is also analytic.

Case Id: $U = U_\gamma \cap U_\delta$, where $U_\gamma \in U_\Gamma$ and $U_\delta \in U_\Delta$. Associated with each of U_γ and U_δ we have coordinate charts $\psi_\gamma \in \Psi_\Gamma$ and $\psi_\delta \in \Psi_\Delta$, respectively. Say $\psi_\gamma = S_\gamma \circ \varphi_\gamma \circ P$ and ψ_δ of the form given in (5.2.1). We note that since U intersects neither the geodesic associated with the grafting of the cylinder nor the geodesic associated with the simple shearing, for every $\tau \in U$ we have $\tau \in (E(c_j))^C \cap U_\delta \subset \widehat{T}$, where j denotes the cylinder associated with the grafting. Thus, on U we have $\psi_\delta = S_\delta \circ g_\delta^j \circ \varphi_\delta \circ P$. Now, consider the transition maps $\psi_\gamma \circ \psi_\delta^{-1}$ and $\psi_\delta \circ \psi_\gamma^{-1}$.

$$\begin{aligned}
\psi_\gamma \circ \psi_\delta^{-1} &= (S_\gamma \circ \varphi_\gamma \circ P) \circ (S_\delta \circ g_\delta^j \circ \varphi_\delta \circ P)^{-1} \\
&= S_\gamma \circ \varphi_\gamma \circ P \circ P^{-1} \circ \varphi_\delta^{-1} \circ (g_\delta^j)^{-1} \circ S_\delta^{-1} \\
&= S_\gamma \circ \varphi_\gamma \circ \varphi_\delta^{-1} \circ (g_\delta^j)^{-1} \circ S_\delta^{-1}
\end{aligned}$$

Note that we define the transition map $\psi_\gamma \circ \psi_\delta^{-1}$ only on the overlap region U . Since the set U does not itself intersect the inserted cylinder (or the boundary along which we weld the cylinder to the Riemann surface T via the grafting map $(g_\delta^j)^{-1}$), on U

the inverse of the grafting map acts as either the identity map or as a translation. In either case, the action of $(g_\delta^j)^{-1}$ is (locally) analytic. For the same reason, on U we have that S_δ^{-1} and S_γ each act as either identity maps or translations; they are thus (locally) analytic. Next, we note that since the maps φ_γ and φ_δ were borrowed from the conformal structure on the original torus T , $\varphi_\alpha \circ \varphi_\delta^{-1}$ is analytic, where defined. Thus, the transition map $\psi_\gamma \circ \psi_\delta^{-1}$ is the composition of analytic maps on U , and is therefore analytic. Similarly, $\psi_\delta \circ \psi_\gamma^{-1}$ is also analytic.

Case Ie: $U = U_\alpha \cap U_\xi$, where $U_\alpha \in U_A$ and $U_\xi \in U_\Xi$. Associated with U_α and U_ξ we have coordinate charts $\psi_\alpha \in \Psi_A$ and $\psi_\xi \in \Psi_\Xi$, respectively. Say $\psi_\alpha = \varphi_\alpha \circ P$ and $\psi_\xi = S_\xi \circ g_\xi \circ \varphi_\xi \circ P$. Now, consider the transition maps $\psi_\alpha \circ \psi_\xi^{-1}$ and $\psi_\xi \circ \psi_\alpha^{-1}$.

$$\begin{aligned}\psi_\xi \circ \psi_\alpha^{-1} &= (S_\xi \circ g_\xi \circ \varphi_\xi \circ P) \circ (\varphi_\alpha \circ P)^{-1} \\ &= S_\xi \circ g_\xi \circ \varphi_\xi \circ P \circ P^{-1} \circ \varphi_\alpha^{-1} \\ &= S_\xi \circ g_\xi \circ \varphi_\xi \circ \varphi_\alpha^{-1}\end{aligned}$$

Note that we define the transition map $\psi_\xi \circ \psi_\alpha^{-1}$ only on the set U . Since U does not itself intersect either the geodesic associated with U_ξ , on U the shearing and grafting maps act as either identity maps or as translations. In either case, the action of g_ξ and S_ξ are (locally) analytic. Next, we note that since the maps φ_α and φ_ξ were borrowed from the conformal structure on the original torus T , $\varphi_\xi \circ \varphi_\alpha^{-1}$ is analytic, where defined. Thus, the transition map $\psi_\xi \circ \psi_\alpha^{-1}$ is the composition of analytic maps on U , and is therefore itself analytic. Similarly, $\psi_\alpha \circ \psi_\xi^{-1}$ is also analytic.

Case If: $U = U_\gamma \cap U_\xi$, where $U_\gamma \in U_\Gamma$ and $U_\xi \in U_\Xi$. Associated with U_γ and U_ξ we have coordinate charts $\psi_\gamma \in \Psi_\Gamma$ and $\psi_\xi \in \Psi_\Xi$, respectively. Say $\psi_\gamma = S_\gamma \circ \varphi_\gamma \circ P$ and $\psi_\xi = g_\xi \circ \varphi_\xi \circ P$. Now, consider the transition maps $\psi_\gamma \circ \psi_\xi^{-1}$ and $\psi_\xi \circ \psi_\gamma^{-1}$.

$$\begin{aligned}\psi_\xi \circ \psi_\gamma^{-1} &= (S_\xi \circ g_\xi \circ \varphi_\xi \circ P) \circ (S_\gamma \circ \varphi_\gamma \circ P)^{-1} \\ &= S_\xi \circ g_\xi \circ \varphi_\xi \circ P \circ P^{-1} \circ \varphi_\gamma^{-1} \circ S_\gamma^{-1} \\ &= S_\xi \circ g_\xi \circ \varphi_\xi \circ \varphi_\gamma^{-1} \circ S_\gamma^{-1}\end{aligned}$$

Note that we define the transition map $\psi_\xi \circ \psi_\gamma^{-1}$ only on the set U . Since U does not

itself intersect either the geodesic associated with the set U_γ or the geodesic associated with the set U_ξ , on U the maps S_γ^{-1} , g_ξ , and S_ξ each act as either identity maps or translations. In either case, the action of each on U is (locally) analytic. Finally, we note that since the maps φ_γ and φ_ξ were borrowed from the conformal structure on the original torus T , $\varphi_\xi \circ \varphi_\gamma^{-1}$ is analytic, where defined. Thus, the transition map $\psi_\xi \circ \psi_\gamma^{-1}$ is the composition of analytic maps on U , and is therefore itself analytic. Similarly, $\psi_\gamma \circ \psi_\xi^{-1}$ is also analytic.

Case Ig: $U = U_\delta \cap U_\xi$, where $U_\delta \in U_\Delta$ and $U_\xi \in U_\Xi$. Associated with U_δ and U_ξ we have coordinate charts $\psi_\delta \in \Psi_\Delta$ and $\psi_\xi \in \Psi_\Xi$, respectively. Say $\psi_\xi = S_\xi \circ g_\xi \circ \varphi_\xi \circ P$ and ψ_δ is of the form given in (5.2.1). Since U intersects neither the geodesic associated with U_δ nor the geodesic associated with U_ξ , for every $\tau \in U$ we have $\tau \in (E(c_j))^c \cap U_\delta \subset \widehat{T}$, where j denotes the cylinder associated with the grafting. Thus, on U we have $\psi_\delta = S_\delta \circ g_\delta^j \circ \varphi_\delta \circ P$. Now, consider the transition maps $\psi_\xi \circ \psi_\delta^{-1}$ and $\psi_\delta \circ \psi_\xi^{-1}$.

$$\begin{aligned} \psi_\delta \circ \psi_\xi^{-1} &= (S_\delta \circ g_\delta^j \circ \varphi_\delta \circ P) \circ (S_\xi \circ g_\xi \circ \varphi_\xi \circ P)^{-1} \\ &= S_\delta \circ g_\delta^j \circ \varphi_\delta \circ P \circ P^{-1} \circ \varphi_\xi^{-1} \circ g_\xi^{-1} \circ S_\xi^{-1} \\ &= S_\delta \circ g_\delta^j \circ \varphi_\delta \circ \varphi_\xi^{-1} \circ g_\xi^{-1} \circ S_\xi^{-1} \end{aligned}$$

Again, the transition map $\psi_\delta \circ \psi_\xi^{-1}$ is defined only on the overlap region U . Since this set intersects neither the geodesic associated with U_δ nor the geodesic associated with U_ξ , on U the maps S_δ , S_ξ^{-1} , g_δ^j , and g_ξ^{-1} each reduces to either the identity map or a translation, and thus each is (locally) analytic. Since the maps φ_δ and φ_ξ were borrowed from the conformal structure on the original torus T , $\varphi_\delta \circ \varphi_\xi^{-1}$ is analytic, where defined. Thus, the transition map $\psi_\delta \circ \psi_\xi^{-1}$ is the composition of analytic maps on U , and is therefore itself analytic. Similarly, $\psi_\xi \circ \psi_\delta^{-1}$ is also analytic.

Case Ih: $U = U_{\xi_1} \cap U_{\xi_2}$, where $U_{\xi_1}, U_{\xi_2} \in U_\Xi$. Associated with U_{ξ_1} and U_{ξ_2} we have coordinate charts $\psi_{\xi_i} \in \Psi_\Xi, i = 1, 2$. Say $\psi_{\xi_i} = S_{\xi_i} \circ g_{\xi_i} \circ \varphi_{\xi_i} \circ P, i = 1, 2$. Now,

consider the transition maps $\psi_{\xi_1} \circ \psi_{\xi_2}^{-1}$ and $\psi_{\xi_2} \circ \psi_{\xi_1}^{-1}$.

$$\begin{aligned}
\psi_{\xi_1} \circ \psi_{\xi_2}^{-1} &= (S_{\xi_1} \circ g_{\xi_1} \circ \varphi_{\xi_1} \circ P) \circ (S_{\xi_2} \circ g_{\xi_2} \circ \varphi_{\xi_2} \circ P)^{-1} \\
&= S_{\xi_1} \circ g_{\xi_1} \circ \varphi_{\xi_1} \circ P \circ P^{-1} \circ \varphi_{\xi_2}^{-1} \circ g_{\xi_2}^{-1} \circ S_{\xi_2}^{-1} \\
&= S_{\xi_1} \circ g_{\xi_1} \circ \varphi_{\xi_1} \circ \varphi_{\xi_2}^{-1} \circ g_{\xi_2}^{-1} \circ S_{\xi_2}^{-1}
\end{aligned}$$

The transition map $\psi_{\xi_1} \circ \psi_{\xi_2}^{-1}$ is defined only on the overlap region U . Since this set intersects neither the geodesic associated with U_{ξ_1} nor the geodesic associated with U_{ξ_2} , on U the maps S_{ξ_1} , $S_{\xi_2}^{-1}$, g_{ξ_1} , and $g_{\xi_2}^{-1}$ each reduces to either the identity map or a translation, and thus each is (locally) analytic. Since the maps φ_{ξ_1} and φ_{ξ_2} were borrowed from the conformal structure on the original torus T , $\varphi_{\xi_1} \circ \varphi_{\xi_2}^{-1}$ is analytic, where defined. Thus, the transition map $\psi_{\xi_1} \circ \psi_{\xi_2}^{-1}$ is the composition of analytic maps on U , and is therefore itself analytic. Similarly, $\psi_{\xi_2} \circ \psi_{\xi_1}^{-1}$ is also analytic.

Case II: Suppose that $U \in U_B$. There are two ways in which U may occur as the result of intersections of sets in \tilde{U} .

Case IIa: $U = U_{\beta_1} \cap U_{\beta_2}$, where $U_{\beta_1}, U_{\beta_2} \in U_B$. Associated with U_{β_1} and U_{β_2} we have coordinate charts $\psi_{\beta_1}, \psi_{\beta_2} \in \Psi_B$. Say $\psi_{\beta_1} = g_{\beta_1}^j \circ \phi_{\beta_1}^j \circ P$ and $\psi_{\beta_2} = g_{\beta_2}^j \circ \phi_{\beta_2}^j \circ P$. Note that since both U_{β_1} and U_{β_2} must necessarily lie in the same finite inserted cylinder, the grafting maps $g_{\beta_1}^j$ and $g_{\beta_2}^j$, are the same map. Now, consider the transition maps $\psi_{\beta_2} \circ \psi_{\beta_1}^{-1}$ and $\psi_{\beta_1} \circ \psi_{\beta_2}^{-1}$.

$$\begin{aligned}
\psi_{\beta_2} \circ \psi_{\beta_1}^{-1} &= (g_{\beta_2}^j \circ \phi_{\beta_2}^j \circ P) \circ (g_{\beta_1}^j \circ \phi_{\beta_1}^j \circ P)^{-1} \\
&= g_{\beta_2}^j \circ \phi_{\beta_2}^j \circ P \circ P^{-1} \circ (\phi_{\beta_1}^j)^{-1} \circ (g_{\beta_1}^j)^{-1} \\
&= g_{\beta_2}^j \circ \phi_{\beta_2}^j \circ (\phi_{\beta_1}^j)^{-1} \circ (g_{\beta_1}^j)^{-1} \\
&= g_{\beta_2}^j \circ (\phi_{\beta_2}^j \circ (\phi_{\beta_1}^j)^{-1}) \circ (g_{\beta_1}^j)^{-1}
\end{aligned}$$

Now, notice that the maps $g_{\beta_1}^j$ and $g_{\beta_2}^j$ have no effect on the analyticity of the maps involved, since both U_{β_1} and U_{β_2} are on the interior of the cylinder $E(c_j)$. The action affecting analyticity takes place in the conformal structure on the cylinder c_j , and $\phi_{\beta_2}^j \circ (\phi_{\beta_1}^j)^{-1}$ is analytic since these maps were taken from this conformal structure.

Thus, as a composition of analytic maps, $\psi_{\beta_2} \circ \psi_{\beta_1}^{-1}$ is analytic. Similarly, $\psi_{\beta_1} \circ \psi_{\beta_2}^{-1}$ is analytic.

Case IIb: $U = U_\beta \cap U_\delta$, where $U_\beta \in U_B$ and $U_\delta \in U_\Delta$. Associated with each of U_β and U_δ we have coordinate charts $\psi_\beta \in \Psi_B$ and $\psi_\delta \in \Psi_\Delta$, respectively. Say $\psi_\beta = g_\beta^j \circ \phi_\beta^j \circ P$ and ψ_δ are of the form given in (5.2.1). Note that since U does not intersect any geodesic associated with the grafting of the cylinder, for every $\tau \in U$ we have $\tau \in E(c_j) \cap U_\delta \subset \widehat{T}$, where j denotes the cylinder associated with the grafting. Thus, on U we have $\psi_\delta = g_\delta^j \circ \phi_\delta^j \circ P$. Now, consider the transition maps $\psi_\beta \circ \psi_\delta^{-1}$ and $\psi_\delta \circ \psi_\beta^{-1}$.

$$\psi_\beta \circ \psi_\delta^{-1} = (g_\beta^j \circ \phi_\beta^j \circ P) \circ (g_\delta^j \circ \phi_\delta^j \circ P)^{-1}$$

This case, thus reduces to Case IIa, and the transition maps $\psi_\beta \circ \psi_\delta^{-1}$ and $\psi_\delta \circ \psi_\beta^{-1}$ are analytic.

Case III: Suppose that $U \in U_\Gamma$. Then, $U = U_{\gamma_1} \cap U_{\gamma_2}$, where $U_{\gamma_1}, U_{\gamma_2} \in U_\Gamma$. Associated with each of U_{γ_1} and U_{γ_2} we have coordinate charts $\psi_{\gamma_1}, \psi_{\gamma_2} \in \Psi_\Gamma$. Say $\psi_{\gamma_1} = S_\gamma \circ \varphi_{\gamma_1} \circ P$ and $\psi_{\gamma_2} = S_\gamma \circ \varphi_{\gamma_2} \circ P$. Note that the earthquake (shearing) map in each of these coordinate charts is the same, since this earthquake is defined by intersection with a particular weighted geodesic rather than a particular set U . Now, consider the transition maps $\psi_{\gamma_2} \circ \psi_{\gamma_1}^{-1}$ and $\psi_{\gamma_1} \circ \psi_{\gamma_2}^{-1}$.

$$\begin{aligned} \psi_{\gamma_2} \circ \psi_{\gamma_1}^{-1} &= (S_\gamma \circ \varphi_{\gamma_2} \circ P) \circ (S_\gamma \circ \varphi_{\gamma_1} \circ P)^{-1} \\ &= S_\gamma \circ \varphi_{\gamma_2} \circ P \circ P^{-1} \circ \varphi_{\gamma_1}^{-1} \circ S_\gamma^{-1} \\ &= S_\gamma \circ \varphi_{\gamma_2} \circ \varphi_{\gamma_1}^{-1} \circ S_\gamma^{-1} \end{aligned}$$

The action of the pre-composition and post-composition by grafting and shearing maps has no effect on the analyticity; these maps each essentially undo the local behavior of the other. Thus, the transition map $\psi_{\gamma_2} \circ \psi_{\gamma_1}^{-1}$ is analytic. Similarly, $\psi_{\gamma_1} \circ \psi_{\gamma_2}^{-1}$ is also analytic.

Case IV: Suppose that $U \in U_\Delta$. $U = U_{\delta_1} \cap U_{\delta_2}$, where $U_{\delta_1}, U_{\delta_2} \in U_\Delta$. Associated with each of U_{δ_1} and U_{δ_2} we have coordinate charts $\psi_{\delta_1}, \psi_{\delta_2} \in \Psi_\Delta$. Say ψ_{δ_1} and ψ_{δ_2}

are each of the form given in (5.2.1). We may decompose the set U into three disjoint sets, $U = U_\alpha \cup L \cup U_\beta$, where $U_\alpha \in U_A$, $U_\beta \in U_B$, and $L = \partial U_\alpha \cap \partial U_\beta$, as shown in Figure 5.7. We have already shown that the transition maps $\psi_{\delta_1} \circ \psi_{\delta_2}^{-1}$ and $\psi_{\delta_2} \circ \psi_{\delta_1}^{-1}$ are analytic on each of the sets U_α and U_β . These transition maps, though, are also clearly continuous on all of U . Since the image of $L \subset U$ in the plane has measure zero, any map which is K -quasiconformal on the image of $U \setminus L$ is also K -quasiconformal on L [33]; special cases of this result are often given in texts on complex analysis [18]. Thus, since the transition maps are analytic (1-quasiconformal) on the images of U_α and U_β , the transition maps are analytic on all of U .

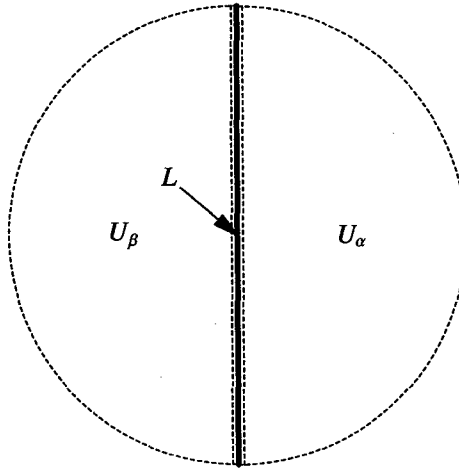


Figure 5.7: Partition of U into U_α , U_β , and L

Case V: Suppose that $U \in U_\Xi$. Then, $U = U_{\xi_1} \cap U_{\xi_2}$, where $U_{\xi_1}, U_{\xi_2} \in U_\Xi$. Associated with each of U_{ξ_1} and U_{ξ_2} we have coordinate charts $\psi_{\xi_1}, \psi_{\xi_2} \in \Psi_\Xi$. Say $\psi_{\xi_1} = S_{\xi_1} \circ g_{\xi_1} \circ \varphi_{\xi_1} \circ P$ and $\psi_{\xi_2} = S_{\xi_2} \circ g_{\xi_2} \circ \varphi_{\xi_2} \circ P$. Note that since the geodesic intersected by each of U_{ξ_1} and U_{ξ_2} is the same, we have $S_{\xi_1} = S_{\xi_2}$ and $g_{\xi_1} = g_{\xi_2}$. Now, consider the transition maps $\psi_{\xi_2} \circ \psi_{\xi_1}^{-1}$ and $\psi_{\xi_1} \circ \psi_{\xi_2}^{-1}$.

$$\begin{aligned}
 \psi_{\xi_1} \circ \psi_{\xi_2}^{-1} &= (S_{\xi_1} \circ g_{\xi_1} \circ \varphi_{\xi_1} \circ P) \circ (S_{\xi_2} \circ g_{\xi_2} \circ \varphi_{\xi_2} \circ P)^{-1} \\
 &= S_{\xi_1} \circ g_{\xi_1} \circ \varphi_{\xi_1} \circ P \circ P^{-1} \circ \varphi_{\xi_2}^{-1} \circ g_{\xi_2}^{-1} \circ S_{\xi_2}^{-1} \\
 &= S_{\xi_1} \circ g_{\xi_1} \circ \varphi_{\xi_1} \circ \varphi_{\xi_2}^{-1} \circ g_{\xi_2}^{-1} \circ S_{\xi_2}^{-1}
 \end{aligned}$$

The maps φ_{ξ_1} and φ_{ξ_2} were borrowed from the conformal structure on T , so $\varphi_{\xi_1} \circ \varphi_{\xi_2}^{-1}$ is analytic. The action of the pre-composition and post-composition by grafting and shearing maps has no effect on the analyticity; these maps each essentially undo the local behavior of the other. Thus, the analyticity of the transition map $\psi_{\xi_1} \circ \psi_{\xi_2}^{-1}$ is shown. Similarly, $\psi_{\xi_2} \circ \psi_{\xi_1}^{-1}$

Thus, the transition maps in the structure $(\tilde{U}, \tilde{\Psi})$ are analytic. \square

Corollary 5.2.1. *Complex earthquakes are maps on the Teichmüller space of tori.*

Proof. Proposition 5.2.1 guarantees that the image \hat{T} of a torus T under a complex earthquake is a new torus. That is, the earthquake has mapped a point in the Teichmüller space of tori to a new point in that space. \square

5.3 Density of Euclidean Earthquakes

Having shown that given a point T in the Teichmüller space of tori and a finite complex Euclidean earthquake on that surface, the earthquake produces a new surface \hat{T} in the Teichmüller space of tori, we turn to Problem 5.3.1.

Problem 5.3.1. *Is there an analogue to Thurston's Earthquake Theorem for tori? That is, can we produce any surface in the Teichmüller space of tori by applying an earthquake to the torus T ? If so, is it possible to do so under the restrictions of Thurston's theorem, using exactly one class of these transformations (positive shearing, negative shearing, positive grafting, negative grafting)? Finally, is the earthquake in some sense unique?*

Taking the components of Problem 5.3.1 one at a time, in Theorem 5.3.1 we show that we may, in fact, apply an earthquake to a given torus T and obtain as the image any given surface in the Teichmüller space of tori.

Theorem 5.3.1. *Let T and \hat{T} be arbitrary fixed points in the Teichmüller space of tori. There exists a finite lamination (\mathcal{L}, σ) on T and an associated earthquake E on T induced by this lamination such that $E(T) = \hat{T}$. Moreover, there also exists a*

sequence of measured geodesic laminations $\{(\mathcal{L}_k, \sigma_k)\}_{k=k_0}^\infty$ on T and earthquake maps $\{E_k\}_{k=k_0}^\infty$ on T induced by these laminations such that $E_k(T) \rightarrow \widehat{T}$ as $k \rightarrow \infty$ and the generators of the surfaces $E_k(T)$ converge uniformly to the canonical generators of \widehat{T} .

Proof. Let T and \widehat{T} be arbitrary fixed points in the Teichmüller space of tori. In this space, we normalize so that one generator for the fundamental group of all tori in the group is $z + 1$. Thus the fundamental regions for the surfaces T and \widehat{T} are each determined by the complex numbers ω and $\widehat{\omega}$ in \mathbb{H} , respectively, as shown in Figure 5.8 [29, 30].

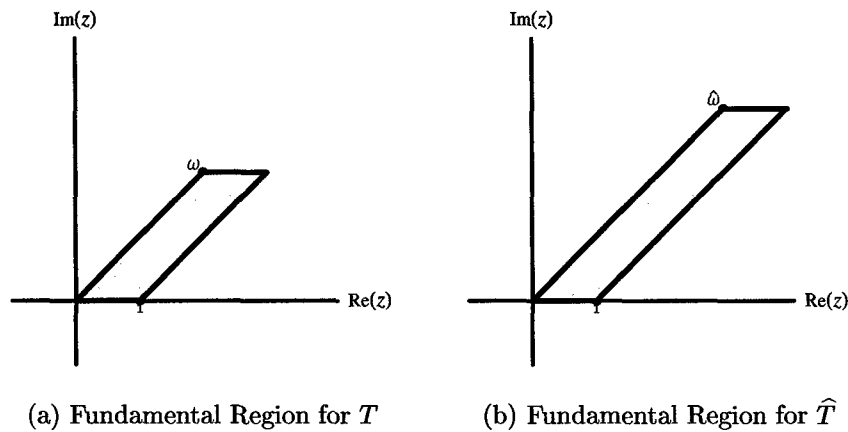


Figure 5.8: Fundamental Regions in the Normalized Teichmüller Space of Tori

To demonstrate the result we explicitly describe a sequence of finite measured geodesic laminations $\{(\mathcal{L}_k, \sigma_k)\}_{k=k_0}^\infty$ on the fundamental region for T . We construct these laminations so that the image of T under each associated earthquake is the surface \widehat{T} and the sequence of images of T have generators converging uniformly to the canonical generators of \widehat{T} . For each $k \geq k_0 \in \mathbb{N}$, let

$$\mathcal{L}_k = \{L_k^j\}_{j=1}^k = \left\{ \left(\frac{j}{k+1} \operatorname{Re}(\omega) + t \right) + i \left(\frac{j}{k+1} \operatorname{Im}(\omega) \right) : 0 \leq t \leq 1 \right\}_{j=1}^k.$$

Examples of such laminations are shown in Figure 5.9.

To complete the construction of the finite measured geodesic lamination, we need only define the measure σ_k . Let $\delta_k^1 = \frac{1}{k}(\operatorname{Re}(\widehat{\omega}) - \operatorname{Re}(\omega))$, and let $\delta_k^2 = \frac{1}{k}(\operatorname{Im}(\widehat{\omega}) - \operatorname{Im}(\omega))$.

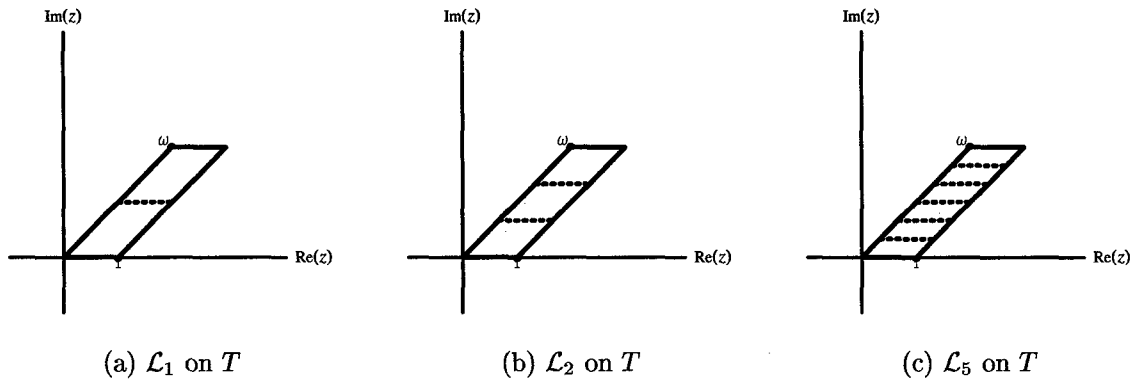


Figure 5.9: Laminations on a Fundamental Region for a Torus

We will require that k be large enough that

$$\delta_k^1 < 1 \tag{5.3.1}$$

and

$$\delta_k^2 > - \left| \frac{\text{Im}(\omega)}{\text{Re}(\omega)} \right|. \tag{5.3.2}$$

Clearly, we can always choose k large enough that these relations are satisfied, since $\delta_k^1, \delta_k^2 \rightarrow 0$ as $k \rightarrow \infty$. Let k_0 be the smallest natural number such that (5.3.1) and (5.3.2) are satisfied. Now, let $k \geq k_0$ and define $\sigma_k : \mathcal{L}_k \rightarrow \mathbb{C}$ by $\sigma_k(L_k^j) = \delta_k^1 + i\delta_k^2$ for each $j = 1, 2, \dots, k$. The effect of the constraints given in (5.3.1) and (5.3.2) is two-fold. First, inequality (5.3.1) ensures that we never shear so far that the resulting fundamental region is “split,” and no shearing will twist the surface a full revolution. This requirement is certainly not necessary, since shearing lengths greater than one will simply indicate that the generators change homotopy classes. We impose the restriction here for convenience and clarity of the construction. The second constraint is similar in its effect, ensuring that the fundamental regions remain contiguous.

Notice that if $0 < \text{Im}(\hat{\omega}) < \text{Im}(\omega)$, and the grafting actions defined by the lami-

nations thus described are negative, then for $j = 1, 2, \dots, k - 1$, we have

$$\begin{aligned} \left(\frac{j+1}{k+1} \operatorname{Im}(\omega) - \frac{j}{k+1} \operatorname{Im}(\omega) \right) - \delta_k^2 &= \frac{1}{k+1} \operatorname{Im}(\omega) - \frac{1}{k} (\operatorname{Im}(\hat{\omega}) - \operatorname{Im}(\omega)) \\ &> -\frac{1}{k} (\operatorname{Im}(\hat{\omega}) - \operatorname{Im}(\omega)) \\ &= \frac{1}{k} (\operatorname{Im}(\omega) - \operatorname{Im}(\hat{\omega})) \\ &> 0. \end{aligned}$$

Thus the weights have been constructed so that the earthquake is always well-defined. That is, we avoid the complications which arise if too much of the surface is removed in the execution of a grafting associated with a negative imaginary weight; removing “too much” may interfere with the action of other geodesics (by removing them) or reduce the torus to a degenerate surface.

We have defined a sequence $\{(\mathcal{L}_k, \sigma_k)\}_{k=k_0}^{\infty}$ of finite measured geodesic laminations on the fundamental region for T . Associated with each lamination $(\mathcal{L}_k, \sigma_k)$ we have an earthquake E_k . Applying the finite earthquakes associated with these laminations, we obtain a sequence of tori, $\{\hat{T}_k\}_{k=k_0}^{\infty}$; more precisely, we have a sequence of fundamental regions, each determining a torus. An illustration of the action of the earthquakes on T determined by the laminations described is shown in Figure 5.10, where we have $k_0 = 2$. The resulting regions are clearly fundamental regions for the image surface \hat{T} , so the first part of the theorem is shown.

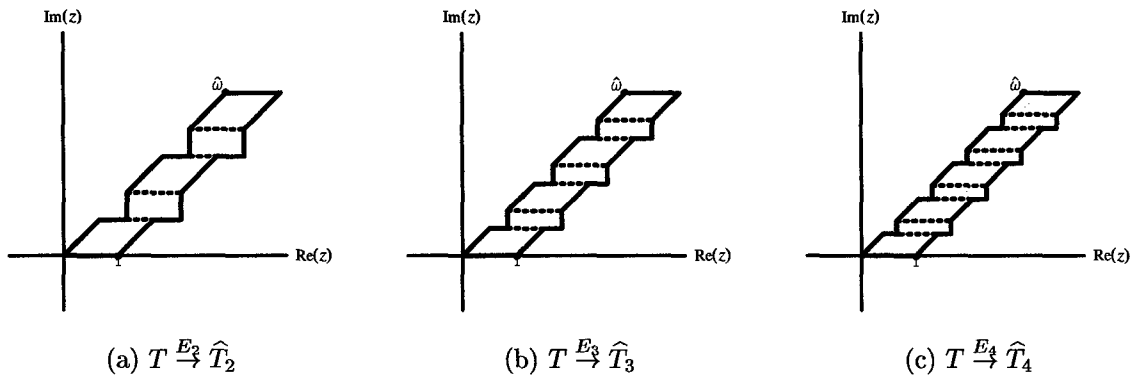


Figure 5.10: Convergent Euclidean Earthquakes on a Torus T

Now, as points in the (normalized) Teichmüller space of tori the sequence $\{\widehat{T}_k\}_{k=k_0}^{\infty}$ is a constant sequence. We wish to show that generators in this sequence of tori, which are not constant, converge uniformly to the canonical generators of the given torus \widehat{T} , $z + 1$ and $z + \hat{\omega}$. Define a “distance” between the surface $E_k(T) = \widehat{T}_k$ and $E(T) = \widehat{T}$ in terms of their respective fundamental regions by

$$\begin{aligned} d(E_k(T), \widehat{T}) &= \sup_{\tau \in T} |E_k(\tau) - E(\tau)| \\ &= \max_{\tau \in T} |E_k(\tau) - E(\tau)| \\ &= \frac{1}{2} \sqrt{3(\delta_2^k)^2 - (\delta_1^k)^2}. \end{aligned}$$

From this, uniform convergence of the fundamental regions as $k \rightarrow \infty$ is clear since

$$\begin{aligned} &\lim_{k_0 < k \rightarrow \infty} \left(\sup_{\tau \in T} |E_k(\tau) - E(\tau)| \right) \\ &= \lim_{k_0 < k \rightarrow \infty} \left(\max_{\tau \in T} |E_k(\tau) - E(\tau)| \right) \\ &= \lim_{k_0 < k \rightarrow \infty} \left(\frac{1}{2} \sqrt{3(\delta_2^k)^2 - (\delta_1^k)^2} \right) \\ &= \lim_{k_0 < k \rightarrow \infty} \left(\frac{1}{2k} \sqrt{3(\operatorname{Im}(\hat{\omega}) - \operatorname{Im}(\omega))^2 - (\operatorname{Re}(\hat{\omega}) - \operatorname{Re}(\omega))^2} \right) \\ &= 0. \end{aligned}$$

Thus, the fundamental regions for the tori $\{\widehat{T}_k\}_{k=k_0}^{\infty}$ converge uniformly to the fundamental region of \widehat{T} defined by the canonical generators $z + 1$ and $z + \omega$; that is, the generators converge uniformly to the canonical generators of \widehat{T} as desired. Thus, the result is shown. \square

We notice that in the construction used to prove Theorem 5.3.1 we had a sequence of distinct earthquakes on the torus T , each producing \widehat{T} as the image of T under the earthquake action. This leads immediately to the fact that the earthquakes transforming one surface into another are not unique in the Euclidean case as they were in the hyperbolic case, when we allow all of left and right shearing and positive and negative grafting. The construction used in Theorem 5.3.1 requires both real

and imaginary parts (shearing and grafting maps) taken from both the positive and negative reals. In order to translate ω to $\hat{\omega}$ (for arbitrary $\hat{\omega}$) with shearing and grafting maps, we must have the freedom to move along both axes of translation and in both directions along each. We are thus led to Conjecture 5.3.1.

Conjecture 5.3.1. *Let two arbitrary points, T and \hat{T} , in the Teichmüller space of tori be given. There does not exist, in general, a sequence of measured geodesic laminations $\{(\mathcal{L}_k, \sigma_k)\}_{k=1}^{\infty}$ of T and earthquake maps $\{E_k\}_{k=1}^{\infty}$ on T induced by these laminations such that $E_k(T) \rightarrow \hat{T}$ as $k \rightarrow \infty$, where $\sigma_k : \mathcal{L}_k \rightarrow \Lambda \subset \mathbb{C}$, for Λ equal to any one of*

$$\{z \in \mathbb{C} : \operatorname{Re}(z) \geq 0, \operatorname{Im}(z) = 0\}, \quad (5.3.3)$$

$$\{z \in \mathbb{C} : \operatorname{Re}(z) \leq 0, \operatorname{Im}(z) = 0\}, \quad (5.3.4)$$

$$\{z \in \mathbb{C} : \operatorname{Re}(z) = 0, \operatorname{Im}(z) \geq 0\}, \text{ or} \quad (5.3.5)$$

$$\{z \in \mathbb{C} : \operatorname{Re}(z) = 0, \operatorname{Im}(z) \leq 0\} \quad (5.3.6)$$

for every $k \in \mathbb{N}$.

This conjecture, together with Theorem 5.3.1 and the failure of uniqueness in the earthquakes used to transform one torus into another completes our consideration of Problem 5.3.1.

As an aside, an interesting element of the proof is the constant k_0 chosen to satisfy the inequalities (5.3.1) and (5.3.2). Defined as it is by the relationship between the real and imaginary parts of ω and $\hat{\omega}$, this constant depends upon the Teichmüller distance between T and \hat{T} . That is, k_0 provides an easily calculated indication of the Teichmüller distance between the two surfaces.

5.4 Discrete Complex Earthquake Maps on Tori

Since Euclidean complex earthquake maps on tori are easily constructible, we do not have the pressing need for a numerical method to reproduce their actions as in the case of complex earthquakes on hyperbolic surfaces. In the interest of a complete

description of earthquakes on compact Riemann surfaces and a complete characterization of the action and convergence of discrete earthquakes on those surfaces, we have Problem 5.4.1.

Problem 5.4.1. *Can we approximate the action of complex earthquakes on tori with discrete conformal maps (circle packing), as we did for earthquakes on hyperbolic Riemann surfaces in Chapter IV?*

An (affirmative) answer to the question thus posed is given in Theorem 5.4.1. This theorem is an analogue of Theorem 4.5.1, in which we proved the convergence of discrete earthquakes on hyperbolic surfaces. Note that we construct these discrete Euclidean earthquakes in exactly the same manner as we constructed discrete earthquakes on hyperbolic surfaces.

Theorem 5.4.1. *Let T be a compact Euclidean Riemann surface of genus $g = 1$ (a torus) with a finite measured geodesic lamination (\mathcal{L}, σ) . Let $\{P_k\}$ be a sequence of finite bounded degree packings with mesh decreasing to zero corresponding to Riemann surfaces $\{T_k\}$ such that $T_k \rightarrow T$ as $k \rightarrow \infty$ in the Teichmüller metric. Then the surfaces $E_k(T_k) = \widehat{T}_k$ induced by the discrete Euclidean earthquake maps E_k converge to the surface $E(T) = \widehat{T}$ under the Euclidean earthquake map E induced by (\mathcal{L}, σ) .*

Proof. Let T be a compact Euclidean Riemann surface (a torus), and let (\mathcal{L}, σ) be a finite measured geodesic lamination on T . Note that requiring the mesh of the sequence of bounded degree packings $\{P_k\}$ to approach zero as $k \rightarrow \infty$ is equivalent to requiring that the radii of the circles in the packings approach zero. Thus, we are guaranteed the existence of such a sequence by Corollary 3.5.1. Further, the construction of the surfaces in the proof of Corollary 3.5.1 allows the freedom to control the degree of vertices adjacent to the geodesics along which we shear and graft.

The Teichmüller distance between the packable surfaces T_k and T is going to zero, so for each $k \in \mathbb{N}$ there exists a map $f_k : T_k \rightarrow T$ that respects the marking on T

and is $1 + \varepsilon_k$ -quasiconformal, where $\varepsilon_k \rightarrow 0$ as $k \rightarrow \infty$, (i.e., as $k \rightarrow \infty$, $f_k \rightarrow f$, where f is conformal). Note that we choose a consistent set of generators (markings) for each surface, so that the Teichmüller space is well defined. More precisely, the map f_k consists of a map from the Euclidean plane to itself through a map between the surfaces and their respective conformal structures. Where no ambiguity arises, however, we will speak about the map as $f_k : T_k \rightarrow T$.

Let $\{c_j\}_{j=1}^m$, be the cylinders grafted into the Riemann surface T by the finite earthquake E . For each $j = 1, 2, \dots, m$, let $\{c_{j_k}\}_{k \in \mathbb{N}}$ be a sequence of surfaces admitting a circle packing of finite uniformly bounded degree so that $c_{j_k} \rightarrow c_j$ as $k \rightarrow \infty$ in the Teichmüller metric. Further, require that the mesh of the packing on c_{j_k} goes to zero as $k \rightarrow \infty$ for each $j = 1, 2, \dots, m$. Thus, for each $k \in \mathbb{N}$ there exists a map $f_{j_k} : c_{j_k} \rightarrow c_j$ that is $1 + \varepsilon_{j_k}$ -quasiconformal, where $\varepsilon_{j_k} \rightarrow 0$ as $k \rightarrow \infty$, (i.e., as $k \rightarrow \infty$, $f_{j_k} \rightarrow f_j$, where f_j is conformal).

Let \widehat{T} be the image of T under the action of the earthquake E , and for each $k \in \mathbb{N}$ let \widehat{T}_k be the image of T_k under the action of a combinatorial earthquake E_k . We construct these combinatorial earthquakes by describing laminations on the surfaces T_k corresponding to the lamination on T . Let $k \in \mathbb{N}$. Corresponding to each geodesic on L^i on T , we choose a geodesic L_k^i on T_k in the same homotopy class as L^i such that the Hausdorff distance between L_k^i and $f_k^{-1}(L^i)$ is minimized. For k sufficiently large, the geodesics $\{L_k^i\}_{i=1}^n$ thus constructed will be pairwise disjoint. Taking the collection of these geodesics, we have a finite measured geodesic lamination (\mathcal{L}_k, σ) on T_k . Notice that we have left the weights σ unchanged; we simply assign to each geodesic in \mathcal{L}_k the weight on the corresponding geodesic in T . Now, we have finite measured geodesic laminations on each T_k , $k \in \mathbb{N}$, and we may carry out the discrete shearing and welding operations of combinatorial earthquakes. We also construct a set of secondary geodesics on T_k describing the second side of cylinders to be removed by a negative grafting action. On the torus T there is a geodesic \widetilde{L}^i corresponding to the end of the cylinder to be removed opposite L^i . This is illustrated in Figure 5.11. By construction, the set of geodesics and secondary geodesics are pairwise disjoint,

and no geodesic or secondary geodesic is contained in the portion of the torus (to be removed) between L^i and \tilde{L}^i . We then construct secondary geodesics \tilde{L}_k^i just as we constructed the geodesics L_k^i .

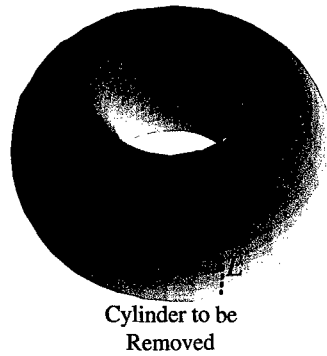


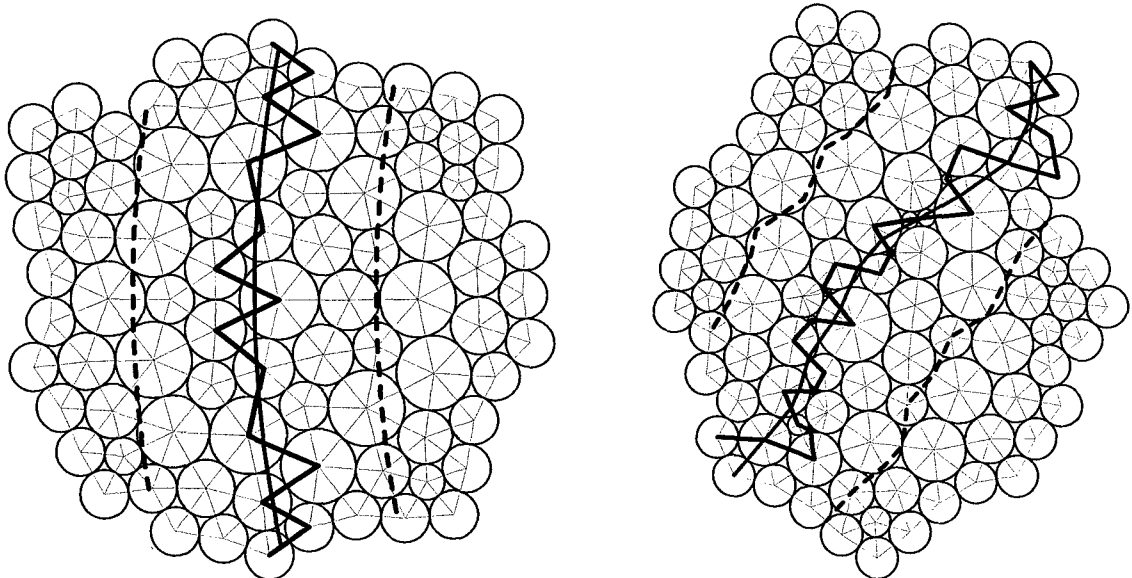
Figure 5.11: Secondary Geodesics on T

Let \hat{T} be the image of T under the action of the earthquake E , and for each $k \in \mathbb{N}$ let \hat{T}_k be the image of T_k under the action of the combinatorial earthquake E_k .

Around each geodesic L^i and each secondary geodesic $\tilde{L}^i, i = 1, 2, \dots, n$, on T we place a collar, a neighborhood of uniform width, so that no two such neighborhoods intersect. Call these collars C^i and \tilde{C}^i . Since the geodesics in the finite lamination are disjoint by construction, we know that there exists such a collar about each geodesic. Similarly, about each geodesic L_k^i and each secondary geodesic $\tilde{L}_k^i, i = 1, 2, \dots, n$ in the lamination \mathcal{L}_k on T_k there exist collars C_k^i and \tilde{C}_k^i such that the collection of these collars on T_k is pairwise disjoint. We require that the collars C_k^i and \tilde{C}_k^i on T_k have width less than $\frac{1}{2}$ the width of the corresponding collars on T . Now, since $T_k \rightarrow T$ in the Teichmüller metric, the maps between T_k and T are going to conformal maps and the markings on T_k are converging to the markings on T . Thus, for k sufficiently large, the images of the collars C_k^i and \tilde{C}_k^i under the map f_k are contained in the collars C^i and \tilde{C}^i , respectively, (i.e., $f_k(C_k^i) \subsetneq C^i$ for all k sufficiently large). Further, since the mesh of the packings on T_k goes to zero, for k sufficiently large, the discrete

geodesics ℓ_k^i and $\tilde{\ell}_k^i$ corresponding to L_k^i and $\tilde{L}_k^i, i = 1, 2, \dots, n$, lie strictly within the interior of the collars C_k^i and \tilde{C}_k^i , respectively.

Consider the images of the collars C_k^i under the action of the discrete earthquake E_k . If the geodesic L_k^i about which we built the collar C_k^i has real weight, and thus induces only a discrete shearing action on the discrete geodesic, then there is no difficulty in defining what we will call a quasicollar on \hat{T}_k as the image of C_k^i under E_k . The image of the discrete geodesic ℓ_k^i and the image of the geodesic L_k^i are contained in this quasicollar. This is shown in Figure 5.12, where the geodesic L_k^i is shown as a solid gray curve, the discrete geodesic ℓ_k^i is shown as a solid black, piecewise linear curve, and the collar C_k^i is denoted by dashed curves.



(a) Geodesic, Discrete Geodesic, and Collar on T_k (b) Images under a Discrete Shearing Map

Figure 5.12: Geodesics, Discrete Geodesics, and Quasicollars

The case in which the weight on L_k^i has non-zero imaginary part is somewhat more problematic. The action of the earthquake when the imaginary component is positive will divide the collar into two disjoint sets. Since the grafting (imaginary) component of the earthquake involves the insertion of a cylinder, however, we may extend these disjoint regions into the interior of the cylinder in such a way that we

create quasicollars about the ends of the inserted cylinder. Since the inserted cylinder has non-zero height, we may construct these quasicollars so that they are disjoint. The action of the earthquake when the imaginary component of the weight is negative removes a portion of the surface, but our construction is such that this removal simply creates a new quasicollar, and the image of the discrete geodesic ℓ_k^i and the image of the geodesic L_k^i are contained in this quasicollar. When the imaginary part of the weight is negative, the action of the combinatorial earthquake removes the surface between the discrete geodesics, removing one side of the collar about each geodesic. The remaining portions of each collar join together along the seam created by joining the two discrete geodesics, to create a quasicollar.

Define a pullback map $P_k : \widehat{T}_k \rightarrow \{T_k, c_{1_k}, \dots, c_{m_k}\}$ by letting $P_k(\hat{\tau})$ be the unique pre-image $\tau \in T_k$ of the point $\hat{\tau} \in \widehat{T}_k$ under the combinatorial earthquake E_k . Note that since the degree of the vertices in the complex on \widehat{T}_k is bounded and since, by construction, the angles in the packing on T_k are bounded away from zero, the map P_k is $1 + \hat{\varepsilon}_k$ -quasiconformal. Further, at any point isolated from the combinatorial geodesics, as $k \rightarrow \infty$ the number of generations of circles on the packed surfaces between that point and the combinatorial geodesics goes to infinity; thus, at any such point, Lemma 3.2.4, the Packing Lemma, guarantees that the dilatation of the maps P_k goes to 1 as $k \rightarrow \infty$, (i.e., as $k \rightarrow \infty$, on points isolated from the combinatorial geodesics, $P_k \rightarrow \widehat{P}$, where \widehat{P} is conformal).

We showed in Theorem 5.2.1 that \widehat{T} is a Riemann surface. Thus, since each of T , \widehat{T} , T_k , and \widehat{T}_k are Riemann surfaces, they each have a conformal structure; in the case of T_k and \widehat{T}_k , they inherit their conformal structures from their packings. Let $\{\varphi_\nu\}_{\nu \in \Upsilon}$, $\{\psi_\nu\}_{\nu \in N}$, $\{\varphi_{k_\nu}\}_{\nu \in \Upsilon}$, and $\{\psi_{k_\nu}\}_{k_\nu \in N_k}$ be the collection of coordinate charts in the conformal structure on T , \widehat{T} , T_k , and \widehat{T}_k , respectively. Note that the structure on \widehat{T} will be the structure described in Section 5.2. Now, we consider a collection of maps $\hat{f}_k : \widehat{T}_k \rightarrow \widehat{T}$, each defined on open sets in \widehat{T}_k . Let $U \subset \widehat{T}_k$.

Case I: Suppose $U \subset \widehat{T}_k$ is an open set such that U does not intersect the interior of any quasicollar, and U does not intersect any cylinder inserted by the earthquake E_k .

Associated with this open set in \widehat{T}_k we have a coordinate chart $\psi_{k\nu}$ from the conformal structure on \widehat{T}_k . Now, the map $P^{-1} \circ f_k \circ P_k \circ \psi_{k\nu}^{-1}$ takes an open subset of the plane \mathbb{C} corresponding to the pair $(U, \psi_{k\nu})$ to an open subset $U_\alpha \subset \widehat{R}$ so that $U_\alpha \in U_A$, as described in Section 5.2. Corresponding to U_α , we take from the conformal structure on \widehat{T} described in Section 5.2 a coordinate chart ψ_α . Thus we have the following:

$$\begin{aligned} \psi_\alpha \circ P^{-1} \circ f_k \circ P_k \circ \psi_{k\nu}^{-1} &= \varphi_\alpha \circ P \circ P^{-1} \circ f_k \circ P_k \circ \psi_{k\nu}^{-1} \\ &= \varphi_\alpha \circ f_k \circ P_k \circ \psi_{k\nu}^{-1}. \end{aligned}$$

Since φ_α and $\psi_{k\nu}^{-1}$ are conformal (or 1-quasiconformal) and the maps f_k and P_k are $(1 + \varepsilon_k)$ -quasiconformal and $(1 + \hat{\varepsilon}_k)$ -quasiconformal, respectively, the map thus described is $(1 + \varepsilon_k)(1 + \hat{\varepsilon}_k)$ -quasiconformal, by Lemma 2.4.1. Note that ε_k and $\hat{\varepsilon}_k$ are independent of the set U , since they depend only on the maps f_k and P_k , which are globally $(1 + \varepsilon_k)$ -quasiconformal and $(1 + \hat{\varepsilon}_k)$ -quasiconformal, respectively. By construction, U is isolated in \widehat{R}_k from the images of the geodesics defining the earthquake E_k , and $\varepsilon_k, \hat{\varepsilon}_k \rightarrow 0$ as $k \rightarrow \infty$. Thus, as $k \rightarrow \infty$, the map $\psi_\alpha \circ P^{-1} \circ f_k \circ P_k \circ \psi_{k\nu}^{-1} : \widehat{R}_k \rightarrow \widehat{R}$ approaches a conformal map.

Case II: Suppose $U \subset \widehat{T}_k$ is an open set such that U does not intersect the interior of any quasicollar, and U is contained in the interior of some cylinder inserted by the earthquake E_k . Associated with this open set in \widehat{T}_k we have a coordinate chart $\psi_{k\nu}$. Now, the map $P^{-1} \circ f_{j_k} \circ P_k \circ \psi_{k\nu}^{-1}$ takes an open subset of the plane \mathbb{C} corresponding to the pair $(U, \psi_{k\nu})$ to an open subset $U_\beta \subset \widehat{R}$ so that $U_\beta \in U_B$, as described in Section 5.2. Corresponding to U_β , we take from the conformal structure on \widehat{T} described in Section 5.2 a coordinate chart ψ_β . Thus we have the following:

$$\begin{aligned} \psi_\beta \circ P^{-1} \circ f_{j_k} \circ P_k \circ \psi_{k\nu}^{-1} &= g_\beta^j \circ \phi_\beta^j \circ P \circ P^{-1} \circ f_{j_k} \circ P_k \circ \psi_{k\nu}^{-1} \\ &= g_\beta^j \circ \phi_\beta^j \circ f_{j_k} \circ P_k \circ \psi_{k\nu}^{-1}. \end{aligned}$$

Since $g_\beta^j \circ \phi_\beta^j$ and $\psi_{k\nu}^{-1}$ are conformal (or 1-quasiconformal) and the maps f_{j_k} and P_k are $(1 + \varepsilon_{j_k})$ -quasiconformal and $(1 + \hat{\varepsilon}_k)$ -quasiconformal, respectively, the map thus described is $(1 + \varepsilon_{j_k})(1 + \hat{\varepsilon}_k)$ -quasiconformal. Again, we note that the constants

describing the deviation from conformality, ε_{j_k} and $\hat{\varepsilon}_k$, are independent of the choice of U . By construction, U is isolated in \hat{T}_k from the images of the geodesics defining the earthquake E_k , and $\varepsilon_{j_k}, \hat{\varepsilon}_k \rightarrow 0$ as $k \rightarrow \infty$. Thus, as $k \rightarrow \infty$, the map $\psi_\beta \circ P^{-1} \circ f_{j_k} \circ P_k \circ \varphi_{k\nu}^{-1} : \hat{T}_k \rightarrow \hat{T}$ approaches a conformal map.

Case III: Suppose that U is a small open subset of \hat{T}_k such that U intersects $E_k(\ell_k^i)$ for some $i = 1, 2, \dots, n$, and U intersects the boundary of the quasicollar \hat{C}_k^i associated with L_k^i . Corresponding to U we have a coordinate chart $\psi_{k\nu}$. Now, we have three cases to consider depending on the imaginary part of the weight on the geodesic L^i .

Case IIIa: Suppose $\text{Im}(\sigma(L^i)) = 0$; that is, the earthquake action on the geodesic L^i involves only a shearing action. This gives that the map P_k takes U to a subset of T_k such that $P_k(U) \not\subset C_k^i$ and $P_k(U) \cap \ell_k^i \neq \emptyset$, as shown in Figure 5.13.

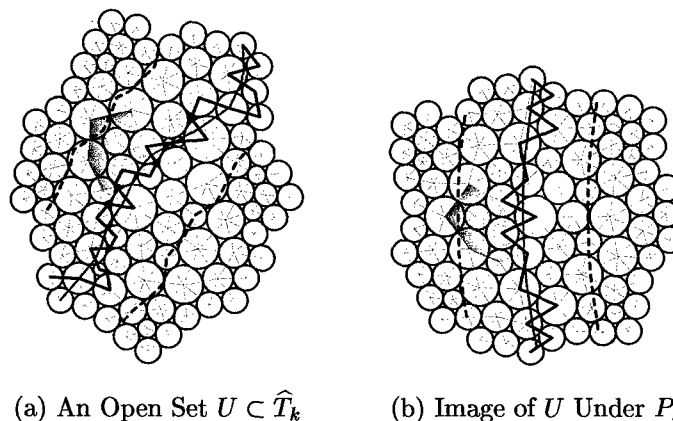


Figure 5.13: Pullback of Geodesics, Discrete Geodesics, and Quasicollars

Note that in Figure 5.13b we have included the refining edges associated with the shearing so that there is a bijection between individual triangles in Figure 5.13a and Figure 5.13b.

Now, we wish to send this set $P_k(U)$ to a subset of T , but there is a geometric difficulty to be resolved. The "halves" of $P_k(U)$ have as one portion of their boundaries a segment of the discrete geodesic ℓ_k^i . We need these segments of their boundaries to lie on the actual geodesic L_k^i in T_k . The problem is easily resolved, at the expense of

admitting some quasiconformality in our eventual transformation, by the application of a Euclidean projection p_k^i , as illustrated in Figure 5.14.

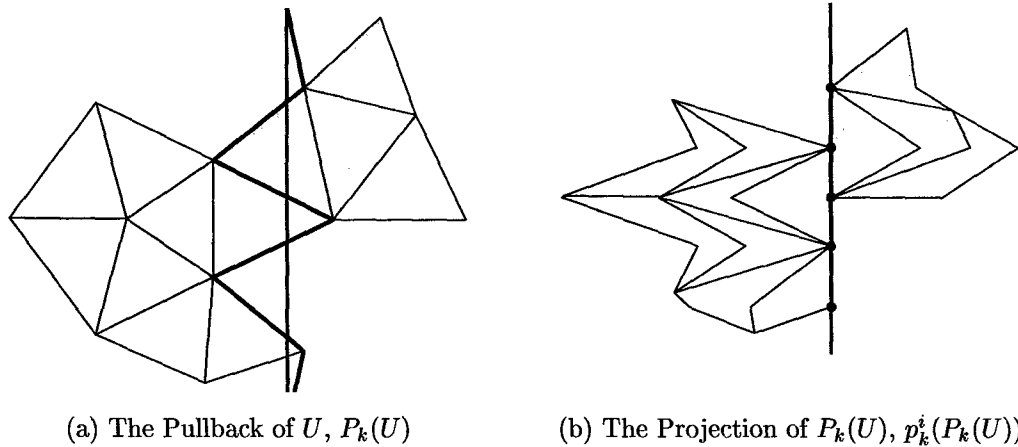


Figure 5.14: Projection of Geodesics, Discrete Geodesics, and Quasicollars

This p_k^i map on the set $P_k(U)$ is $1 + \tilde{\varepsilon}_k$ -quasiconformal, but Proposition 4.2.1 guarantees that p_k^i converges uniformly to the identity; so $\tilde{\varepsilon}_k \rightarrow 0$ as $k \rightarrow \infty$. Further, the constant $\tilde{\varepsilon}_k$ is independent of the choice of U . This independence is a result of two facts. First, the projection associated with any given geodesic L^i and the accompanying discrete geodesic ℓ_k^i has a quasiconformality constant uniform across the entire geodesic. Second, there are only finitely many geodesics for which we must use these projections. Taking the maximum such quasiconformal constant as $\tilde{\varepsilon}_k$, we have independence of the choice for U .

Corresponding to the set $p_k^i(P_k(U)) \subset T_k$, or more precisely to some open subset of T_k containing $p_k^i(P_k(U)) \subset T_k$, we have a coordinate chart φ_{k_v} which takes $p_k^i(P_k(U))$ to a subset of a fundamental region for T_k in the plane \mathbb{C} . The image of $p_k^i(P_k(U)) \cap L_k^i$ under this map is thus an arc of a Euclidean geodesic (a line) in \mathbb{C} . There exists a conformal map (comprising translation, rotation, and scaling) $M_k^U : \mathbb{C} \rightarrow \mathbb{C}$ such that $M_k^U(\varphi_{k_v}(p_k^i(P_k(U)))) \cap L_k^i$ is a small arc of a Euclidean geodesic in \mathbb{C} that is the projection of the geodesic L^i in T . We may choose this arc of the projection of L^i sufficiently small that the set $M_k^U(\varphi_{k_v}(p_k^i(P_k(U))))$ is contained in a single

fundamental region for T .

A second difficulty arising from the projection operation must be addressed. If we were to apply a shearing map on the lift of the geodesic L^i which separates the “halves” of $M_k^U(\varphi_{k_v}(p_k^i(P_k(U))))$ using the weight associated with L^i , the sides will not necessarily match along the geodesic, as illustrated in Figure 5.15.

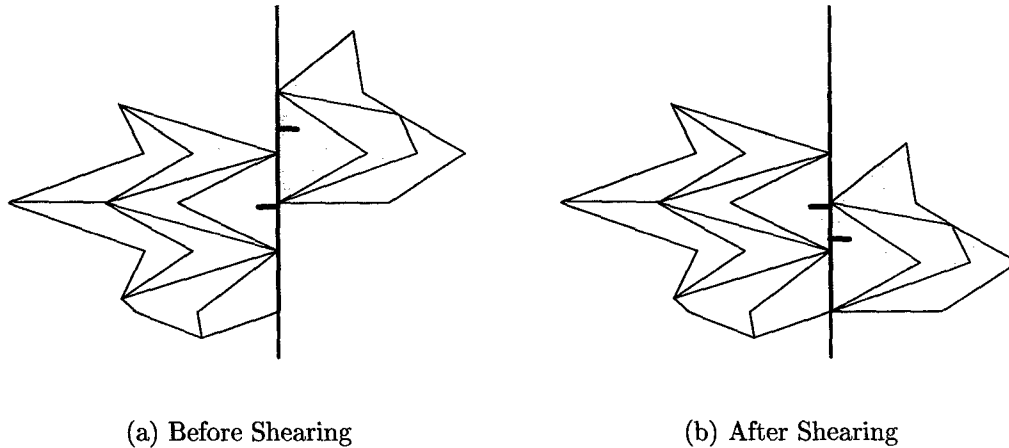


Figure 5.15: Misalignment under Pullback, Projection, and Shearing

The difference along the geodesic is a quasisymmetry on one half of the intersection with L^i , however, and extends to a $1 + \bar{\varepsilon}_k$ -quasiconformal map, Q_k^U , in the corresponding half of $M_k^U(\varphi_{k_v}(p_k^i(P_k(U))))$ [24, 33]. Recall, however, that the quasisymmetry and associated quasiconformal map arise as a result of the need for a Euclidean projection p_k^i to correct the difference between the geodesic L_k^i and the discrete geodesic ℓ_k^i . Lemma 4.1.1 guarantees that $\ell_k^i \rightarrow L_k^i$ uniformly as $k \rightarrow \infty$. Thus, $\bar{\varepsilon}_k \rightarrow 0$ as $k \rightarrow \infty$. Further, since the quasiconformality of M_k^U depends only on the quasisymmetry associated with the projection p_k^i , $\bar{\varepsilon}_k$ is independent of the choice of U .

Corresponding to the set $Q_k^U(M_k^U(\varphi_{k_v}(p_k^i(P_k(U)))) \subset \mathbb{C}$, we have a map from the conformal structure on T , φ_v^{-1} , taking this set to an open set on T intersecting the geodesic L^i . (Again, the coordinate chart really comes from an open set containing the set of interest.) Notice that as a result of applying the correction Q_k^U , the two halves of this image (on either side of the lift to \mathbb{C} of the geodesic L^i) now match

the action of the shearing caused by P^{-1} . We now apply P^{-1} , to obtain a set $V \subset \widehat{T}$. Corresponding to this open set we have a coordinate chart from the conformal structure on \widehat{T} defined in Section 5.2. Since $V \in U_\Gamma$, as described in Section 5.2, we have a coordinate chart ψ_γ corresponding to V . This gives the following:

$$\begin{aligned} & \psi_\gamma \circ P^{-1} \circ \varphi_v^{-1} \circ Q_k^U \circ M_k^U \circ \varphi_{k_v} \circ p_k^i \circ P_k \circ \varphi_{k_v}^{-1} \\ = & S_\gamma \circ \varphi_\gamma \circ P \circ P^{-1} \circ \varphi_v^{-1} \circ Q_k^U \circ M_k^U \circ \varphi_{k_v} \circ p_k^i \circ P_k \circ \varphi_{k_v}^{-1} \\ = & S_\gamma \circ \varphi_\gamma \circ \varphi_v^{-1} \circ Q_k^U \circ M_k^U \circ \varphi_{k_v} \circ p_k^i \circ P_k \circ \varphi_{k_v}^{-1}. \end{aligned}$$

This map is $(1 + \bar{\varepsilon}_k)(1 + \tilde{\varepsilon}_k)(1 + \hat{\varepsilon}_k)$ -quasiconformal, where this quasiconformality is independent of the choice for U . Now, consider the dilatation at a point $u \in U$. If u is not contained in the set $E_k(\ell_k^i)$, then Lemma 3.2.4, the packing Lemma, guarantees that the dilatation at u goes to 1 since each of $\bar{\varepsilon}_k, \tilde{\varepsilon}_k, \hat{\varepsilon}_k \rightarrow 0$ as $k \rightarrow \infty$. Thus, this map from \widehat{T}_k to \widehat{T} converges to a conformal map, except perhaps on the image of the discrete geodesic ℓ_k^i under the earthquake E_k . But this set has measure zero, and the map is continuous. Thus, the limit map is conformal on all of U [33].

Case IIIb: Suppose $\text{Im}(\sigma(L^i)) > 0$; that is, the earthquake action on the geodesic L^i is a positive grafting action (and potentially a shearing action as well). The situation here is somewhat more complicated than the previous case since the map P_k takes the portion of U on the inserted cylinder to a cylinder c_{j_k} and the remaining points of U to a subset of T_k . We will deal with the maps on these two subsets of U separately.

First, consider that subset of U which is taken to T_k . Call this subset U_1 . $P_k(U_1) \not\subset C_k^i$ and $P_k(U_1) \cap \ell_k^i \neq \emptyset$. Now, we wish to send this set $P_k(U_1)$ to a subset of T , but there is a geometric difficulty to be resolved. $P_k(U_1)$ has as one portion of its boundary a segment of the discrete geodesic ℓ_k^i ; we need this segment of the boundary to lie on the actual geodesic L_k^i in T_k . As before, this problem is easily addressed, at the expense of admitting some quasiconformality into our eventual transformation, by the application of a Euclidean projection p_k^i . This map on the set $P_k(U_1)$ is $1 + \tilde{\varepsilon}_k$ -quasiconformal, but Proposition 4.2.1 guarantees that p_k^i converges uniformly to the

identity; so $\tilde{\varepsilon}_k \rightarrow 0$ as $k \rightarrow \infty$. As in Case IIIa, $\tilde{\varepsilon}_k$ is independent of the choice of U .

Corresponding to the set $p_k^i(P_k(U_1)) \subset T_k$, or more precisely to some open subset of T_k containing $p_k^i(P_k(U_1)) \subset T_k$, we have a coordinate chart φ_{k_v} which takes $p_k^i(P_k(U_1))$ to a subset of a fundamental region for T_k in the plane \mathbb{C} . The image of $p_k^i(P_k(U_1)) \cap L_k^i$ under this map is thus an arc of a Euclidean geodesic in \mathbb{C} . There exists a conformal map (comprising a translation, rotation, and scaling) $M_k^{U_1} : \mathbb{C} \rightarrow \mathbb{C}$ such that $M_k^{U_1}(\varphi_{k_v}(p_k^i(P_k(U_1)))) \cap L_k^i$ is an arc of the Euclidean geodesic in \mathbb{C} that is the lift of the geodesic L^i in T . We may choose this arc small enough that the set $M_k^{U_1}(\varphi_{k_v}(p_k^i(P_k(U_1))))$ is contained in a single fundamental region for T .

Again, we will require a correction to compensate for the effect of the Euclidean projection p_k^i . Call this correction Q_k^U , and note that this map is a quasismetry on the intersection with the lift of the geodesic L^i and is $(1 + \tilde{\varepsilon}_k)$ -quasiconformal, as in Case IIIa. This quasiconformality constant $\tilde{\varepsilon}_k$ is independent of the choice for U . Corresponding to the set $Q_k^U(M_k^{U_1}(\varphi_{k_v}(p_k^i(P_k(U_1)))) \subset \mathbb{C}$, we have a map from the conformal structure on T , φ_v^{-1} , taking this set to an open set on T intersecting the geodesic L^i . (Again, the coordinate chart really comes from an open set containing the set of interest.) We now apply P^{-1} , to obtain a set $V_1 \subset \hat{T}$ adjoining the edge of an inserted cylinder c_j .

Now, consider that subset of U which is taken into c_{j_k} . Call this subset U_2 . $P_k(U_2) \subset c_{j_k}$ and $P_k(U_2)$ intersects the boundary of the cylinder c_{j_k} . We take this set into the cylinder c_j via the $1 + \tilde{\varepsilon}_k$ -quasiconformal map f_{j_k} , where $\tilde{\varepsilon}_k$ is independent of the choice of U , since we may choose $\tilde{\varepsilon}_k$ as the maximum of the constants associated with the finitely many cylinders $\{c_j\}$. We then apply the map P^{-1} to obtain a set $V_2 \subset \hat{T}$.

The way we have constructed these maps, in particular the application of the map Q_k^U , ensures that the set $V = V_1 \cup V_2 \subset \hat{T}$ is an element of the collection U_Δ as described in Section 5.2. Corresponding to this set V we have a coordinate chart ψ_δ from the conformal structure on \hat{T} given in Section 5.2. This gives the following

piecewise map $\Pi_k : \widehat{T}_k \rightarrow \widehat{T}$:

$$\Pi_k(u) = \begin{cases} \psi_\beta \circ P^{-1} \circ \varphi_\nu^{-1} \circ Q_k^U \circ M_k^{U_1} \circ \varphi_{k\nu} \circ p_k^i \circ P_k \circ \psi_{k\nu}^{-1}(u) & \text{if } u \in U_1 \subset \widehat{T}_k \\ \psi_\beta \circ P^{-1} \circ f_{j_k} \circ P_k \circ \psi_{k\nu}^{-1}(u) & \text{if } u \in U_2 \subset \widehat{T}_k. \end{cases}$$

The first of these maps, for $u \in U_1$, is $(1 + \bar{\varepsilon}_k)(1 + \tilde{\varepsilon}_k)(1 + \hat{\varepsilon}_k)$ -quasiconformal. The second map, for $u \in U_2$, is $(1 + \varepsilon_{j_k})(1 + \hat{\varepsilon}_k)$ -quasiconformal. As we have shown, these constants are independent of the choice of U . Now, consider the dilatation at a point $u \in U$. If u is not contained in the set $E_k(\ell_k^i)$, then Lemma 3.2.4, the packing Lemma, guarantees that the dilatation at u goes to 1 since each of $\bar{\varepsilon}_k, \tilde{\varepsilon}_k, \hat{\varepsilon}_k, \varepsilon_{j_k} \rightarrow 0$ as $k \rightarrow \infty$. Thus, this piecewise map Π_k from \widehat{T}_k to \widehat{T} converges to a conformal map Π , except perhaps on the image of the discrete geodesic ℓ_k^i under the earthquake E_k . But this set has measure zero, and the map is continuous. Thus, the map Π is conformal on all of U [33].

Case IIIc: Suppose $\text{Im}(\sigma(L^i)) < 0$; that is, the earthquake action on the geodesic L^i is a negative grafting action (and potentially a shearing action as well). Here, the map P_k divides the set U into two disjoint sets, separated by an inserted cylinder; essentially, the first step in this action is the inverse of the action described in Case IIIb. As in Case IIIb, we will consider these sets separately.

Consider the subset of U whose image borders the discrete geodesic ℓ_k^i ; call this subset U_1 . $P_k(U_1) \subset C_k^i$ and $P_k(U_1) \cap \ell_k^i \neq \emptyset$. Now, we wish to send this set $P_k(U_1)$ to a subset of T , but there is a geometric difficulty to be resolved. $P_k(U_1)$ has as one portion of its boundary a segment of the discrete geodesic ℓ_k^i ; we need this segment of the boundary to lie on the actual geodesic L_k^i in T_k . As before, this problem is easily addressed, at the expense of admitting some quasiconformality into our eventual transformation, by the application of a Euclidean projection p_k^i . This map on the set $P_k(U_1)$ is $1 + \tilde{\varepsilon}_k$ -quasiconformal, but Proposition 4.2.1 guarantees that p_k^i converges uniformly to the identity; so $\tilde{\varepsilon}_k \rightarrow 0$ as $k \rightarrow \infty$. As in Case IIIa, $\tilde{\varepsilon}_k$ is independent of the choice of U .

Corresponding to the set $p_k^i(P_k(U_1)) \subset T_k$, or more precisely to some open sub-

set of T_k containing $p_k^i(P_k(U_1)) \subset T_k$, we have a coordinate chart $\varphi_{k_{v_1}}$ which takes $p_k^i(P_k(U_1))$ to a subset of a fundamental region for T_k in the plane \mathbb{C} . The image of $p_k^i(P_k(U_1)) \cap L_k^i$ under this map is thus an arc of a Euclidean geodesic in \mathbb{C} . There exists a conformal map (comprising a translation, rotation, and scaling) $M_k^{U_1} : \mathbb{C} \rightarrow \mathbb{C}$ such that $M_k^{U_1}(\varphi_{k_{v_1}}(p_k^i(P_k(U_1)))) \cap L_k^i$ is an arc of the Euclidean geodesic in \mathbb{C} that is the lift of the geodesic L^i in T . We may choose this arc small enough that the set $M_k^{U_1}(\varphi_{k_{v_1}}(p_k^i(P_k(U_1))))$ is contained in a single fundamental region for T .

Again, we will require a correction to compensate for the effect of the Euclidean projection p_k^i . Call this correction Q_k^U , and note that this map is a quasimetry on the intersection with the lift of the geodesic L^i and is $(1 + \bar{\varepsilon}_k)$ -quasiconformal, as in Case IIIa. Again, the quasiconformality constant $\bar{\varepsilon}_k$ is independent of the choice for U .

Corresponding to the set $Q_k^U(M_k^{U_1}(\varphi_{k_{v_1}}(p_k^i(P_k(U_1)))) \subset \mathbb{C}$, we have a map from the conformal structure on T , $\varphi_{v_1}^{-1}$, taking this set to an open set on T intersecting the geodesic L^i . (Again, the coordinate chart really comes from an open set containing the set of interest.) We now apply P^{-1} , to obtain a set $V_1 \subset \widehat{T}$.

Now, consider the subset of U whose image borders the discrete (*secondary*) geodesic $\tilde{\ell}_k^i$; call this subset U_2 . We map this set to \widehat{T} in essentially the same manner as we mapped U_1 to \widehat{T} . The differences lie in distinct choices from the conformal structures on T_k and T , a different choice for the conformal map M , and in not applying a correction map Q (since we need only correct on one side of the geodesic). Thus we will have a map

$$P^{-1} \circ \varphi_{v_2}^{-1} \circ M_k^{U_2} \circ \varphi_{k_{v_2}} \circ p_k^i \circ P_k \circ \psi_{k_{v_2}}^{-1}$$

which takes U_2 to a set $V_2 \subset \widehat{T}$

The way we have constructed these maps, in particular the application of the map Q_k^U , ensures that the set $V = V_1 \cup V_2 \subset \widehat{T}$ is an element of the collection U_{Ξ} as described in Section 5.2. Corresponding to this set V we have a coordinate chart ψ_{ξ} from the conformal structure on \widehat{T} given in Section 5.2. This gives the following

piecewise map $\Pi_k : \widehat{T}_k \rightarrow \widehat{T}$:

$$\Pi_k(u) = \begin{cases} \psi_\xi \circ P^{-1} \circ \varphi_{v_1}^{-1} \circ Q_k^U \circ M_k^{U_1} \circ \varphi_{k_{v_1}} \circ p_k^i \circ P_k \circ \psi_{k_v}^{-1}(u) & \text{if } u \in U_1 \subset \widehat{T}_k \\ \psi_\xi \circ P^{-1} \circ f_{j_k} \circ P_k \circ \psi_{k_v}^{-1}(u) & \text{if } u \in U_2 \subset \widehat{T}_k. \end{cases}$$

The first of these maps, for $u \in U_1$, is $(1 + \bar{\varepsilon}_k)(1 + \tilde{\varepsilon}_k)(1 + \hat{\varepsilon}_k)$ -quasiconformal. The second map, for $u \in U_2$, is $(1 + \tilde{\varepsilon}_k)(1 + \hat{\varepsilon}_k)$ -quasiconformal. As we have shown, each of these constants is independent of the choice of U . Now, consider the dilatation at a point $u \in U$. If u is not contained in the set $E_k(\ell_k^i)$, then Lemma 3.2.4, the packing Lemma, guarantees that the dilatation at u goes to 1 since each of $\bar{\varepsilon}_k, \tilde{\varepsilon}_k, \hat{\varepsilon}_k, \varepsilon_{j_k} \rightarrow 0$ as $k \rightarrow \infty$. Thus, this piecewise map Π_k from \widehat{T}_k to \widehat{T} converges to a conformal map Π , except perhaps on the image of the discrete geodesic ℓ_k^i under the earthquake E_k . But this set has measure zero, and the map is continuous. Thus, the map Π is conformal on all of U [33].

Thus, as $k \rightarrow \infty$ the maps from \widehat{T}_k to \widehat{T} are becoming conformal, and, by construction, the markings on surfaces \widehat{T} and \widehat{T}_k are consistent. Therefore, the surfaces \widehat{T}_k converge to a surface conformally equivalent to \widehat{T} with equivalent markings; but this is equivalent to saying $\widehat{T}_k \rightarrow \widehat{T}$ (in the Teichmüller metric) as $k \rightarrow \infty$, and the result is shown. \square

We now give several examples of finite earthquakes, both shearing and grafting, on a compact torus T , and we approximate these earthquakes using the circle packing techniques given.

Example 5.4.1. Let T be the point in the normalized Teichmüller space of tori defined by the generators $z + 1$ and $z + \omega$, where $\omega = \frac{7}{5} + i\frac{2\sqrt{3}}{5} \in \mathbb{H}$. We place a geodesic L on this surface such that the segment between $\frac{13}{80} + i\frac{13\sqrt{3}}{80}$ and $\frac{93}{80} + i\frac{13\sqrt{3}}{80}$ is an arc of the lift of that geodesic through the canonical fundamental region for T . This fundamental region for T and the geodesic arc described are shown in Figure 5.16a. Place a weight of $\sigma(L) = -\frac{6}{10}$ on the geodesic. The action of the (right) earthquake induced by this finite geodesic lamination on T is shown in Figure 5.16b. Note

that though the generators of the image surface \widehat{T} are not the canonical generators associated with the image point in the Teichmüller space of tori, the position in Teichmüller space is determined by the point $\hat{\omega} = 1 + i\frac{2\sqrt{3}}{5} \in \mathbb{H}$ [29, 30].

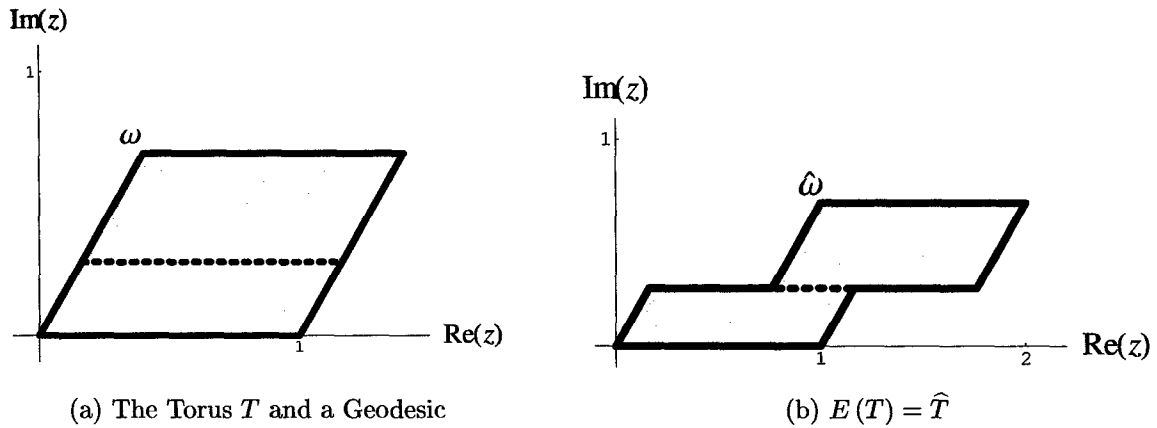


Figure 5.16: Explicit Shearing Action on a Torus

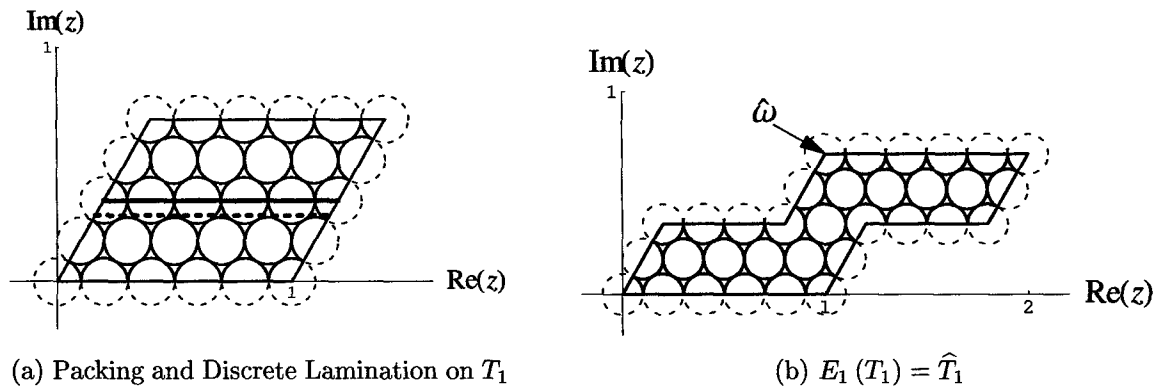


Figure 5.17: Packing, Discrete Lamination, and Earthquake on a Torus

The torus T shown in Figure 5.16a is itself a packable surface, so we may place a packing on the surface as shown in Figure 5.17a. To remain consistent with the notation of Theorem 5.4.1, we will call this packed surface T_1 though there is no difference between T_1 and T itself. Also in Figure 5.17a we show the geodesic L (as a dashed segment) and the discrete geodesic approximating L (as a solid segment). Now, we execute the discrete (combinatorial) earthquake E_1 determined by the dis-

crete geodesic and the weight on L to obtain the surface \widehat{T}_1 shown in Figure 5.17b. Note that the discrete earthquake, in this case a right shearing action, respects the combinatorics of the packing on T_1 , as described in Figure 3.12. The discrete earthquake results in a normalized point in the Teichmüller space of tori determined by the point $1 + \frac{2\sqrt{3}}{5}i \in \mathbb{H}$. Thus, the discrete approximation exactly mimics the action of the true earthquake. This will always occur when the packing on our surface is as regular as the packing shown (a regular hex packing) and the shearing respects the combinatorics of the triangulation.

Example 5.4.2. In this example, we repeat the process given in Example 5.4.1, changing only the weight; here we use $\sigma(L) = \frac{5}{8}$. All other parameters for the surface and (right) earthquake described in Example 5.4.1 are unchanged. When we execute the earthquake E induced by these parameters, we obtain the surface \widehat{T} in the normalized Teichmüller space of tori determined by the point $\widehat{\omega} = \frac{41}{40} + \frac{2\sqrt{3}}{5}i \in \mathbb{H}$.

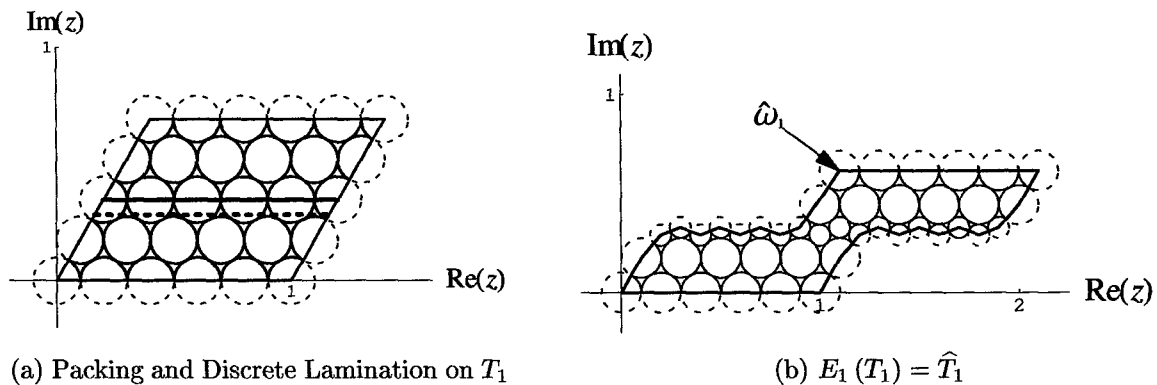


Figure 5.18: Discrete Shearing Map on a “Coarsely” Packed Torus

Again, the surface T is itself packable, and we place a packing on the surface as shown in Figure 5.18a to obtain the surface T_1 , identical to T . Now, the seemingly minor change in the weight on L results in a combinatorial earthquake which does not respect the combinatorics of the triangulation on T_1 . Thus, we must refine the packing, as shown in Figure 4.3. This results in new circles added to the packing when we execute the combinatorial earthquake E_1 , which should alter the result

obtained in Example 5.4.1. In Figure 5.18b we see that, after normalization, the action of the E_1 on the packable torus T_1 results in a torus determined by the point $\hat{\omega}_1 = 1.1 + 0.615973i \in \mathbb{H}$.

Since the combinatorial earthquake E_1 did not result in the desired image \hat{T} , we refine the packing to obtain a new packable surface T_2 . While we continue with notation consistent with Theorem 5.4.1, T_2 is again identical to T . The refinement we use is the hex refinement described in Section 3.3. This new packing, the geodesic, and discrete geodesic are shown in Figure 5.19a. Note that the refinement results in the selection of a new edge path for the discrete geodesic which is closer to true geodesic. Now, we execute the combinatorial earthquake E_2 on T_2 to obtain a new torus determined, by the point $\hat{\omega}_2 = 1.05 + 0.654396i \in \mathbb{H}$, as shown in Figure 5.19b.

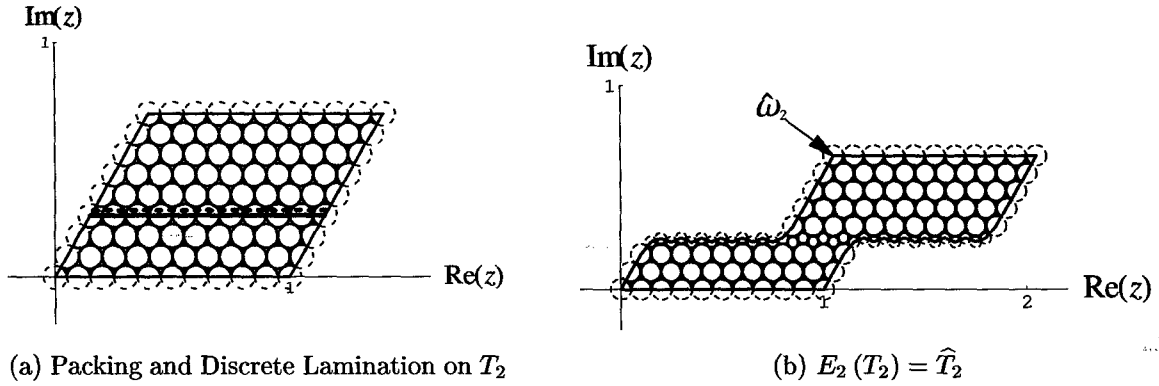


Figure 5.19: Discrete Shearing Map on a “Finely” Packed Torus

Note that we are now “closer” to the desired destination surface \hat{T} . That is, if we denote the Teichmüller distance between two points S and \hat{S} in the normalized Teichmüller space of tori by $d_T(S, \hat{S})$, and we recall that this distance corresponds to the hyperbolic distance between the points $\omega_S, \omega_{\hat{S}} \in \mathbb{H}$ [29], we have the following:

$$d_T(T, \hat{T}_1) = d_{\mathbb{H}}(\omega, \hat{\omega}_1) = d_{\mathbb{H}}\left(\frac{41}{40} + \frac{2\sqrt{3}}{5}i, 1.1 + 0.615973i\right) = 0.1641895$$

$$d_T(T, \hat{T}_2) = d_{\mathbb{H}}(\omega, \hat{\omega}_2) = d_{\mathbb{H}}\left(\frac{41}{40} + \frac{2\sqrt{3}}{5}i, 1.05 + 0.654396i\right) = 0.06806798.$$

Thus, one iteration of hex refinement improves our approximation by a factor of approximately 2.41214. In these computations, we use the formula

$$d_{\mathbb{H}}(z, w) = \cosh^{-1} \left(1 + \frac{|z - w|^2}{2\operatorname{Im}(z)\operatorname{Im}(w)} \right), \quad (5.4.1)$$

giving the hyperbolic distance in the half-plane model between points $z, w \in \mathbb{H}$ [2].

Example 5.4.3. As in Example 5.4.1 and Example 5.4.2, we let T be the point in the normalized Teichmüller space of tori defined by the generators $z + 1$ and $z + \omega$, where $\omega = \frac{7}{5} + i\frac{2\sqrt{3}}{5} \in \mathbb{H}$. We place a geodesic L on this surface such that the segment between $\frac{13}{80} + i\frac{13\sqrt{3}}{80}$ and $\frac{93}{80} + i\frac{13\sqrt{3}}{80}$ is an arc of the lift of that geodesic through the canonical fundamental region for T . This fundamental region for T and the geodesic arc described are shown in Figure 5.20a. Place a weight of $\sigma(L) = \frac{1}{4}i$ on the geodesic. The action of the (grafting) earthquake induced by this finite geodesic lamination on T is shown in Figure 5.20b. Note that though the generators of the image surface \widehat{T} are not the canonical generators associated with the image point in the Teichmüller space of tori, the position in Teichmüller space is determined by the point $\widehat{\omega} = \frac{2}{5} + \frac{5+8\sqrt{3}}{20}i$ [29, 30].

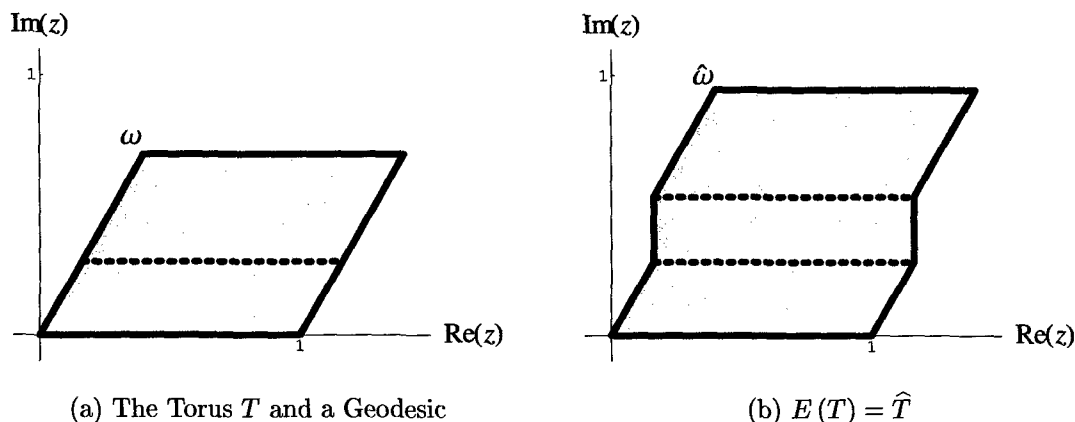


Figure 5.20: Explicit Grafting Action on a Torus

The surface T is itself packable, and we place a packing on the surface as shown in Figure 5.21a to obtain the surface T_1 , identical to T .

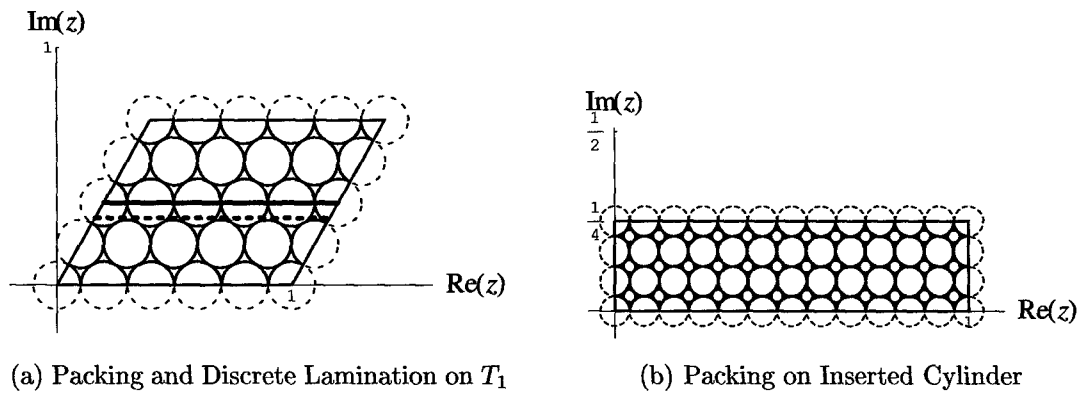


Figure 5.21: Packing and Discrete Lamination on a Torus and a Packed Cylinder

Now, using the technique shown in Figure 4.4, we graft together the combinatorics in the packings in Figure 5.20a and Figure 5.20b. That is, we execute the discrete earthquake E_1 to obtain the packed torus \widehat{T}_1 shown in Figure 5.22a. The torus \widehat{T}_1 is normalized so it is uniquely described by the point $\widehat{\omega}_1 = .499124 + 1.00916i \in \mathbb{H}$. Thus we may calculate the distance in the Teichmüller metric between \widehat{T} and \widehat{T}_1 , $d_T(\widehat{T}, \widehat{T}_1) = 0.122204$.

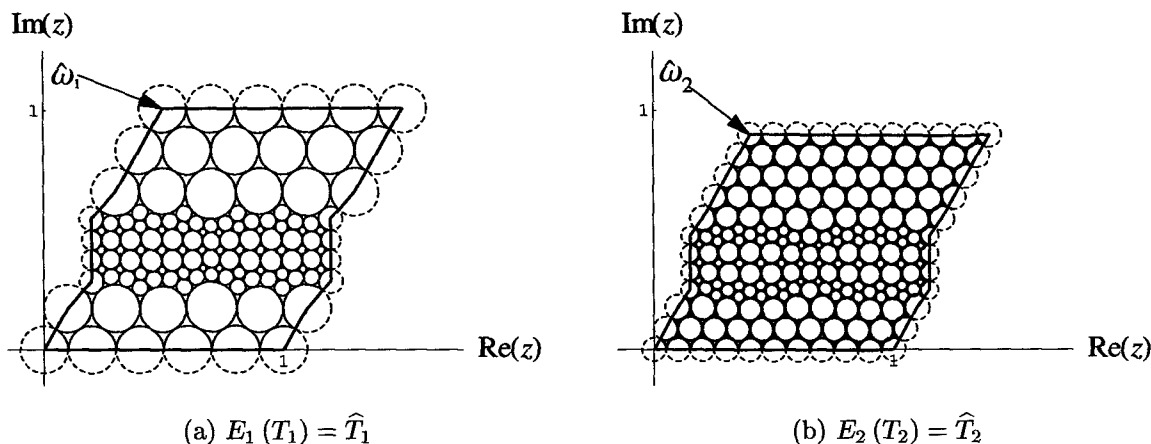


Figure 5.22: Discrete Grafting Maps on a Torus T

As in Example 5.4.2, we may improve our approximation of \widehat{T} through a refinement of the original surfaces. We hex refine the circle packing on T to obtain a new surface T_2 ; as before, T_2 is identical to the original torus T , but we wish to remain

consistent with the notation of Theorem 5.4.1. Note that we have only refined the packing on the torus; the packing on the cylinder remains unchanged in the grafting earthquake E_2 on T_2 . The image, $E_2(T_2) = \widehat{T}_2$, of the earthquake E_2 is shown in Figure 5.22b. The torus \widehat{T}_2 is normalized so that it is uniquely described by the point $\hat{\omega}_2 = 0.404856 + 0.899675i \in \mathbb{H}$. The Teichmüller distance between \widehat{T} and \widehat{T}_2 is given by $d_T(\widehat{T}, \widehat{T}_2) = 0.0471377$. Thus, one iteration of hex refinement improved our approximation of \widehat{T} by a factor of 2.5925.

5.5 Earthquakes on Other Surfaces

We are now in a position to give a complete characterization of earthquakes on compact Riemann surfaces. We recall that, as a consequence of the Uniformization Theorem [15], compact Riemann surfaces fall into a finite number of categories. We have described the action of earthquakes on the Teichmüller spaces of compact tori and compact hyperbolic Riemann surfaces (n -holed tori with $n \geq 2$). Among the remaining surfaces, only the sphere is compact. The Teichmüller space of the sphere is the trivial (one-point) space. We may thus easily define an earthquake on the Riemann sphere and obtain trivial transformations in the Teichmüller space of the sphere.

BIBLIOGRAPHY

- [1] Roger W. Barnard and G. Brock Williams. "Combinatorial Excursions in Moduli Space." *Pacific Journal of Mathematics*, Volume 205, Number 1, 2002, pp. 3-30.
- [2] Alan F. Beardon. *The Geometry of Discrete Groups*. Springer-Verlag, New York, 1983.
- [3] Gennady Belyĭ. "On Galois Extensions of a Maximal Cyclotomic Field." *Mathematics of the USSR Izvestija*, Volume 14, 1979, pp. 247-256 (English).
- [4] Alan F. Beardon and Kenneth Stephenson. "The Uniformization Theorem for Circle Packings." *Indiana University Mathematics Journal*, Volume 39, 1990, pp. 1383-1425.
- [5] Francis Bonahon. *Closed Curves on Surfaces*. Preprint.
- [6] Francis Bonahon. "Earthquakes on Riemann Surfaces and on Measured Geodesic Laminations." *Transactions of the American Mathematical Society*. Volume 330, Number 1, 1992, pp 69-95.
- [7] Francis Bonahon. "Geodesic Laminations on Surfaces" in *Laminations and Foliations in Dynamics, Geometry, and Topology. Contemporary Mathematics*. Volume 269, 2001, pp. 1-37.
- [8] Philip L. Bowers and Kenneth Stephenson. "Circle Packings in Surfaces of Finite Type: An *In Situ* Approach with Application to Moduli Space." *Topology*, Volume 32, Number 1, 1993, pp. 157-183.
- [9] Philip L. Bowers and Kenneth Stephenson. "A 'Regular' Pentagonal Tiling of the Plane." *Conformal Geometry and Dynamics*, Volume 1, 1997, pp.58-86.
- [10] Philip L. Bowers and Kenneth Stephenson. "The Set of Circle Packing Points in the Teichmüller Space of a Surface of Finite Conformal Type is Dense." *Mathematical Proceedings of the Cambridge Philosophical Society*, Volume 111, Number 3, 1992, pp. 487-513.
- [11] Philip L. Bowers and Kenneth Stephenson. *Uniformizing Dessins and Belyĭ Maps Via Circle Packing (Memoirs of the American Mathematical Society)*. American Mathematical Society, 2004.
- [12] Robert Brooks. "Circle Packings and Co-compact Extensions of Kleinian Groups." *Inventiones Mathematicae*, Volume 86, 1986, pp. 461-469.
- [13] James Ward Brown and Ruel V. Churchill. *Complex Variables and Applications, 6th ed.* McGraw-Hill, New York, 1996.

- [14] Peter Buser. *Geometry and Spectra of Compact Riemann Surfaces*. Birkhäuser, Boston, 1992.
- [15] Constantin Carathéodory. *Conformal Representation*. Dover, New York, 1932.
- [16] Andrew J. Casson and Steven A. Bleiler. *Automorphisms of Surfaces after Nielsen and Thurston*. London Mathematical Society Student Texts, Volume 9, Cambridge University Press, Cambridge, 1998.
- [17] Charles R. Collins and Kenneth Stephenson. "A Circle Packing Algorithm." *Computational Geometry: Theory and Applications*, Volume 25, 2003, pp. 233-256.
- [18] John B. Conway. *Functions of One Complex Variable I, 2nd ed.* Springer-Verlag, New York, 1978.
- [19] Heinrich Dörrie. *100 Great Problems of Elementary Mathematics: Their History and Solutions*. Dover, New York, 1965.
- [20] Tomasz Dubejko and Kenneth Stephenson. "Circle Packing: Experiments in Discrete Analytic Function Theory." *Experimental Mathematics*, Volume 4, Number 4, 1995, pp. 307-348.
- [21] Albert Fathi, et al. "Travaux de Thurston sur les Surfaces [The Works of Thurston on Surfaces]." *Astérisque, Séminaire Orsay*, Volume 66-67, Société Mathématique de France, Paris, 1979.
- [22] Frederick P. Gardiner and William J. Harvey. "Universal Teichmüller Space." *Handbook of Complex Analysis, Volume 1: Geometric Function Theory*, R. Kühnau, Editor, Elsevier, 2002, pp. 457-492.
- [23] Frederick P. Gardiner, Jun Hu, and Nikola Lakic. "Earthquake Curves." *Contemporary Mathematics*, Volume 311, 2002, pp. 141-195.
- [24] Frederick P. Gardiner and Nikola Lakic. *Quasiconformal Teichmüller Theory*. Mathematical Surveys and Monographs, Volume 76, American Mathematical Society, 2000.
- [25] Jun Hu. "Earthquake Measure and Cross-Ratio Distortion." *Contemporary Mathematics*, Volume 355, 2004, pp. 258-308.
- [26] Nora Hartsfield and Gerhard Ringel. *Pearls in Graph Theory: A Comprehensive Introduction*. Academic Press, San Diego, 1990.
- [27] Zheng-Xu He and Burt Rodin. "Convergence of Circle Packings of Finite Valence to Riemann Mappings." *Communication in Analysis and Geometry*. Volume 1, 1993, pp. 31-41.

- [28] Zheng-Xu He and Oded Schramm. "On the Convergence of Circle Packings to the Riemann Map." *Inventiones Mathematicae*. Volume 125, Number 2, 1996, pp. 285-305.
- [29] Yoichi Imayoshi and Masahiko Taniguchi. *An Introduction to Teichmüller Spaces*. Springer-Verlag, New York, 1992.
- [30] Gareth A. Jones and David Singerman. *Complex Functions: An Algebraic and Geometric Viewpoint*. Cambridge University Press, Cambridge, 1987.
- [31] Paul Koebe. "Kontaktprobleme der Konformen Abbildung." *Berichte über die Verhandlungen der Sächsischen Akademie der Wissenschaften zu Leipzig*, Volume 88, 1936, pp. 141-164.
- [32] Steven P. Kerckhoff. "The Nielsen Realization Problem." *Annals of Mathematics*. Volume 117, 1983, pp.235-265.
- [33] Olli Lehto and Kaarlo I. Virtanen. *Quasiconformal Mappings of the Plane, 2ed*. Springer-Verlag, Berlin, Heidelberg, New York, 1973.
- [34] Thomas Babington Macaulay. "Horatius." *Lays of Ancient Rome*. IndyPublish.com, McLean, Virginia, July 2002.
- [35] Curtis T. McMullen. "Complex Earthquakes and Teichmüller Theory." *Journal of the American Mathematical Society*, Volume 11, Number 2, 2001, pp. 283-320.
- [36] D. Minda and Burt Rodin. "Circle Packing and Riemann Surfaces." *Journal D'Analyse Mathématique*, Volume 57, 1991, pp. 221-249.
- [37] Bojan Mohar. "Circle Packing of Maps in Polynomial Time." *European Journal of Combinatorics*. Volume 18, 1997, pp. 785-805.
- [38] Tristan Needham. *Visual Complex Analysis*. Oxford University Press, 1997.
- [39] Burt Rodin and Dennis Sullivan. "The Convergence of Circle Packings to the Riemann Mapping." *Journal of Differential Geometry*, Volume 26, 1987, pp. 349-360.
- [40] Dragomir Šarić. "Real and Complex Earthquakes." To appear in *Transactions of the American Mathematical Society*, Electronically published at <http://www.ams.org/tran/0000-000-00/S0002-9947-05-03651-2/home.html>.
- [41] Kevin P. Scannell and Michael Wolf. "The Grafting Map of Teichmüller Space." *Journal of the American Mathematical Society*, Volume 15, Number 4, 2002, pp. 893-927.

- [42] Kenneth Stephenson. *An Introduction to Circle Packing: The Theory of Discrete Analytic Functions*. Cambridge University Press, 2005.
- [43] Kenneth Stephenson. "A Probabilistic Proof of Thurston's Conjecture on Circle Packings." *Rendiconti del Seminario Mate. e Fisico di Milano*, Volume 66, 1996, pp. 201-291.
- [44] Kenneth Stephenson. *CirclePack software*, downloaded from <http://www.math.utk.edu/~kens> (1992-2004).
- [45] Kenneth Stephenson. "Circle Packing: A Mathematical Tale." *Notices of the American Mathematical Society*, Volume 50, Number 11, 2003, pp. 1376-1388.
- [46] Kenneth Stephenson. "Circle Packing and Discrete Analytic Function Theory." *Handbook of Complex Analysis, Volume 1: Geometric Function Theory*, R. Kühnau, Editor, Elsevier, 2002, pp. 333-370.
- [47] Kenneth Stephenson. "The Approximation of Conformal Structures Via Circle Packing." *Computational Methods and Function Theory 1997, Proceedings of the Third CMFT Conference*, World Scientific, 1999, pp. 551-582.
- [48] John Stillwell. *Geometry of Surfaces*. Springer-Verlag, New York, 1992.
- [49] William P. Thurston. "Earthquakes in two-dimensional hyperbolic geometry." *Low-Dimensional Topology and Kleinian Groups* (Coventry/Durham, 1984), London Mathematical Society Lecture Note Series, Volume 112, Cambridge University Press, 1986, pp. 90-112.
- [50] William P. Thurston. "The Finite Riemann Mapping Theorem." Invited Talk, An International Symposium at Purdue University on the occasion of the proof of the Bieberbach Conjecture, 1985.
- [51] William P. Thurston. "The Geometry and Topology of 3-Manifolds." Princeton University Notes, preprint.
- [52] Peter Waterman and Scott Wolpert. "Earthquakes and Tesselations of Teichmüller Space." *Transactions of the American Mathematical Society*, Volume 278, Number 1, 1983, pp. 157-167.
- [53] G. Brock Williams. "Discrete Approximations of Conformal Weldings Using Circle Packing." *Indiana University Mathematics Journal*, Volume 53, Number 3, 2004, pp. 765-804.
- [54] G. Brock Williams. "Earthquakes and Circle Packing." *Journal D'Analyse Mathématique*, Volume 85, 2001, pp. 371-396.
- [55] Stephen Wolfram. *The Mathematica Book, 5th ed.* Wolfram Media/Cambridge University Press, 2003.

APPENDIX

APPENDIX A: DRAWING THE LAMINATION ON \mathbb{D}

A well known property of cross-ratios found in most complex analysis textbooks (see, for example, [13]) states that the relation

$$\frac{(w - w_1)(w_2 - w_3)}{(w - w_3)(w_2 - w_1)} = \frac{(z - z_1)(z_2 - z_3)}{(z - z_3)(z_2 - z_1)} \quad (\text{A.1})$$

implicitly defines the unique Möbius transformation (or fractional linear transformation) which maps distinct points z_1, z_2 , and z_3 in the finite complex plane onto distinct points w_1, w_2 , and w_3 in the finite complex plane. Solving this relation for w , we obtain an explicit expression for this unique Möbius transformation. This action is realized in the *Mathematica* code below. In the notation of the code given, the map obtained has the property that $a = z_1, b = z_2, c = z_3, d = w_1, e = w_2$, and $f = w_3$.

```
Mobius[{a_, b_, c_}, {d_, e_, f_}] :=
  Chop[N[
    ((ade-dbe-adf+bef+dcf-ecf)z+(-adec+dbec+adbf-abef-dbcf+aecf))/
    ((-db+ae+dc-ec-af+bf)z+(adb-abe-adc+bec+acf-bcf))]]]
```

The *Mathematica* code below takes two points m and n on the unit circle and computes a parametric description for the unique hyperbolic geodesic between the two points. We do this by composing a parametrization of the diameter between $z = -1$ and $z = 1, \gamma(t) = -1 + 2t, 0 \leq t \leq 1$, and the appropriate Möbius transformation sending this diameter to the desired hyperbolic geodesic, computed using the command `Mobius[]` from above.

```
Eqn[m_, n_] :=
  Block[{p, q, r},
    p=Exp[I(Min[Arg[m], Arg[n]])];
    q=Exp[I(Max[Arg[m], Arg[n]])];
    r=Exp[I(Arg[m]+Arg[n])/2];
    FullSimplify[{Re[Mobius[{1, I, -1}, {p, r, q}]/.z->(-1+2t)],
      Im[Mobius[{1, I, -1}, {p, Exp[Ir], q}]/.z->(-1+2t)}]]]
```

The following *Mathematica* function takes a list of $n \geq 1$ pairs of distinct points on the unit circle, $\{\{z_{1,1}, z_{1,2}\}, \{z_{2,1}, z_{2,2}\}, \dots, \{z_{n,1}, z_{n,2}\}\}$, and draws the lamination consisting of the geodesics connecting $z_{i,1}$ and $z_{i,2}, 1 \leq i \leq n$.

```
Lamination[pts_] :=
  ParametricPlot[Evaluate[
    Union[{{Cos[2 Pi t], Sin[2 Pi t]}},
      Table[Eqn[pts[[i]]], {i, 1, Length[pts]}]], {t, 0, 1},
    AspectRatio->Automatic, Axes->None, PlotRange->All]
```

APPENDIX B: ACTION OF A FINITE LEFT EARTHQUAKE

The following *Mathematica* code explicitly defines, as a function of z , the comparison map associated with the i th geodesic having left and right endpoints x and y , respectively, and weight u .

```
ComparisonMap[i_,{x_,y_},u_,z_]:=
Simplify[((yExp[u]-x)z+yx(1-Exp[u]))/((Exp[u]-1)z+(y-xExp[u]))]
```

The following code defines a piecewise function for the application of the shearing map for a left earthquake. Note that this map is the comparison map, above, on one domain and the identity map elsewhere.

```
M[i_,z_]:= Which[
  Arg[Q[[i,1,2]]]<Arg[Q[[i,1,1]]],
    Which[
      Or[Arg[z]<Arg[Q[[i,1,2]]],Arg[z]>Arg[Q[[i,1,1]]]],
        ComparisonMap[i,{Q[[i,1,1]],Q[[i,1,2]]},Q[[i,2]]},z],
      True,z],
  Arg[Q[[i,1,2]]]>Arg[Q[[i,1,1]]],
    Which[
      And[Arg[z]<Arg[Q[[i,1,2]]],Arg[z]>Arg[Q[[i,1,1]]]],
        ComparisonMap[i,{Q[[i,1,1]],Q[[i,1,2]]},Q[[i,2]]},z],
      True,z]]
```

The *Mathematica* function below takes as its input a list of points $S \subset \partial\mathbb{D}$ and a description, L , of the finite measured geodesic lamination associated with S . $S = \{s_1, s_2, \dots, s_n\}$ is a list of complex numbers and may be expressed in either polar or rectangular form. L is a list of the form

$$L = \{ \{ \{ p_{1,1}, p_{1,2} \}, \mu_1 \}, \{ \{ p_{2,1}, p_{2,2} \}, \mu_2 \}, \dots, \{ \{ p_{n-3,1}, p_{n-3,2} \}, \mu_{n-3} \} \},$$

where $\{p_{i,1}, p_{i,2}\}$ describes the i th geodesic in the tree of triangles, and μ_i is the weight associated with the i th geodesic. (Recall that a finite lamination on n vertices is comprised of $n - 3$ disjoint, hyperbolic geodesics.) In this notation, $p_{i,1}$ and $p_{i,2}$, $1 \leq i \leq n - 3$, are the left and right endpoints of the i th geodesic, respectively. Note that this code calls the function `M[]`, above, which then calls the function `ComparisonMap[]`.

```
Earthquake[S_,L_]:=
Block[{P=S,Q=L},
Do[
  Do[P[[k]]=M[j,P[[k]]],{k,1,Length[P]}];
  Do[Q[[k,1,1]]=M[j,Q[[k,1,1]]],{k,1,Length[Q]}];
  Do[Q[[k,1,2]]=M[j,Q[[k,1,2]]],{k,1,Length[Q]}];,
{j,1,Length[Q]}];
{P,Q}]
```

APPENDIX C: COMPUTING A MEASURED GEODESIC LAMINATION

The `Complement[]` command in *Mathematica* delivers the complement of one set relative to another. The result returned by the function is sorted in canonical order. The following function returns the list $x \setminus y$ without altering the original order of elements in x . [55]

```
UnsortedComplement[x_List,y_List]:=
  Replace[x,Dispatch[#:→Sequence[]]&/@Union[y]],1]
```

The following *Mathematica* function is a cross-ratio given in [24] linked to the amount points of S are moved to the left by a finite left earthquake. This command is used in computing the lamination and associated measure.

```
cr[a_,b_,c_,d_]:=((d - c)(b - a))/((c - b)(a - d))
```

Now, given a set of points $S = \{s_1, s_2, \dots, s_n\}$ and their images $h(S)$ the algorithm below generates the unique finite lamination \mathcal{L} and a non-negative measure σ associated with S such that, up to post-composition by a Möbius transformation h is the restriction to S of the finite left earthquake h_σ . This inductive algorithm is suggested as an exercise in [24] and examined in more detail in [23].

```
FindLam[pre_,post_]:=
Block[{StartPts,ImagePts,T,a,b,c,a1,b1,c1,L,A,q,test,i,j,k,s,K,TTemp},
  StartPts=pre;ImagePts=post;L={};
  While[Length[StartPts]>=4,
    K=Table[
      {Mod[i,Length[StartPts]]+1,
       Mod[i+1,Length[StartPts]]+1,
       Mod[i+2,Length[StartPts]]+1},{i,0,Length[StartPts]-1}];
    T=Table[
      {{StartPts[[K[k,1]]],StartPts[[K[[k,2]]]]},
       StartPts[[K[[k,3]]]]},
      {ImagePts[[K[k,1]]],ImagePts[[K[[k,2]]]]},
      ImagePts[[K[[k,3]]]]},{k,1,Length[K]};
    dist=
    Table[Table[
      Log[
        Chop[N[
          cr[T[[i,2,1]],T[[i,2,2]],T[[i,2,3]],
            UnsortedComplement[ImagePts,T[[i,2]]][[j]]]/
          cr[T[[i,1,1]],T[[i,1,2]],T[[i,1,3]],
            UnsortedComplement[StartPts,T[[i,1]]][[j]]]]],
        {j,1,Length[StartPts]-3}],{i,1,Length[T]};
```

```

q=Infinity;
test=Table[True,{i,1,Length[dist[[1]]]};
Do[Which[
  And[Table[dist[[j,i]]>=0,{i,1,Length[dist[[j]]]}]==test,
    Min[dist[[j]]]<q],
  q=Min[dist[[j]]];],{j,1,Length[dist]};
AppendTo[L,{T[[Position[dist,q][[1,1]],1,3]],
  T[[Position[dist,q][[1,1]],1,1]],q}];
ImagePts=Drop[ImagePts,
  {Position[StartPts,
    T[[Position[dist,q][[1]][[1]],1,2]][[1,1]]}];
StartPts=Drop[StartPts,
  {Position[StartPts,
    T[[Position[dist,q][[1]][[1]],1,2]][[1,1]]}];
];L]

```

APPENDIX D: COMPUTING THE PACKING LABEL

One of the fundamental results in the theory and practice of circle packing is that given any assignment of positive numbers to the boundary vertices of a triangulation \mathcal{K} , there exists an essentially unique locally univalent circle packing for \mathcal{K} whose boundary circles have these numbers as their radii [42]. This essentially unique circle packing is determined by the so-called **packing label**, a list of the vertices in the triangulation \mathcal{K} and an associated radius for each. The first difficulty in programming a circle packing algorithm is the calculation of these radii.

The following *Mathematica* function is an implementation of the law of cosines giving the angle determined by two legs of a triangle created by connecting the centers of three mutually tangent circles. The values $x, y,$ and z represent the radii of the three circles. The angle calculated is the angle at the center of the circle with radius x .

```
T[x_,y_,z_]:=N[ArcCos[((x+y)+(x+z)-(y+z))/(2(x+y)(x+z))]]
```

The *Mathematica* function below takes a description of the complex \mathcal{K} and a list of boundary vertices along with an assigned radius for each boundary vertex, and it returns the essentially unique Euclidean packing label associated with those inputs. The algorithm which this function implements was suggested by the meta-code described in Practicum I of [44].

```
PackingLabel[K_,B_]:= Block[{e,n,m,R,A,o,G,c,t},
e=.00001;
n=Length[K];
m=Length[B];
R=Table[1.,{i,1,n}];
Do[R[[B[[i,1]]]]]=B[[i,2]],{i,1,m}];
A=Complement[Table[i,{i,1,n}],Table[B[[i,1]],{i,1,m}]];
o=n-m;
G=Table[2*Pi,{i,1,o}];
Do[G[[i]]=
  T[R[[K[[A[[i]],1]]]],R[[Last[K[[A[[i]],2]]]]],
  R[[First[K[[A[[i]],2]]]]]+
  Sum[T[R[[K[[A[[i]],1]]]],R[[K[[A[[i]],2,j]]]],
  R[[K[[A[[i]],2,j+1]]]],
  {1,Length[K[[A[[i]],2]]-1}],
{i,1,o}];
c=2;
t=Max[Table[Abs[2*Pi-G[[i]]],{i,1,o}]];
While[t>e,
  Do[If[G[[i]]<2*Pi,R[[A[[i]]]]]=R[[A[[i]]]]-1/c,
  R[[A[[i]]]]]=R[[A[[i]]]]+1/c,
  {i,1,o}];
```

```

Do[If[R[[A[[i]]]]<0,R[[A[[i]]]]=N[1/(2c)],{i,1,o}];
c=c+1;
Do[G[[i]]=
  T[R[[K[[A[[i]],1]]],R[[Last[K[[A[[i]],2]]]]],
  R[[First[K[[A[[i]],2]]]]]+
  Sum[T[R[[K[[A[[i]],1]]],R[[K[[A[[i]],2,j]]]],
  R[[K[[A[[i]],2,j+1]]]],
  {j,1,Length[K[[A[[i]],2]]-1}],
{i,1,o}];
t=Max[Table[Abs[2*Pi-G[[i]]],{i,1,o}]];];

```

R]

The key to this algorithm is the adjustment of the radii at each step. In the implementation shown, we add and subtract terms in a harmonic series as appropriate to correct the angle sum; a correction step is included to prevent negative radii. This method, chosen for simplicity, is quite slow. There are, however, many other algorithms for the computation of packing labels [17, 37, 44].

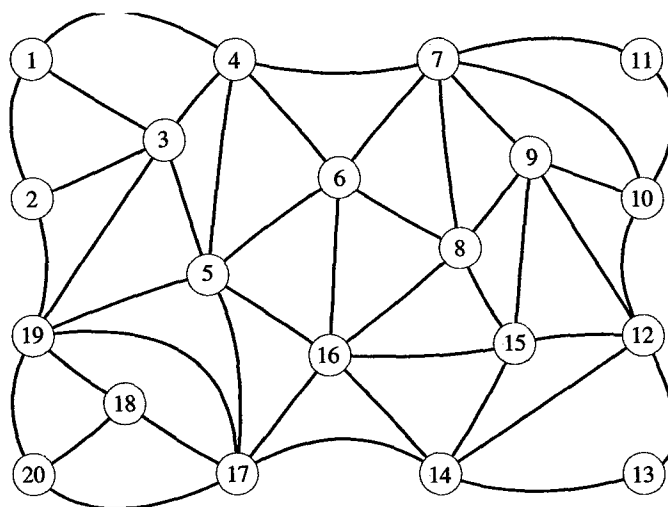


Figure D.1: A Triangulation \mathcal{K}

In Figure D.1, we see a triangulation \mathcal{K} with 20 vertices. If we give each of the boundary vertices a positive radius, in order to achieve a locally univalent packing we need to compute the remaining radii. We assign each boundary vertex a radius of 1, and we use the algorithm described to generate a complete list of the radii in the packing, given in the second column of Table D.1. As stated above, the algorithm is very slow; 448397 iterations were required to achieve results to within 10^{-5} . If we assign different radii to the boundary vertices, we obtain a different set of values for the radii of the interior vertices. That is, the packing label is, as we have already stated, unique. For example, if we assign a radius of 1 to the vertices 1,11,13, and

20 and a radius of $\frac{1}{2}$ to the vertices 2,4,7,10,12,14,17, and 19 we obtain the packing label given in the third column of Table D.1.

Table D.1: Computed Packing Labels for \mathcal{K}

Vertex	Computed Radius for B_1	Computed Radius for B_2
1	1	1
2	1	$\frac{1}{2}$
3	0.663959	0.377904
4	1	$\frac{1}{2}$
5	0.767825	0.394196
6	0.502727	0.253292
7	1	$\frac{1}{2}$
8	0.409361	0.205468
9	0.493900	0.247294
10	1	$\frac{1}{2}$
11	1	1
12	1	$\frac{1}{2}$
13	1	1
14	1	$\frac{1}{2}$
15	0.461162	0.231158
16	0.645202	0.324809
17	1	$\frac{1}{2}$
18	0.154701	0.093836
19	1	$\frac{1}{2}$
20	1	1

As we have already stated, there are other algorithms by which we may calculate the packing label. While the algorithm given above is certainly convergent, its convergence rate is extremely slow. The *Mathematica* command **PackingLabel2[]**, given below, takes as its input the same arguments as the **PackingLabel[]**, but the convergence is significantly faster. The radii computed above (requiring 448397 passes through the algorithm coded in **PackingLabel[]**) are recalculated using the algorithm coded in **PackingLabel2[]**, requiring only 96 passes through the modified algorithm. In this new algorithm, rather than changing the radius associated with every interior vertex on each pass through the algorithm, here we make only one change with every pass through the algorithm. Also, rather than changing the radii by an amount determined by a convergent alternating series, at each step we solve the equation

$$2\pi = \sum_{i=1}^n \theta_i(r), \quad (\text{D.1})$$

where r is the radius of the circle at the center of a flower and $\theta_i(r)$ is the central angle of a triangle created by joining the legs of three adjacent circles in the circle packing. This is illustrated in Figure D.2.

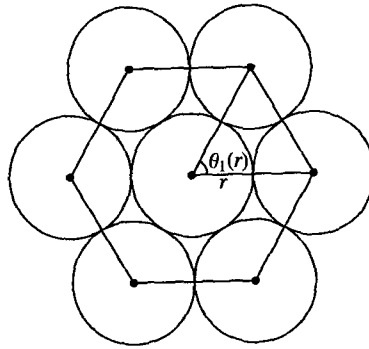


Figure D.2: Angle Sums

```

PackingLabel2[K_,B_]:= Block[{e,n,m,R,A,o,G,c,t,d,r,i,j,a},
e=.00001; n=Length[K]; m=Length[B];
R=Table[1.,{i, 1, n}];
Do[R[[B[[i,1]]]]=B[[i,2]],{i,1,m}];
A=Complement[Table[i,{i,1,n}],Table[B[[i,1]],{i,1,m}]];
o=n-m;
G=Table[2*Pi,{i,1,o}]; Do[G[[i]]=
  T[R[[K[[A[[i]],1]]]],R[[Last[K[[A[[i]],2]]]]],
  R[[First[K[[A[[i]],2]]]]]+
  Sum[T[R[[K[[A[[i]],1]]]],R[[K[[A[[i]],2,j]]]],
  R[[K[[A[[i]],2,j+1]]]]],
  {1,Length[K[[A[[i]],2]]-1}],
{i,1,o}];
t=Max[Table[Abs[2*Pi-G[[i]]],{i,1,o}]];
While[t>e,
d=Position[Table[Abs[2*Pi-G[[i]]],{i,1,o}],t][[1,1]];
R[[K[[A[[d]],1]]]]=
  FindRoot[2*Pi==T[r,R[[Last[K[[A[[d]],2]]]]],
  R[[First[K[[A[[d]],2]]]]]+
  Sum[T[r,R[[K[[A[[d]],2,j]]]],R[[K[[A[[d]],2,j+1]]]]],
  {j,1,Length[K[[A[[d]],2]]-1}],
  {r,R[[K[[A[[d]],1]]]],e,Infinity}][[1,2]];
Do[G[[i]]=
  T[R[[K[[A[[i]],1]]]],R[[Last[K[[A[[i]],2]]]]],
  R[[First[K[[A[[i]],2]]]]]+
  Sum[T[R[[K[[A[[i]],1]]]],R[[K[[A[[i]],2,j]]]],
  R[[K[[A[[i]],2,j+1]]]]],
  {j,1,Length[K[[A[[i]],2]]-1}],
{i,1,o}];
t=Max[Table[Abs[2*Pi-G[[i]]],{i,1,o}]];];R]

```

We note that both `PackingLabel[]` and `PackingLabel2[]` can accommodate and compute valid packing labels for triangulations which have no boundary vertices. That is, we may compute packing labels associated with triangulations on surfaces. For example, Figure D.3 shows a simple triangulation on a torus.

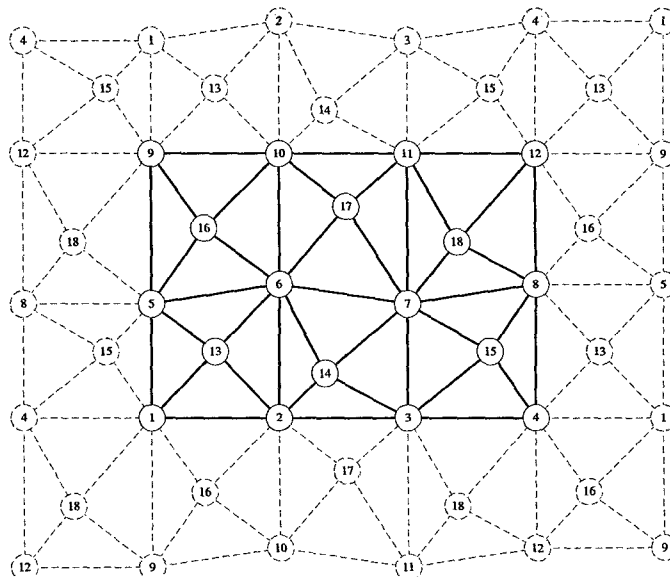


Figure D.3: A Triangulation on a Torus

The packing label for this triangulation gives radius 2.4142 to the vertices labeled 1, 2, ..., 12 and a radius of 1 to the remaining vertices (from the initialization values used in our algorithms).

APPENDIX E: LAYING OUT THE CIRCLE PACKING

Given a packing label R associated with a complex \mathcal{K} , we wish to construct a graphical representation of the essentially unique circle packing they induce. This process is not a numerical process; we merely lay out the circles in their respective positions in the complex plane \mathbb{C} . This is achieved through an accumulation process implemented in the *Mathematica* function `Layout[]`. This function takes as its arguments the variables \mathbf{K} , \mathbf{R} , \mathbf{B} , \mathbf{a} , and \mathbf{g} . \mathbf{K} is a description of the complex \mathcal{K} as a list of vertices and their neighbors in the form

$$\mathbf{K} = \{ \{v^1, \{v_1^1, v_2^1, \dots, v_{k_1}^1\}\}, \dots, \{v^n, \{v_1^n, v_2^n, \dots, v_{k_n}^n\}\} \}$$

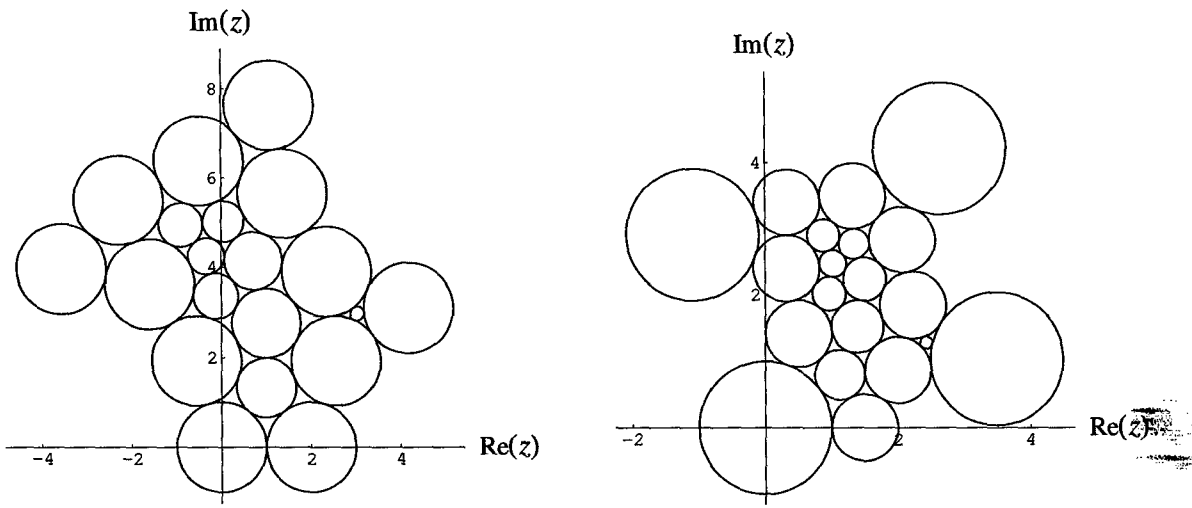
Note that each vertex is simply identified as an integer $1, 2, \dots, n$. The vertices $\{v_1^i, v_2^i, \dots, v_{k_i}^i\}$ surrounding the i th must be listed in counterclockwise order to ensure that the orientation remains consistent. \mathbf{R} is a row vector listing, in order, the radii of each vertex in the packing. \mathbf{B} is a subset of $\{1, 2, \dots, n\}$ naming the boundary vertices. This information would be enough to generate a packing, unique up to rotation and translation (i.e., essentially unique). The remaining parameters, \mathbf{a} and \mathbf{g} , are elements of $\{1, 2, \dots, n\}$ that place the center of a circle in the packing at the origin (the circle associated with the vertex \mathbf{a}) and place the center of an adjacent circle in the packing on the real axis (the circle associated with the vertex \mathbf{g}). The function determines the unique set of centers for the circles in the packing under the normalization imposed by \mathbf{a} and \mathbf{g} . This algorithm was suggested by meta-code given in Practicum I from [44].

```
Layout[K_,R_,B_,a_,g_] := Block[{n,S,P,L,Q,q,u,i,j,b,m,l,p},
n=Length[R]; S=Table[Circle[{0, 0},R[[i]]],{i, 1, n}];
S[[g]]=Circle[{R[[a]]+R[[g]],0},R[[g]]]; P={a,g}; While[Length[P]<n,
  L=Complement[Table[i,{i,1,n}],P];
  Do[
    Q=Table[{L[[j]],K[[L[[j]],2,i]],K[[L[[j]],2,i+1]]},
      {i,1,Length[K[[L[[j]],2]]-1}];
    If[Not[MemberQ[B,L[[j]]]],AppendTo[Q,
      {L[[j]],Last[K[[L[[j]],2]]],First[K[[L[[j]],2]]}];];
  u=Length[Q];
  i=1;
  q=0;
  While[And[i<=u,q===0],
    If[And[MemberQ[P,Q[[i,2]]],MemberQ[P,Q[[i,3]]]],
      b=T[R[[Q[[i,2]]]],R[[Q[[i,3]]]], R[[Q[[i,1]]]]];
      m=N[S[[Q[[i,2]]]][[1,1]]+I*S[[Q[[i,2]]]][[1,2]]];
      l=N[S[[Q[[i,3]]]][[1,1]]+I*S[[Q[[i,3]]]][[1,2]]];
      If[m===0.,
        p=(R[[Q[[i,1]]]]+R[[Q[[i,2]]]])*Exp[I*(Arg[l]+b)];
```

```

S[[L[[j]]]] = Circle[{Re[p], Im[p]}, R[[L[[j]]]]];
P = Sort[AppendTo[P, L[[j]]]];
q = 1;
p = (R[[Q[[i, 1]]]] + R[[Q[[i, 2]]]]) * Exp[I*(Arg[1 - m] + b)] + m;
S[[L[[j]]]] = Circle[{Re[p], Im[p]}, R[[L[[j]]]]];
P = Sort[AppendTo[P, L[[j]]]];
q = 1;
],
i = i + 1;]
],
{j, 1, Length[L]};
]; S]

```



(a) Packing Defined by Column 2 of Table D.1 (b) Packing Defined by Column 3 of Table D.1

Figure E.1: Distinct Circle Packings Induced by Different Boundary Radii

As an example of this packing, consider the complex \mathcal{K} described in Figure D.1 and the two sets of associated radii given in Table D.1. If we let $a = 1$ and $g = 2$ in each case, the function `Layout[]` gives the arrangements of circles shown in Figure E.1.

We may also lay out a packing on a surface. Consider the complex described in Figure D.3 and the associated radii computed in Appendix E. As when we “cut open” a surface along generators of a fundamental group in order to lay out a fundamental region for that surface, we open the complex by removing tangencies, then use the `Layout[]` (with $a = 1$ and $g = 2$) to arrange the circle packing in the plane. The result is shown in Figure E.2.

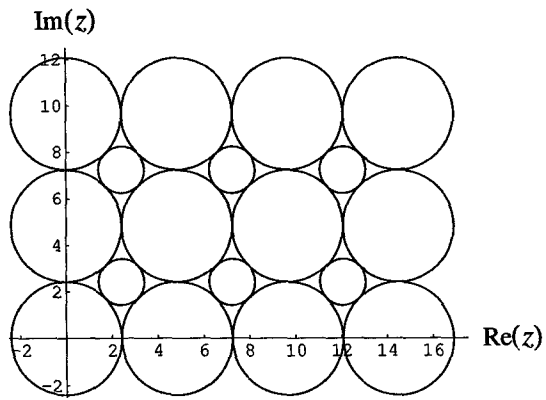


Figure E.2: Circle Packing on a Torus